

# Mapping benthic marine habitats featuring coralligenous bioconstructions: a new protocol approach functional to support geobiological researches

Giuseppe Maruca<sup>1\*</sup>, Mara Cipriani<sup>1\*</sup>, Rocco Dominici<sup>1</sup>, Gianpietro Imbrogno<sup>1</sup>, Giovanni Vespasiano<sup>1</sup>, Carmine Apollaro<sup>1</sup>, Francesco Perri<sup>1</sup>, Fabio Bruno<sup>2</sup>, Antonio Lagudi<sup>2</sup>, Umberto Severino<sup>2</sup>, Valentina A. Bracchi<sup>3</sup>, Daniela Basso<sup>3</sup>, Emilio Cellini<sup>4</sup>, Fabrizio Mauri<sup>4</sup>, Antonietta Rosso<sup>5</sup>, Rossana Sanfilippo<sup>5</sup>, Adriano Guido<sup>1</sup>.

<sup>1</sup>Department of Biology, Ecology and Earth Sciences, University of Calabria, 87036, Rende, Italy;

<sup>2</sup>Department of Mechanical, Energy and Management Engineering, University of Calabria, 87036, Rende, Italy;

<sup>3</sup>Department of Earth and Environmental Sciences, University of Milano–Bicocca, 20126, Milan, Italy;

<sup>4</sup>Regional Agency for the Environment (ARPACAL), Regional Marine Strategy Centre (CRSM), 8890, Crotone Italy.

<sup>5</sup>Department of Biological, Geological and Environmental Sciences, University of Catania, 95129, Catania, Italy;

Correspondence to: Giuseppe Maruca ([giuseppe.maruca@unical.it](mailto:giuseppe.maruca@unical.it)); Mara Cipriani ([mara.cipriani@unical.it](mailto:mara.cipriani@unical.it))

**Abstract.** Seabed mapping represents a very useful tool for seascape characterization and benthic habitat study, and requires advanced technologies for acquiring, processing and interpreting remote data. Particularly, acoustic instruments, such as high-resolution swath bathymetry sounder (*i.e.*, Multibeam Echosounder: MBES), allows to recognize, identify and map the extension of benthic habitats without applying invasive mechanical procedures. Bathymetry and backscatter (BS) data are crucial to perform modern habitat mapping, ~~however they require careful end-product development and, to date, no standardized procedure exists.~~ Although the acquisition and processing of bathymetric data follows standardized procedure (*e.g.*, Hydrographic Organization guidelines), and recent studies proposed recommendation for backscatter acquisition and processing, a broadly validated methodological approach, integrating geomorphometric analysis for benthic habitat mapping, is still lacking. In this work, a ~~protocol~~ new approach for benthic habitat mapping, with focus on coralligenous bioconstructions, was developed using the open-source software QGIS. This ~~protocol~~ methodology, tested within the Isola Capo Rizzuto Marine Protected Area (Calabria, Italy), is designed to be freely reproducible by researchers working in the field of marine ecosystem monitoring and conservation. Through the proposed mapping procedure, it is possible to: i) identify benthic habitats on selected study areas by combining bathymetry and BS data with geomorphological indices performed in QGIS; ii) quantitatively define the 2D and 3D distribution of coralligenous bioconstructions in terms of surface covered, thickness and volume. Moreover, the statistical analysis of quantitative morphometric data allowed for comparison of geometric characteristics of different coralligenous morphotypes. The obtained results, combined with improvement of minimally invasive sampling and geobiological–geochemical characterization, can contribute to the development of protocols aimed at monitoring marine bioconstructed ecosystems, many of which protected by national and international regulations due to their importance for Mediterranean biodiversity preservation, and plan actions for their protection and persistence.

## 1 Introduction

Bioconstructions are geobiological bodies formed in situ by growth of skeletonised organisms and represent habitats that host a great variety of benthic species. They experience a wide array of dynamic phenomena, resulting from the balance

40 between the action of habitat builders, dwelling organisms and bioeroders ~~on a relatively large temporal scale~~ **over decadal**  
 41 **to millennial timescale**. Along the Mediterranean continental shelf, the most conspicuous bioconstructed habitats are  
 42 represented by coralligenous build-ups (Bracchi et al., 2015, 2017, 2022; Basso et al., 2022; Cipriani et al., 2023, 2024),  
 43 vermetid reefs (Picone and Chemello, 2023), sabellariid build-ups (Sanfilippo et al., 2019, 2022; Deias et al., 2023) and  
 44 polychaetes–bryozoan bioconstructions (Guido et al., 2013, 2016, 2017a, b, 2019a, b, 2022), whereas cold–water corals  
 45 occur in deeper settings (Rueda et al. 2019, Foglini et al., 2019). Coralligenous is known as a biocenosis complex  
 46 consisting of a hard biogenic substrate primarily generated by the superimposition of calcareous red algae able to form  
 47 3D structures, supporting a high biodiversity (*e.g.*, Ballesteros, 2006; Bracchi et al., 2022; Rosso et al., 2023; Sciuto et  
 48 al., 2023; Donato et al., 2024). Pérès and Picard (1964) and Pérès (1982) identified Coralligenous as the ecological climax  
 49 **stage** for the Mediterranean circalittoral zone, with some bioconstructions also occurring in dim–light very shallow  
 50 settings (Ballesteros, 2006; Bracchi et al., 2016; Basso et al., 2022). Coralligenous produces various morphotypes on the  
 51 seafloor and plays a key role in the formation and transformation of seascape over geological time (Bracchi et al., 2017;  
 52 Marchese et al., 2020). Architecture and morphology are mainly influenced by biological carbonate production, that  
 53 responds to different factors, like physiography, oceanography, terrigenous supply and climate (Schlager, 1991, 1993;  
 54 Betzler et al., 1997; Bracchi et al., 2017). Based upon the nature of the substrates, coralligenous morphotypes have been  
 55 categorized in two main groups: i) banks, flat frameworks mainly built on horizontal substrata and, and ii) rims, structures  
 56 on submarine vertical cliffs or close to the entrance of submarine caves (Pérès & Picard, 1964; Laborel, 1987; Ballesteros,  
 57 2006; Bracchi et al., 2017; Marchese et al., 2020; Gerovasileiou & Bianchi, 2021). Moreover, Bracchi et al. (2017)  
 58 introduced a new classification for coralligenous morphotypes on sub–horizontal substrate using a shape geometry  
 59 descriptor, in order to ~~improve its knowledge by ensuring an objective description~~ **obtain a more objective description of**  
 60 **these morphologies, classified in:** i) tabular banks, *i.e.*, large tabular structures with a significant lateral continuity that  
 61 completely cover the seafloor, forming an extensive habitat; ii) discrete reliefs, *i.e.*, smaller, distinct structures often  
 62 arranged in clusters that do not fully cover the seafloor, leaving patches of sediment between them; and iii) hybrid banks,  
 63 a category grouping morphologies intermediate between tabular banks and discrete reliefs. These structures can coalesce  
 64 into a larger formation, resembling tabular banks, while still maintain individual characteristics. Hybrid banks often occur  
 65 alongside other habitats, and their distribution is influenced by local sediment and hydrodynamic conditions (Bracchi et  
 66 al., 2017).  
 67 Although coralligenous bioconstructions occur along almost the entire Mediterranean continental shelf, they have been  
 68 mapped only in few areas and their distribution is still underestimated (De Falco et al 2010, 2022; Innangi et al 2024). In  
 69 addition, as known hot spot of biodiversity, along with its low accretion rate of 0.06–0.27 mm/yr and its sensitivity to  
 70 natural and anthropogenic impacts (Di Geronimo et al., 2001; Bertolino et al., 2014; Basso et al., 2022; Cipriani et al.,  
 71 2023, 2024), Coralligenous is acknowledged as a priority habitat for protection under the EU Habitats Directive, is part  
 72 of the Natura 2000 network (92/43/CE), and is subject to specific conservation plans within the framework of the  
 73 Barcelona Convention (UNEP–MAP–RAC/SPA, 2008; UNEP–MAP–RAC/SPA, 2017). Moreover, together with other  
 74 vulnerable settings (*e.g.*, Cold–Water Corals), Coralligenous is monitored under the Marine Strategy Framework  
 75 Directive (MSFD, EC, 2008; SNPA, 2024). As a result, non–destructive methods have been developed to assess the health  
 76 status and ecological quality of this habitat (Bracchi et al., 2022). For all these reasons, seabed mapping can provide a  
 77 very useful tool for seascape characterization and mapping of Coralligenous and other vulnerable habitats (Chiocci et al.,  
 78 2021). In particular, acoustic instruments, such as high–resolution swath bathymetry sounder, side scan sonar and acoustic  
 79 profiling, enable the quick detection and identification of benthic habitats and thus mapping their extension without any  
 80 direct contact that might represent a threat for these vulnerable ecosystems (Bracchi et al., 2017; Chiocci et al., 2021).

Several studies have demonstrated that such technologies, especially when combined with backscatter (BS) data and geometric descriptors, significantly enhance the study of seafloor properties and the discrimination of benthic habitats, such as coral reefs, improving the understanding of their spatial distribution and ecological significance (Fonseca and Mayer, 2007, Lecours et al., 2015; Brown et al., 2012; Lamarche and Lurton, 2018; Abdullah et al., 2024).

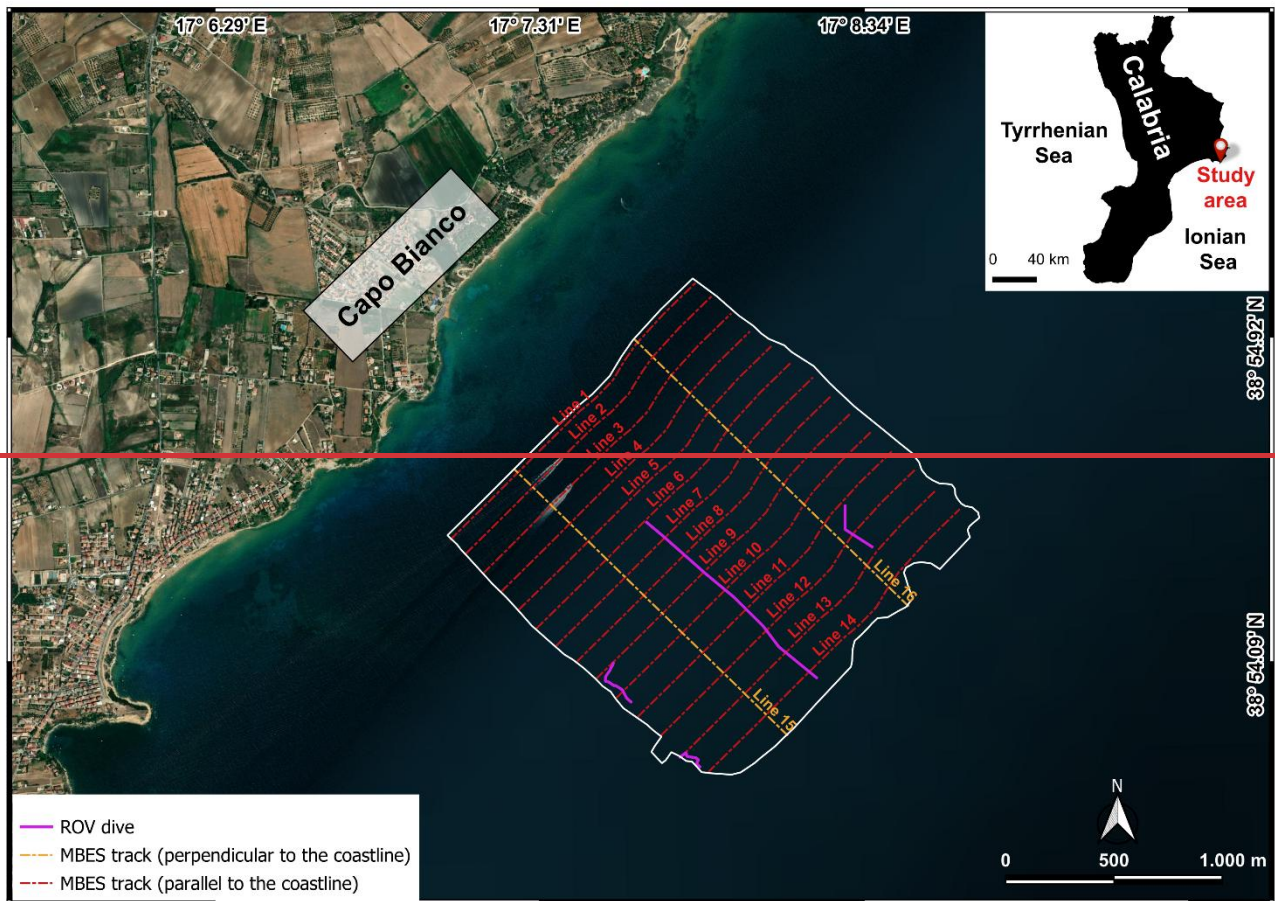
In this work, a semi-automated GIS-based ~~protocol~~ **approach** for benthic habitat mapping was proposed and tested in shallow coastal waters, off Capo Bianco, within the Isola Capo Rizzuto Marine Protected Area (Crotone, Southern Italy). The method combines high-resolution bathymetric and ~~backscatter~~ (BS) data obtained through MBES surveys and geomorphological and geomorphometric indices in order to develop innovative approaches for eco-geomorphological and geobiological characterisation of the seafloor. The benthic habitat mapping ~~protocol~~ here proposed has proven capable not only of identifying marine bioconstructions, but also of quantitatively defining their spatial and three-dimensional distribution in terms of area, volume and height relative to the substrate from which they arise. For these reasons, the procedure represents a powerful tool for accurately delineate the extension of the bioconstructions and evaluate their evolution over time in response to natural and/or anthropogenic changes. Furthermore, the combination of this mapping ~~protocol~~ **approach** with minimally invasive sampling systems and geobiological-geochemical characterization of marine bioconstructions, may represent a potent tool for monitoring these delicate habitats.

## 2 Methodological approach

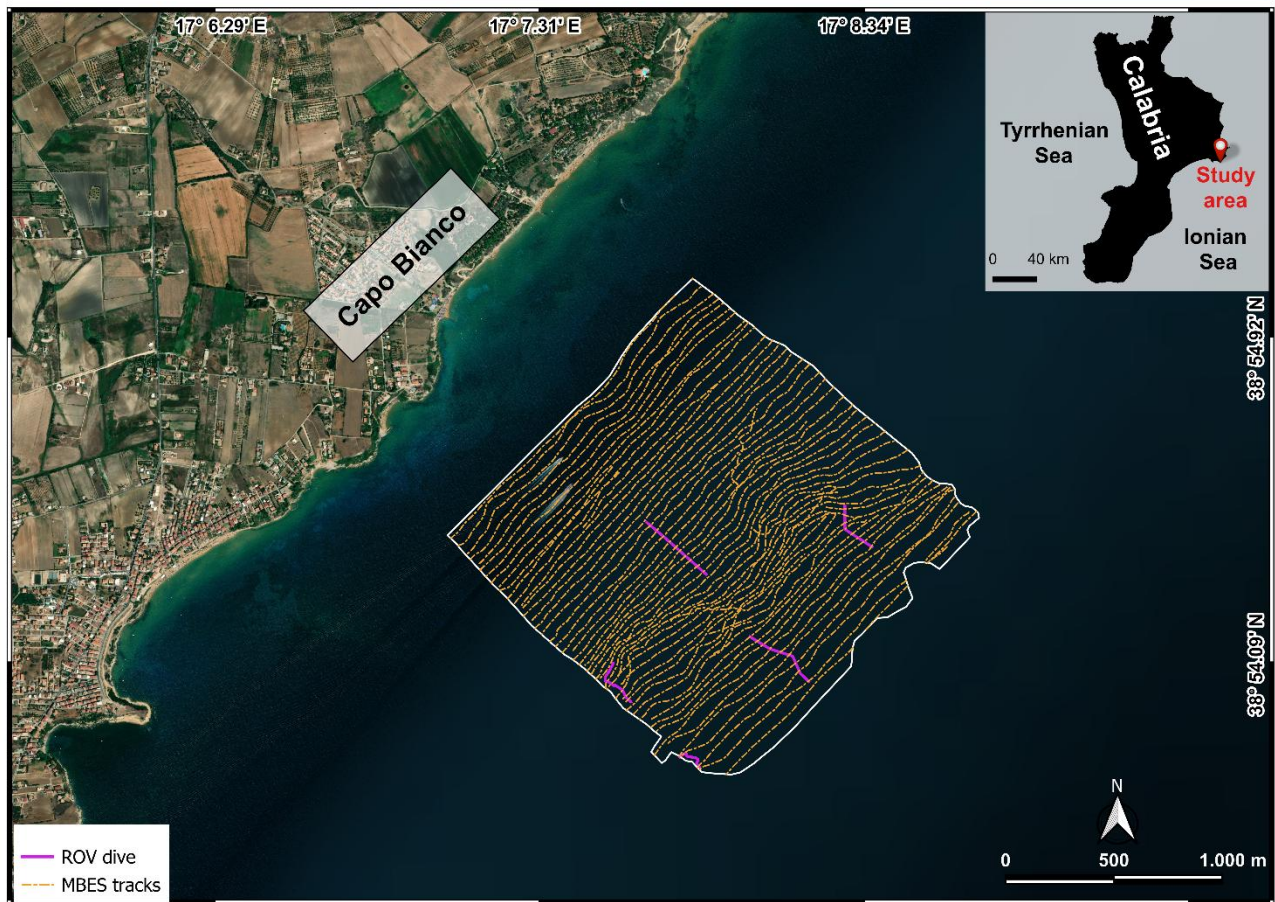
High-resolution acoustic data of the study area offshore Capo Bianco were collected during several MBES surveys (Fig. 1) performed between February and July 2024 as part of the project “Tech4You PP2.3.1: Development of tools and applications for integrated marine communities and substrates monitoring; Action 1: Development of hardware and software systems for three-dimensional detection, sampling and mapping of underwater environments”, in implementation to the previous bathymetric and backscatter data acquisition and elaboration of CRSM-ARPACAL. The ~~protocol~~ **approach** proposed for benthic habitat mapping and defining of spatial and three-dimensional distribution of coralligenous bioconstruction is ~~briefly~~ shown in Figure 2. In particular, mapping operations were conducted using QGIS 3.34.9 “Prizren”. The most representative morphological indices, **represented by slope and seafloor roughness**, were extracted from the Digital Terrain Model (DTM). Due to the large amount of data resulting from the need to obtain a high-resolution mapping of benthic habitats, backscatter and bathymetry values, together with geomorphological-geomorphometric indices, were imported and queried into PostgreSQL, an open-source and free relational database management system (RDBMS) capable of executing queries in SQL language.



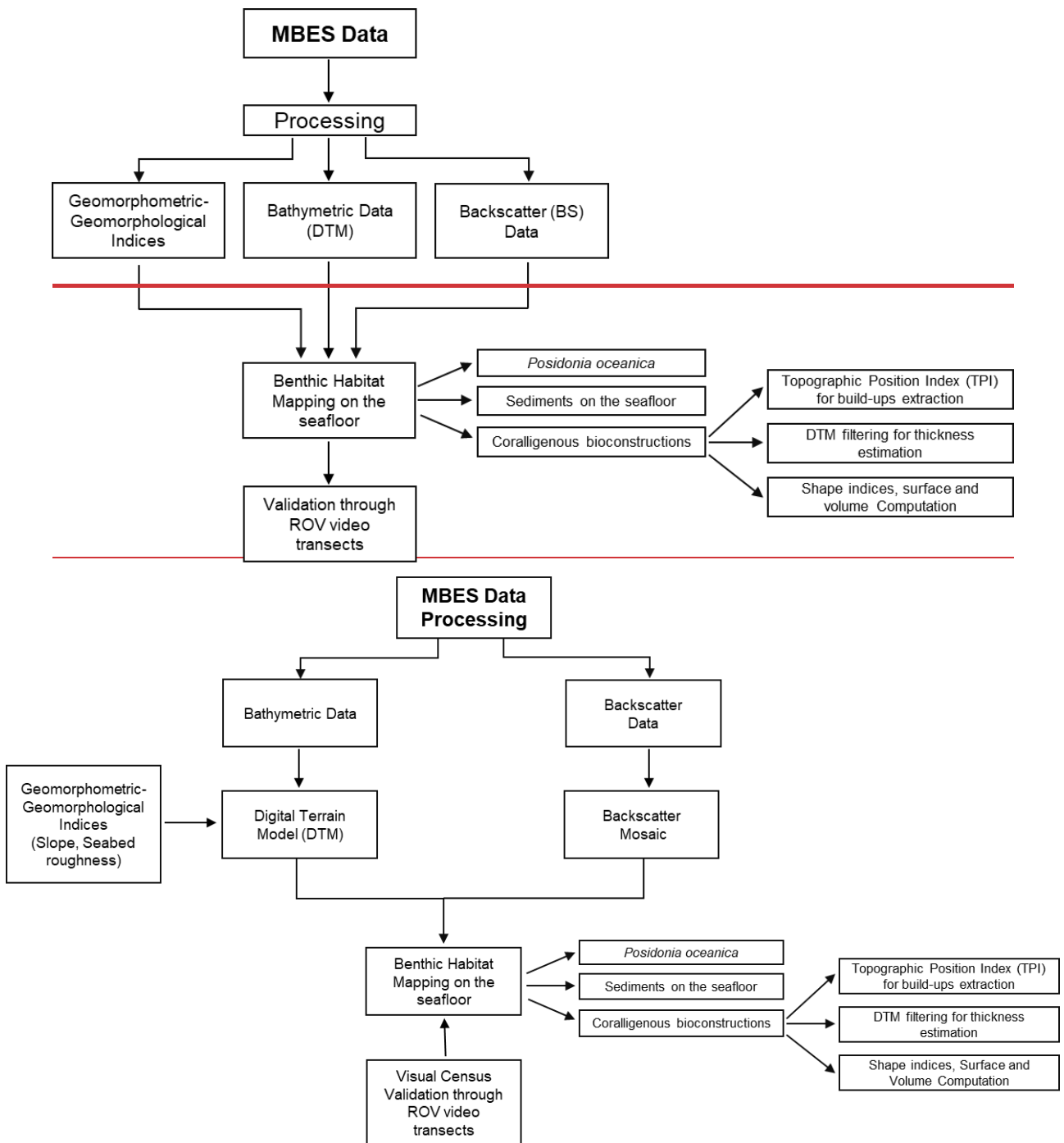
109



110  
111  
112



**Figure 1:** Study area off Capo Bianco (Calabria, Italy) and location of the MBES tracks and ROV–video transect (modified basemap from Esri World Imagery).



**Figure 2:** Conceptual model of the workflow for the development of the proposed benthic habitat mapping model approach.

Once the spatial extension and distribution of the benthic habitat have been defined by combination of bathymetric, backscatter, slope and seafloor roughness data, the extraction of coralligenous build-ups was performed using the Topographic Position Index (TPI), according to Marchese et al. (2020). Moreover, area, Shape Index (SI), maximum diameter (Dmax) thickness and volume were calculated for each extracted polygon. Finally, the benthic habitat mapping model was ground-truthed by visual analysis of ROV-video transect performed along specific paths identified in the within the study area. The underwater video surveys were obtained using a VideoRay Defender equipped with a functional prototype of the optical module dedicated to mapping, comprising a stereo-camera, a high-resolution camera and a

lightning system (Severino et al., 2023). ~~The primary objective of this hardware is to generate high-resolution, scaled 3D models through the use of a stereo camera system.~~ Both cameras have been meticulously calibrated to correct for optical distortions, ensuring accurate and reliable data acquisition. The selected cameras were the GoPro Hero 9 Black, serving as the high-resolution camera, and the Stereolabs ZED2i, serving as the stereo camera. The GoPro Hero 9 Black is a small-sized action camera with a 26.3 MP CMOS sensor capable of acquiring videos at a resolution of 5120×2880 at 30 fps, digital stabilization, and a horizontal field of view up to 128°. The ZED2i is a stereo camera with dual 4 MP sensors of 2 mμ pixel size, a depth range between 0.3 m to 20 m, capable of acquiring video with a resolution of 2208×1242 at 15 fps, and a horizontal field of view of 110°. The stereo-camera communicates with the surface control unit by means of a single-board microcomputer, a NVIDIA Jetson Nano, which supports the CUDA architecture for parallel elaboration. The GoPro Hero 9 Black features Bluetooth Low Energy (BLE) and Wi-Fi communication capabilities. The acquisition parameters for both cameras can be configured via the enclosure using a custom user interface accessible on the surface computer.

## 2.1 Bathymetric and backscatter data

MBES surveys have been carried out using a pole-mounted, ~~Norbit WBMS Basic multibeam sonar system~~ **Norbit iWBMS Long Range Turnkey Multibeam Sonar System** integrated with GNSS/INS (Applanix OceanMaster), **operating with Real Time Kinematic (RTK) corrections, ensuring high positioning accuracy during the surveys.** Data were collected in ~~46~~ **59** tracks with a swath overlap of 20–40 % performed at an average speed of 4.5 knots. ~~Several sound velocity profiles~~ **A total of three sound velocity profiles per day** were collected before starting the acquisition using a Sound Velocity Profiler–Valeport miniSVP. **Considering the absence of freshwater inputs and the relative stability of the water column across the depth range, this was deemed sufficient to ensure reliable sound speed correction.** The MBES survey provided both bathymetry and BS data. The processing of MBES bathymetric data was performed using QPS Qimera and included corrections for tide, heading, heave, pitch and roll. The correction of sound velocity was carried out using profiles obtained with the Valeport miniSVP. Subsequently, the soundings underwent manual cleaning to remove spikes. The bathymetric dataset was exported as a 32-bit raster file with a cell size of 0.05 m. BS data were processed using QPS Fledermaus, and the final output was exported as an 8-bit raster file with 0.05 m cell size.

## 2.2 Geomorphological–geomorphometric indices

Geomorphologic and geomorphometric indices were obtained using SAGA (System for Automated Geoscientific Analysis; Conrad et al., 2015) Next Gen Provider and GDAL plugins. In particular, the slope, expressed in degrees, was calculated using the dedicated function implemented in the GDAL plugin using a ratio of vertical units to horizontal of 1.0 and applying the Zevenbergen–Thorne formula instead of the Horn’s one. Indeed, the Zevenbergen–Thorne method (1987), that considers a second-order finite difference, is more dedicated to geomorphological applications as it uses a particular weighting scheme that emphasizes changes in curvature and terrain shape. Seabed roughness was assessed using the Terrain Roughness Index (TRI), which provides a quantitative measure of terrain heterogeneity (Riley et al., 1999). In particular, TRI values close to 0 indicate fairly regular and uniform surfaces, moderate TRI values correspond to more pronounced irregularities, while high TRI values identify rugged morphologies and/or complex structures on the seafloor. TRI was calculated using SAGA module “Terrain Roughness Index” with the following settings: circle as search mode; a search radius of 0.5 **map units (m.u.)**; gaussian weighting function: a value of 3.00 for the power; a bandwidth of 75.00. The values of these parameters were selected through a trial-and-error method in order to best highlight the heterogeneity of the seabed.



## 164 2.3 Topographic Position Index

165 The Topographic Position Index (TPI) was calculated at the finest possible scale (min radius: 1.00 m.u.; max radius: 5.00  
166 m.u.) according to the DTM resolution and using a Power of 3.00 and a Bandwidth of 150.00. TPI is a morphometric  
167 parameter based on neighbouring areas useful in DTM analysis (Wilson and Gallant, 2000). Specifically, positive TPI  
168 values indicate areas that are higher than the average of their surroundings, TPI values near zero correspond to flat areas  
169 or region with a constant slope, while negative TPI values represent areas lower than their surroundings. In order to  
170 facilitate the extraction of coralligenous build-ups from surrounding seafloor and reduce the occurrence of artifact, a TPI  
171 threshold of 0.2 was used and all the grid cells below this value were not considered as coralligenous bioconstructions.  
172 TPI scale (1.00–5.00 m.u.) and value (0.2) were chosen through a trial-and-error approach in order to preserve the high  
173 resolution of the extraction which is crucial for accurate volume computation.

## 174 2.4 DTM filtering

175 TPI parameters extracted the distribution of the coralligenous build-ups with high-resolution in terms of perimeter  
176 boundary. The thickness calculation for each coralligenous build-up was developed by the creation of a “reference  
177 surface” (without build-ups) using the SAGA “DTM Filter (Slope-Based)” tool implemented in QGIS 3.34.9. This tool  
178 uses concept as described by Vosselman (2000) and can be used to filter a DTM, categorizing its cell into ground and  
179 non-ground (object) cell. A cell is considered ground if there is no other cell within the kernel radius where the height  
180 difference exceeds the allowed maximum terrain slope at the distance between the two cells. The thickness estimation of  
181 each coralligenous build-up was obtained by subtracting the average depth of each polygon extracted using TPI from the  
182 average depth value of the reference surface at that specific zone.  
183 After estimating the height of each build-up relative to the seabed on which it developed, the Shape Index (SI–McGarigal  
184 et al., 1995) was calculated using the module “Polygon Shape Indices” of SAGA in order to describe a seafloor landscape  
185 characterized by distinct Coralligenous morphotypes. Finally, covered surface and volume of each polygon were  
186 calculated using vector field operation implemented into QGIS.

## 187 3 Geological setting

188 The study area, located offshore Capo Bianco (Isola Capo Rizzuto, Calabria, Italy), belongs to the Crotona Basin (CB)  
189 (Fig. 3). The CB is the widest Neogene basin of the Calabria region, in part partly exposed along the Ionian coast and in  
190 part documented offshore. It represents a segment of the Ionian fore arc basin located on the internal part on the inner  
191 portion of the Calabrian accretionary wedge (Cavazza et al., 1997; Bonardi et al., 2001; Minelli and Faccenna, 2010). The  
192 basin infill, developed within the context of rollback subduction, was controlled by south-eastward migration of the  
193 Calabrian arc and the opening of the Tyrrhenian Sea (Serravallian–Tortonian onward) (Malinverno and Ryan, 1986;  
194 Faccenna et al., 2001; Milia and Torrente, 2014). The basin infill is structured into several distinct tectono-stratigraphic  
195 sequences, which reflect an extensional to transtensional tectonic regime, occasionally interrupted by transpressional to  
196 compressional events (Malinverno and Ryan, 1986; Faccenna et al., 2001; Reitz and Seeber, 2012; Zecchin et al., 2012;  
197 Massari and Prosser, 2013; Milia and Torrente, 2014).  
198 Since the mid-Pleistocene, this region experienced a significant uplift (Westaway, 1993; Westaway and Bridgland, 2007;  
199 Faccenna et al., 2011; 0.70–1.25 m/ky; Zecchin et al., 2004), which, combined with glacio-eustatic sea level fluctuations,  
200 led to the formation in the Crotona Peninsula of five orders of marine terraces in the Crotona Peninsula along the Ionian  
201 coast of Calabria (Palmentola et al., 1990; Westaway, 1993; Westaway and Bridgland, 2007; Santoro et al., 2009;

202 **Faccenna et al., 2011; Bracchi et al., 2014; Santagati et al., 2024), -Zecchin et al. (2004) recognized five orders of terraces**  
 203 **in the Crotone peninsula, considering a regional uplift of 0.70–1.25 m/ky. The terraces are spread out along the southern**  
 204 **Crotone area and are unconformably transgressive on which unconformably overlie the Piacenzian–Calabrian marly clays**  
 205 **of the Cutro Formation (Zecchin et al., 2004).**

206 **The Cutro Terrace (1<sup>st</sup> order terrace), represents the oldest and most elevated terrace in the Crotone area, and has been**  
 207 **ascribed to MIS 7 (ca 200 kyr) (Zecchin et al., 2011). It is a mixed marine to continental terrace, consisting of the products**  
 208 **resulting from the succession of two different sedimentary cycles: i) carbonate sedimentation, transitioning into algal**  
 209 **build-ups and biocalcarenite passing into shoreface and foreshore sandstones and calcarenite; ii) predominantly**  
 210 **siliciclastic sediments, comprising shoreface, fluvial channel fill, lagoon–estuarine and lacustrine deposits (Zecchin et al.,**  
 211 **2011). ascribed to MIS 7 by Zecchin et al. (2011), is a mixed marine to continental terrace, consisting of the products of**  
 212 **carbonate (algal build-ups and biocalcarenite passing into shoreface and foreshore deposits) to siliciclastic (shoreface,**  
 213 **fluvial channel fill, lagoon–estuarine and lacustrine deposits) sequences (Zecchin et al., 2011).**

214 **The 2<sup>nd</sup> order is represented by the Campolongo–La Mazzotta terrace, ascribed to MIS 5e by Maunz and Hassler (2000).**  
 215 **These deposits are mainly composed of bioclastic and hybrid sandstones westward and by mostly siliciclastic sandstones**  
 216 **eastwards. Bioclastic deposits and local algal patch reefs, which also contain small colonial corals, are found on La**  
 217 **Mazzotta Hill (Zecchin et al., 2011). (MIS 5e), represented by the Campolongo–La Mazzotta terrace, is characterized by**  
 218 **bioclastic and siliciclastic sandstones, with local bioclastic deposits and algal patch reefs (Maunz and Hassler, 2000,**  
 219 **Zecchin et al., 2011).**

220 **The Le Castella–Capo Cimiti terrace (3<sup>rd</sup> order terrace), was probably associated to the MIS 5c (Maunz and Hassler, 2000;**  
 221 **Zecchin et al., 2004; Nalin et al., 2012). The upper Pleistocene cover thins down northward of Capo Cimiti, along the**  
 222 **present coastline, and is located between 10 m and 65 m of elevation due to normal fault displacement. Carbonate**  
 223 **sediments, represented primarily by algal reefs and secondarily by bioclastic to hybrid sandstones, extensively occur in**  
 224 **the eastern and central parts of the terrace. To the west, bioclastic deposits of lower to upper shoreface environments**  
 225 **dominate (Zecchin et al., 2004; Nalin et al., 2012). probably associated to the MIS 5c (Maunz and Hassler, 2000), shows**  
 226 **extensive algal reefs and shoreface deposits, with elevations variation due to normal fault displacement (Zecchin et al.,**  
 227 **2004; Nalin et al., 2012).**

228 **The Capo Colonna marine terrace (4<sup>th</sup> order terrace), consists of a planar surface gently inclined eastward, with a**  
 229 **sedimentary cover quite continuously exposed along the northern coast of the promontory and covered, in its proximal**  
 230 **segment, by a wedge of colluvium tapering eastward (Bracchi et al., 2014). The terrace deposits correlate either with MIS**  
 231 **5.3 (ca 100 ka; Palmentola et al., 1990; Zecchin et al., 2004, 2009), or MIS 5.1 (ca 80 ka; Gliozzi 1987; Belluomini et al.,**  
 232 **1988; Nalin et al., 2006; Nalin & Massari, 2009). correlated to MIS 5.3 (Palmentola et al., 1990; Zecchin et al., 2004,**  
 233 **2009), or MIS 5.1 (ca 80 ka; Gliozzi 1987; Belluomini et al., 1988; Nalin et al., 2006; Nalin & Massari, 2009), consists**  
 234 **of a planar surface with a sedimentary cover overlaid by a wedge of colluvium tapering (Bracchi et al., 2014).**

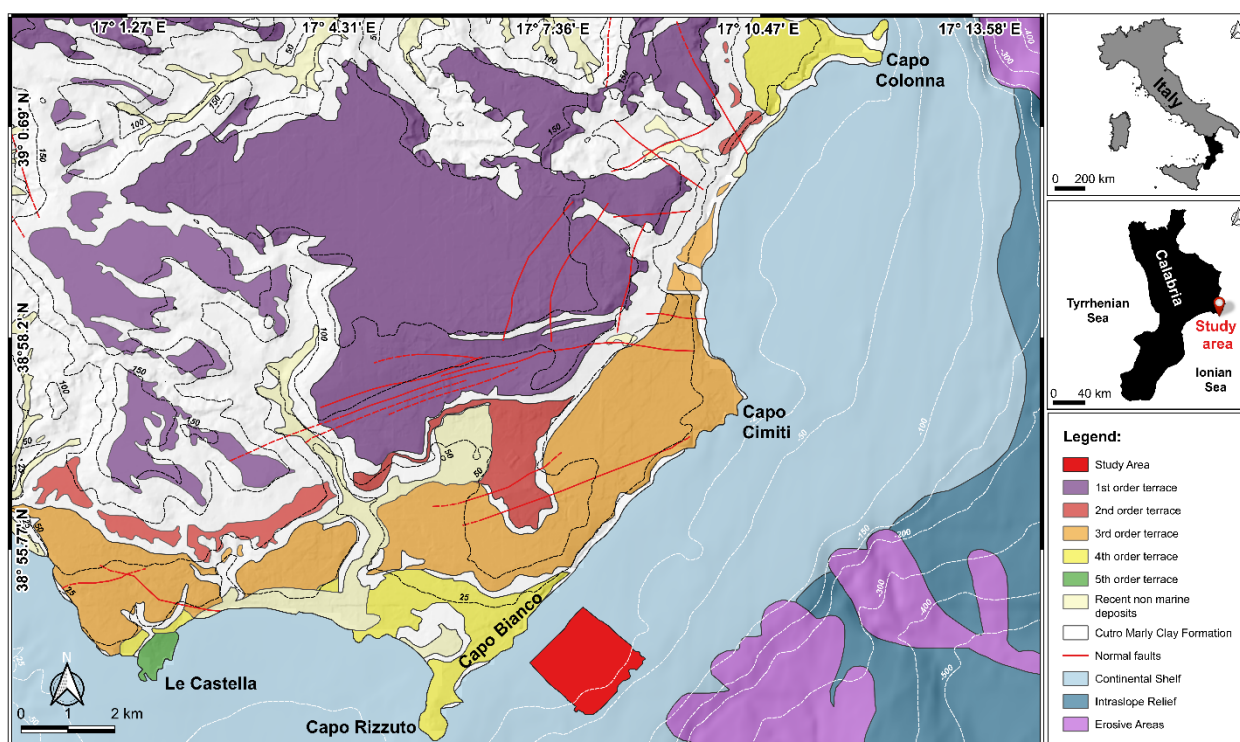
235 **The Le Castella marine terrace (5<sup>th</sup> order terrace) is the youngest. Its deposits, exceptionally well exposed along present–**  
 236 **day coastline, form an unconformity bounded, transgressive–regressive cycle, similar to those observed in other terraces**  
 237 **of the Crotone area (Nalin et al., 2007; Nalin & Massari, 2009; Zecchin et al., 2010; Bracchi et al., 2014; Bracchi et al.,**  
 238 **2016). Zecchin et al. (2004, 2010) identified two different facies for coralline algal build-ups and associated bioclastic**  
 239 **deposits in the lower portion of the cycle. The age of the Le Castella marine terrace deposits remains debated: indeed,**  
 240 **these deposits have been correlated with MIS 5.3 (Gliozzi, 1987), MIS 5.1 (Palmentola et al., 1990) and MIS 3 (Zecchin**  
 241 **et al., 2004; Mauz & Hassler, 2000; Santagati et al., 2024). records an unconformity-bounded transgressive–regressive**  
 242 **cycle (Nalin et al., 2007; Nalin & Massari, 2009; Zecchin et al., 2010; Bracchi et al., 2014; Bracchi et al., 2016), with two**



243 different facies for coralline algal build-ups and associated bioclastic deposits in the lower portion (Zecchin et al., 2004,  
 244 2011). The age of these deposits remains debated, as they have been correlated with MIS 5.3 (Gliozzi, 1987), MIS 5.1  
 245 (Palmentola et al., 1990) and MIS 3 (Zecchin et al., 2004; Mauz & Hassler, 2000; Santagati et al., 2024).

246 The marine terraces exposed in emerged portion near the study area demonstrated extensive carbonate production due to  
 247 the development of algal bioconstruction throughout the Late Pleistocene. This production also appears to currently affect  
 248 the seafloor. However, although the onshore portion of the CB has been well studied, its offshore extension is still less  
 249 known (Pepe et al., 2010). Nevertheless, data from the MaGIC Project related to Sheet 39 “Crotona” covered a vast area  
 250 extending from the Neto Submarine Canyon to the Capo Rizzuto Swell. In this section, the continental shelf reaches up  
 251 to 7 km wide, with the shelf break located at depths of 80–120 m. The slope encompasses the southern portion of the Neto  
 252 Canyon headwall and the Esaro Canyon along with its tributaries. The average continental slope gradient is less than 5°  
 253 and is characterised by an undulating morphology including the Luna and the Capo Rizzuto Swell. The southern section  
 254 of the sheet covers the offshore extension of the Crotona forearc basin (Chiocci et al., 2021). This work aims to enhance  
 255 the understanding of the Crotona Basin offshore features, with focus on underwater bioconstructed habitats.

256



257

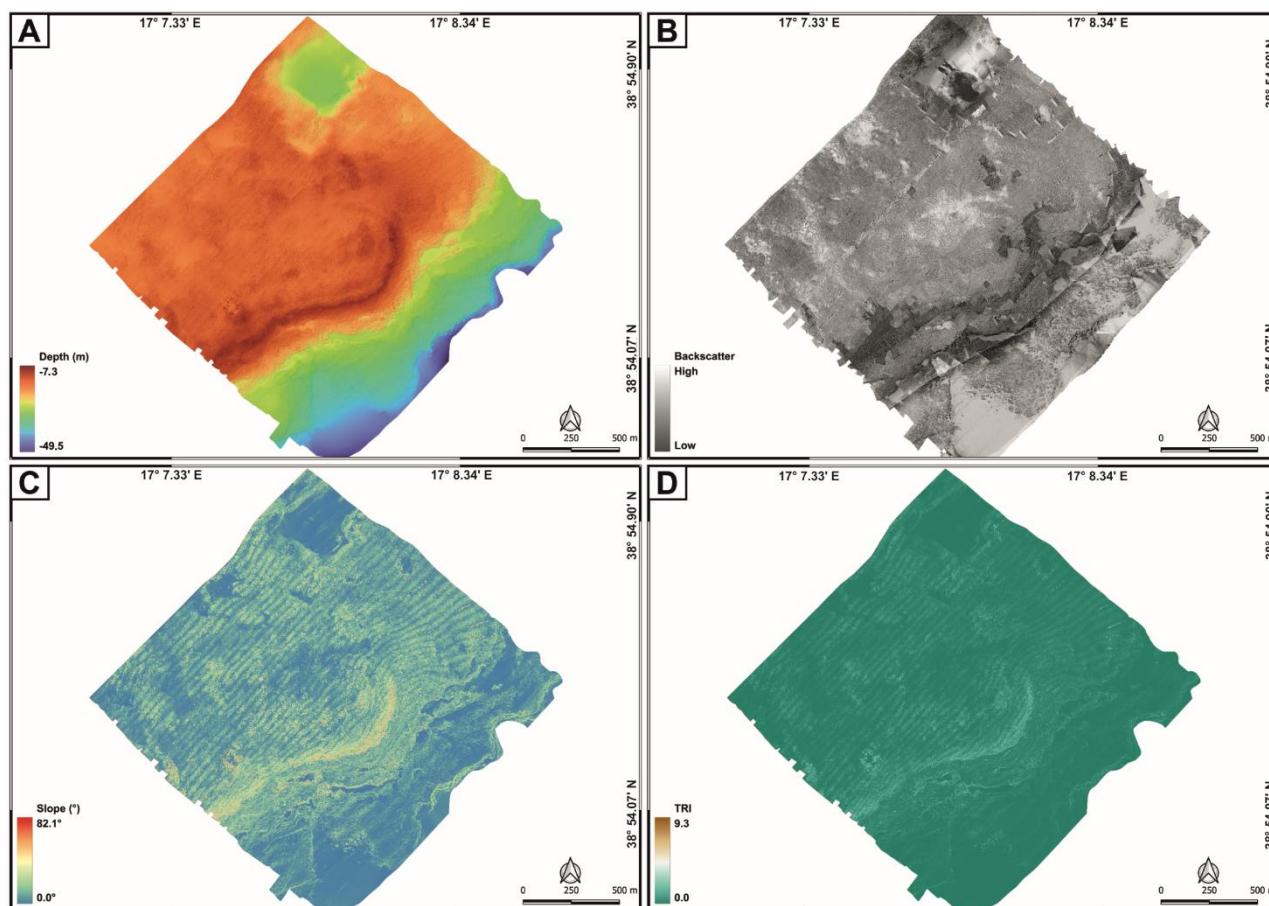
258 **Figure 3:** Conflated geological map of the Crotona peninsula, with the indication of the five order terraces (modified from Bracchi et  
 259 al., 2014), and physiographic domains identified offshore the area in the frame of the MaGIC Project (modified from Chiocci et al.,  
 260 2021).

## 261 4 Results

### 262 4.1 Morphological and morpho-acoustic characteristics of the seafloor

263 The comparison between bathymetric (Fig. 4A) and backscatter (Fig. 4B) data with those related to slope (Fig. 4C) and  
 264 seafloor roughness (Fig. 4D) allowed for the definition of the morphological and morpho-acoustic characteristics of the  
 265 study area off Capo Bianco (Calabria, Italy) and the identification of the benthic habitats. In particular, bathymetric data  
 266 revealed a seafloor with depths ranging from -7.3 m to -49.5 m (Fig. 4A). The transition towards the deeper areas is not  
 267 gradual but shows an evident break in slope (starting from about -15m depth), especially in the central zone of the study

268 area. The shallower portion is characterized by widespread irregularities, while the deeper areas appear generally more  
 269 regular, with less pronounced variations. Slope analysis (Fig. 4C) reveals maximum values (up to about 80°) along the  
 270 break in slope, highlighting a steep and well-defined margin. The surrounding areas show lower slopes, with scattered  
 271 peaks associated with seafloor irregularities. The Terrain Ruggedness Index showed: i) a higher roughness along the break  
 272 in slope (where the highest TRI values were recorded) and in its immediate vicinity; ii) the presence of scattered roughness  
 273 associated with irregularities on the seafloor (Fig. 4D).  
 274

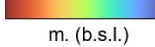


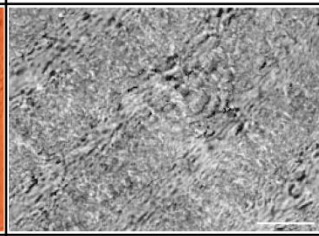

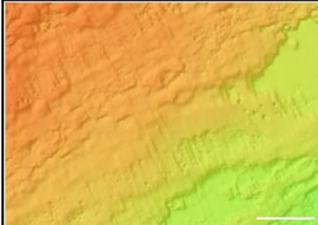
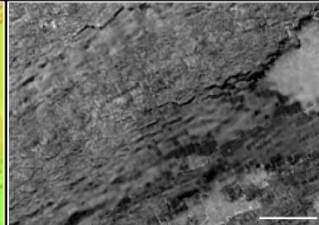


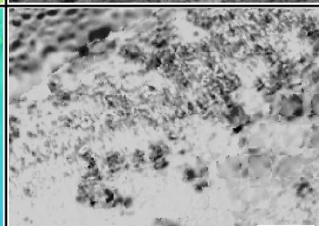

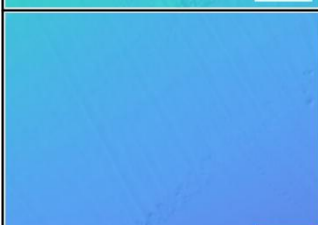
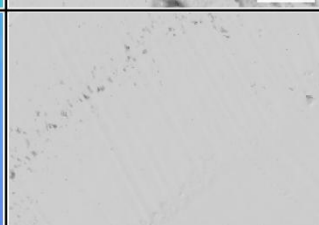



275  
 276 **Figure 4:** Geomorphological characters of the study area expressed through processed bathymetric (A), backscatter (B) data and  
 277 geomorphometric indices, like slope (C) and Terrain Roughness Index (D).

278 Combining bathymetric and backscatter (Fig. 4B) data with slope and seafloor roughness values, different morpho-  
 279 acoustic features were identified (Fig. 5):

- 280 - *Posidonia oceanica* meadows, characterized by an intermittent speckled fabric of moderate backscatter.  
 281 *Posidonia* covers seabed areas characterized by low slopes and slight roughness, spanning a depth range from  
 282 about -6 m to -25 m. In the depth range from -15 m to -25 m, analysis of ROV-video transects showed that  
 283 *Posidonia* meadow forms a mosaic with the coralligenous habitat;
- 284 - banks of Coralligenous, characterized by a complex fabric of moderate to low backscatter. They covered areas  
 285 characterized by moderate to high slopes and medium to high roughness, spanning a depth range from about -  
 286 15 m to -25 m;
- 287 - discrete coralligenous build-ups surrounded by medium to coarse sediment and maerl are characterized by a  
 288 dotted pattern of moderate backscatter. They covered areas characterized by low slopes and medium roughness

- and occupy the area between the end of the banks and the final depth of the MBES survey, at approximately -40 m depth;
- fine to medium sediment, characterized by homogeneous pattern of medium to high backscatter. It covers scattered portions throughout the study area at various depths and is characterized by very low TRI values.

Bathymetry -7.33  -49.51 m. (b.s.l.)	Backscatter High  Low	Seabed image (ROV–video transects)	Seabed Description
			<i>Posidonia oceanica</i> developing on sub–spherical rocky blocks
			Banks of Coralligenous partly covered with <i>Posidonia Oceanica</i>
			Discrete coralligenous build–ups surrounded by medium to coarse sediment and maerl
			Fine to medium sediment

**Figure 5:** Morpho–acoustic features identified by bathymetric and BS data, together with ROV videos interpretation. White scale bar is 20 m.

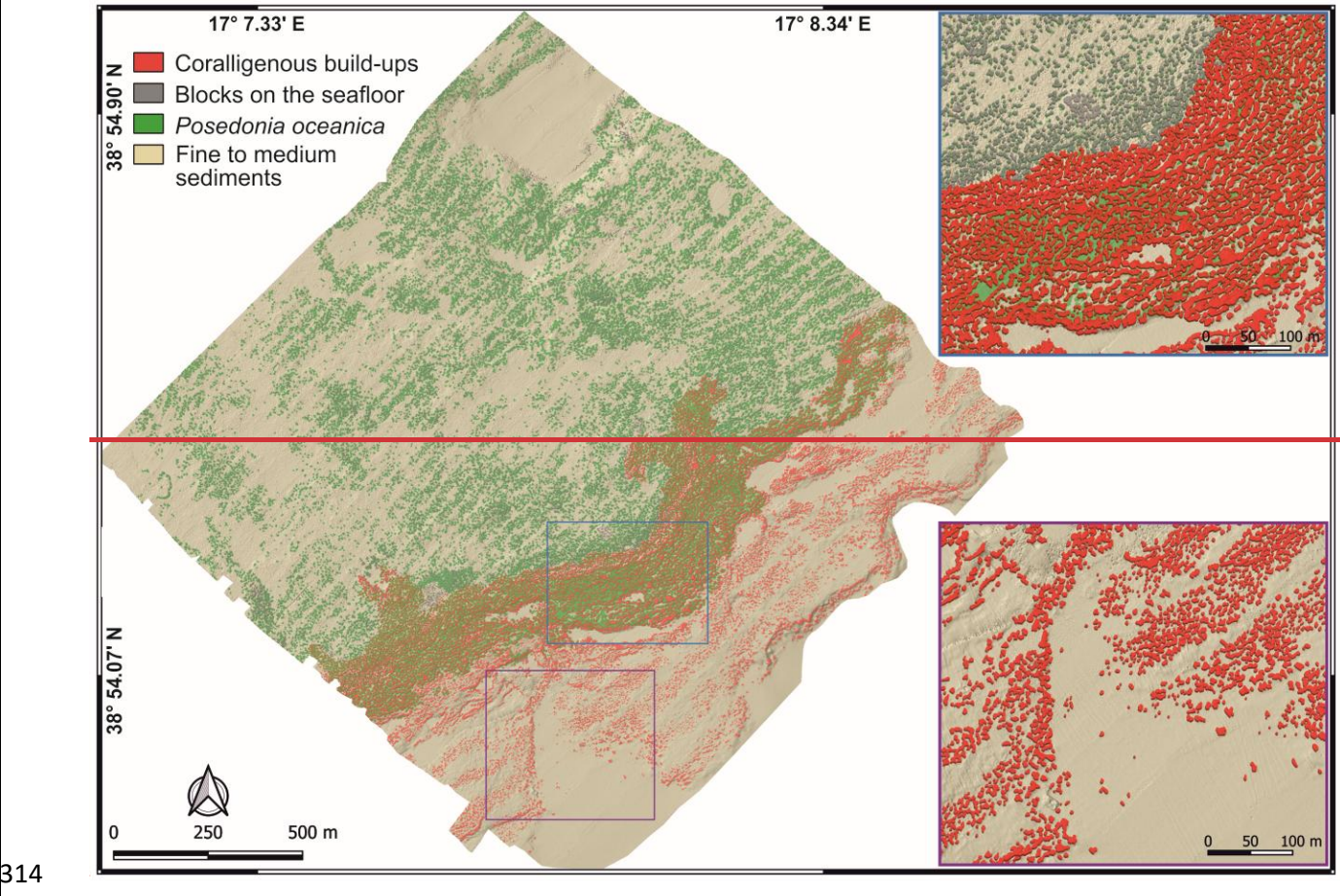
The combination of the various morpho–acoustic features enabled the identification of four main benthic habitats (Fig. 6): i) *Posidonia oceanica* meadows; ii) mosaic of coralligenous and *Posidonia*; iii) Coralligenous *sensu stricto* (*i.e.*, bioconstructions that are not spatially intermixed with *Posidonia oceanica*); iv) fine to medium sediment.

The *Posidonia* habitat, testified by its typical BS signal (intermittent speckled fabric of moderate backscatter), dominate in shallow areas (down to about -15 m depth), where it primarily colonizes rocky substrate. In this area, ROV imagery and bathymetric data also highlight the occurrence of sub-spherical rocky blocks on the seabed, often surrounded by *Posidonia oceanica* (Fig. 5).

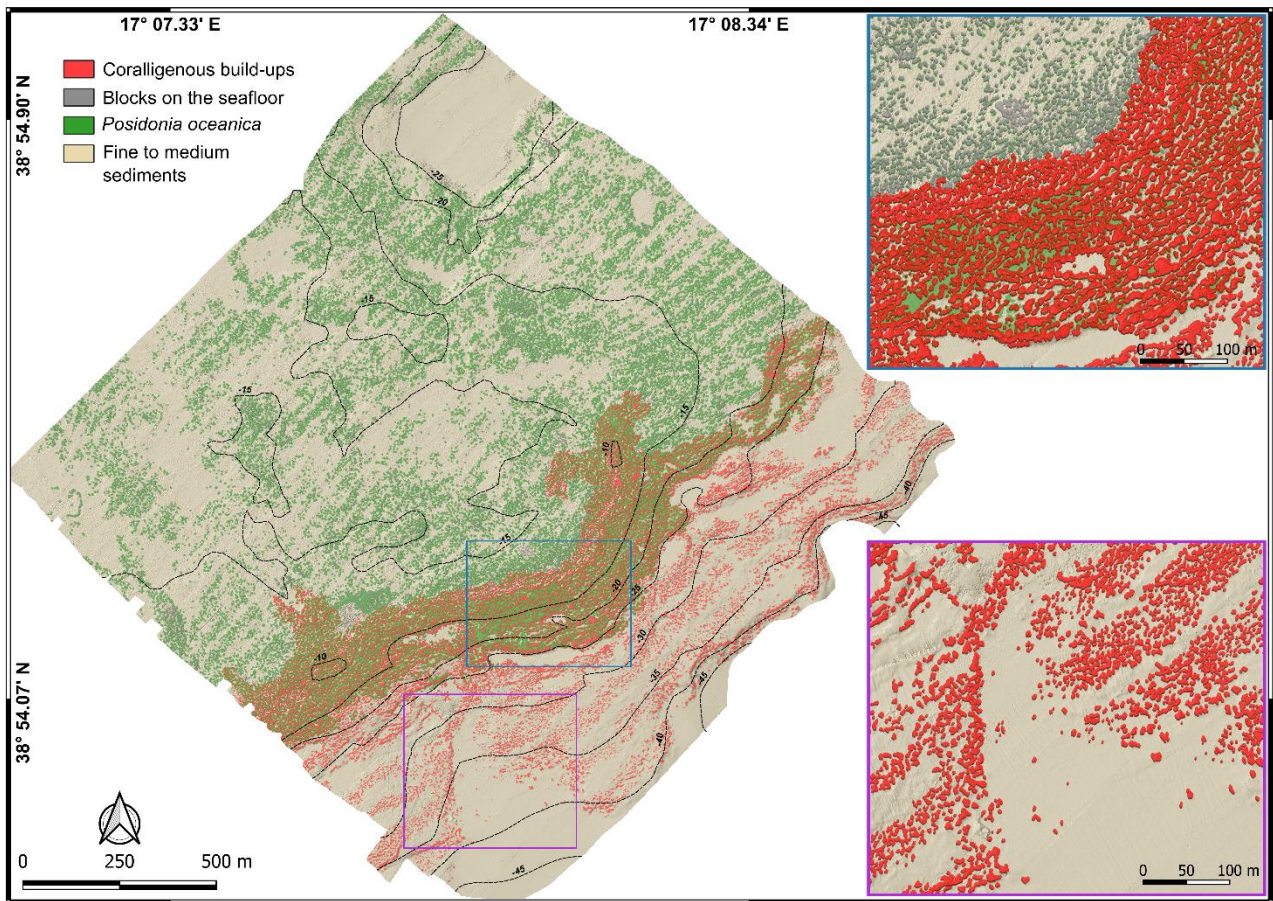
Between -15 m and -25 m, the *Posidonia* backscatter signal gradually attenuates and coralligenous bioconstructions start to be discernible. This transitional belt, that occupies about 0.37 km<sup>2</sup>, was classified as a mosaic of Coralligenous and *Posidonia oceanica*. Visual analysis of ROV-video transects, used as ground-truth, indicates that in this zone



308 bioconstructions, mainly belonging to the banks morphotype, develop on a hard substrate that marks the widespread break  
309 in slope throughout the study area.  
310 Below -25 m, *Posidonia* is no longer detected and the predominant benthic habitat is represented by Coralligenous *sensu*  
311 *stricto*. These bioconstructions, often associated with fine to medium sediment and maerl, predominantly belong to the  
312 discrete reliefs morphotype and tend to align sub-parallel to the shoreline.  
313







**Figure 6:** Mapping model of the underwater benthic habitats in the study area off Capo Bianco (Calabria, Italy). Note, in the blue and purple boxes, two magnifications of representative areas of the model where coralligenous bioconstructions and rocky blocks on the seabed are depicted in 2.5D.

## 4.2 Extraction of coralligenous build-ups

The model extracted 12384 polygons, but only 9211 positive morphologies were finally related to coralligenous build-ups considering the hillshade values and validation from ROV-video transects collected within the study area (Fig. 7A). This means that about 25 % of the polygons extracted using the TPI were found to be artifacts and manually deleted after the re-classification and the polygonization of resulting raster. According to Marchese et al. (2020), the artifacts may be due to: i) occurrence of *Posidonia oceanica* (Innangi et al., 2015) (Fig. 8A); ii) bad roll correction (Fig. 8C), creating false elongated structures; iii) artifacts concentration on DTM boundaries (Fig.8E). While artifacts of types ii) and iii) can be reduced by performing more accurate MBES surveys (*i.e.*, larger coverage, greater overlapping, and narrower swath width), those related to *Posidonia oceanica* represent real morphological features that cannot be removed by improving survey quality. The identification of artifacts was based on specific pattern inconsistent with expected Coralligenous morphologies, and their removal was carried out manually as part of the data cleaning process (Fig. 8B, D, F). The time required for the cleaning phase strongly depends on the quality of the survey execution, the geomorphological and ecological complexity of the study area and the experience of the operator performing the cleaning. These factors can significantly influence the extent and efficiency of manual artifact removal.



335 Regarding the distinction between coralligenous bioconstructions and *Posidonia oceanica* in the mosaic area, the  
 336 separation was primarily based on the characteristics of the backscatter signal. Specifically, as discussed previously,  
 337 *Posidonia* is associated with a moderate, speckled acoustic texture, while coralligenous bioconstructions exhibit a more  
 338 complex and spatially structured acoustic signature. These interpretations were supported by ROV video transects, which  
 339 help to validate the differentiation.

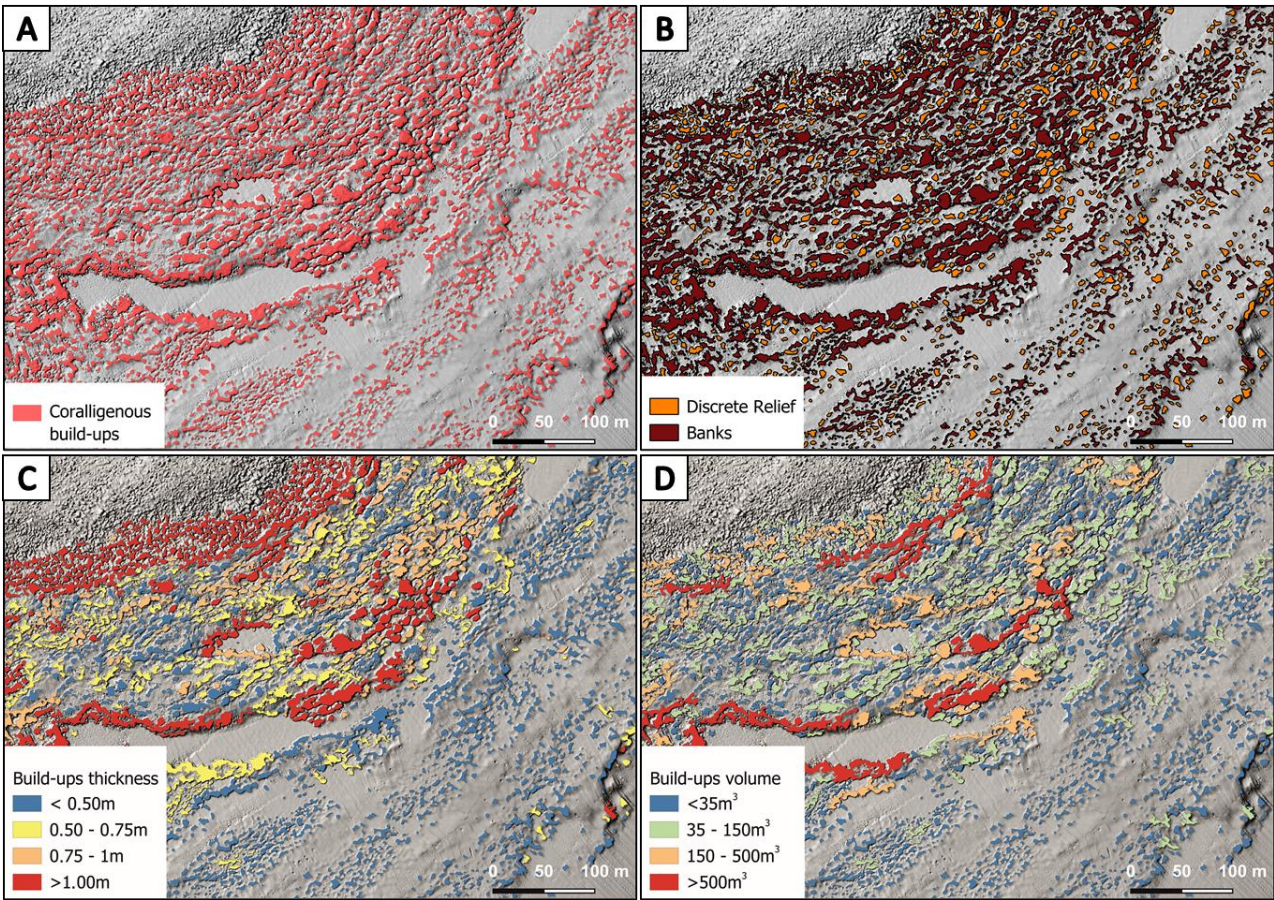
340 ~~Naturally, the time consuming operation of filtering and manually detecting erroneous polygons could be avoided~~  
 341 ~~performing more accurate MBES surveys (i.e., larger coverage, greater overlapping and narrower swath width) free of~~  
 342 ~~artifacts.~~

343

#### 344 4.3 Shape index, thickness, surface and volume of coralligenous build-ups

345 Shape Index (SI) values allowed to distinguish between banks (tabular bank *sensu* Bracchi et al., 2016;  $SI \leq 2$ ) and discrete  
 346 reliefs (discrete reliefs and hybrid banks *sensu* Bracchi et al., 2016;  $SI > 2$ ) (Fig. 7B). Following this approach, it was  
 347 possible to identify 7001 polygons belonging to the morphotype of the banks and 2210 classified as discrete reliefs. As  
 348 shown in Table 1, banks have a greater average thickness (Fig. 7C) compared to discrete reliefs (0.65 m vs 0.49 m,  
 349 respectively) and cover an area of 155677 m<sup>2</sup>, which represents about 5.2 % of the seabed in the study area. In contrast,  
 350 discrete reliefs cover only 2.6 % of the seafloor, with a surface area of 69830 m<sup>2</sup>. The volume (Fig. 7D) occupied by  
 351 discrete reliefs (40806 m<sup>3</sup>) is also significantly lower than that of the banks (116094 m<sup>3</sup>). This data is consistent with the  
 352 fact that discrete reliefs are characterized by smaller extent and thickness compared to the banks.

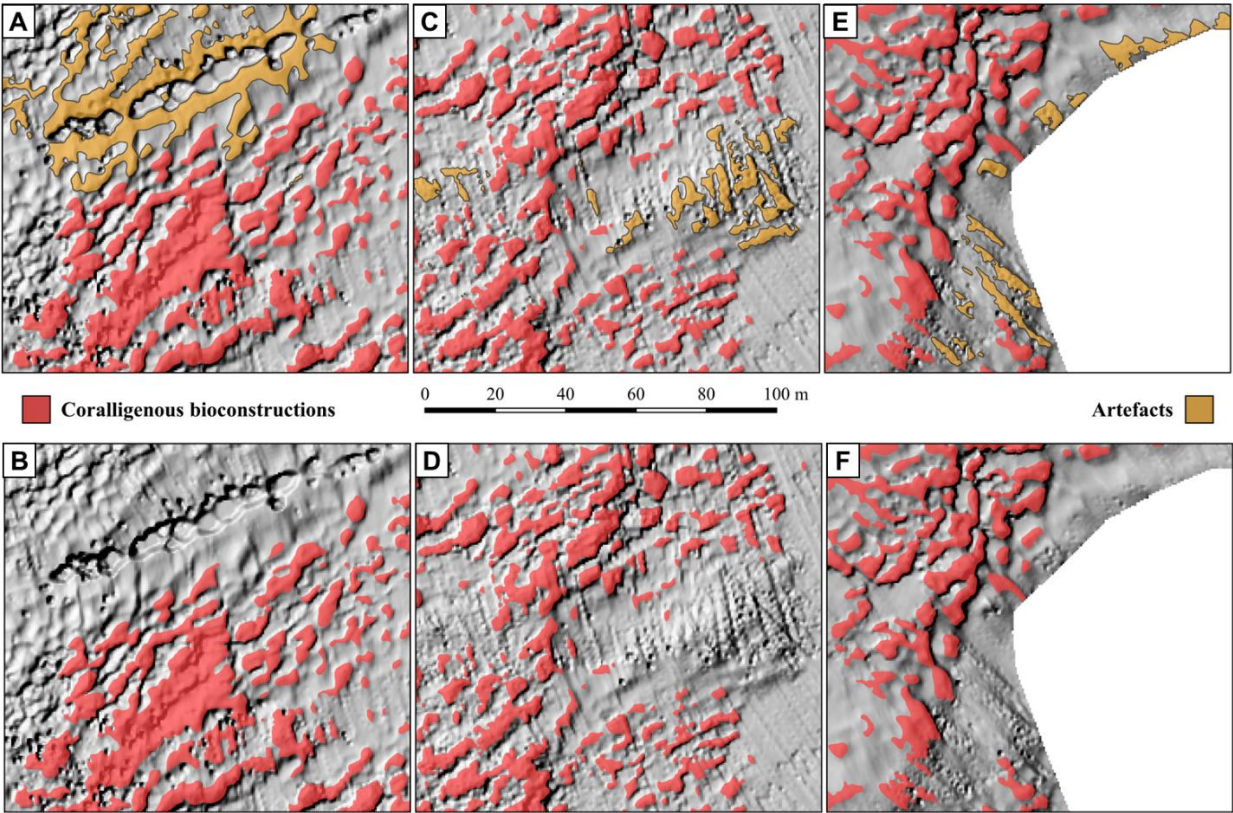
353



354



355 **Figure 7:** (A) Result of build-ups extraction using TPI. (B) Differentiation of coralligenous build-ups into discrete relief and banks based on the SI value. (C) Estimation of build-ups thickness. (D) Calculation of the volume for each coralligenous polygon.



358 **Figure 8:** Examples of artifacts identified during polygon extraction and their manual removal. (A) False positive caused by the presence of *Posidonia oceanica* and (B) the same area after removal; (C) artifact due to bad roll correction and (D) corrected version; (E) artifacts at the boundary of the DTM and (F) cleaned result.

361 **Table 1:** Classification of coralligenous polygons, based on SI values, and results in terms of area and volume.

Morphotype	Shape Index Values	Average Thickness (m)	Area (m <sup>2</sup> )	Volume (m <sup>3</sup> )
Banks	$\leq 2$	0.65	155677	116094
Discrete Reliefs	$> 2$	0.49	69830	40806

## 363 5 DISCUSSION

364 Acoustic techniques, such as high-resolution swath bathymetry sounder (including backscatter), side scan sonar and  
 365 acoustic profiling are optimal tools for quickly recognize and identify the extension of benthic habitats on the seabed and  
 366 map their distribution without mechanical collection of samples, which would damage this delicate ecosystem (Bracchi  
 367 et al., 2017).

368 Conventionally, the segmentation of MBES data sets is carried out manually, despite the process might be inaccurate and  
 369 subjective (Cutter et al., 2003; Bishop et al., 2012). Only few studies have successfully developed object-oriented  
 370 methods that use object-based image analysis (OBIA) or consider a comprehensive set of remote data to accurately  
 371 characterize seabed landforms to document the extension of benthic habitat (Lucieer and Lamarche, 2011; Ismail et al.,  
 372 2015; Janowski et al., 2018; Fakiris et al., 2019). However, geomorphometric techniques can objectively characterize  
 373 submarine habitat and features from the shallow to deep environments (Lecours et al., 2016; Janowski et al., 2018), but a  
 374 standardized technique for seafloor classification has never been developed (Micallef et al., 2012). Recently, Marchese et

al. (2020) proposed a protocol that combines acoustic datasets and geomorphometric analysis, performed using ArcGIS™, in order to define the 2D and 3D complexity of coralligenous build-ups on a sector of the Apulian continental shelf and to quantify how much carbonate is deposited.

Traditionally, the segmentation of MBES data sets have been performed manually, despite the process might be inaccurate and subjective (Cutter et al., 2003; Bishop et al., 2012). Initial attempts at automation employed object-oriented methods using object-based image analysis (OBIA) or considered a comprehensive set of remote data to accurately characterize seabed landforms for documenting the extension of benthic habitat (e.g., Lucieer and Lamarche, 2011; Ismail et al., 2015; Janowski et al., 2018; Fakiris et al., 2019). More recently, the growing availability of high-resolution MBES data has encouraged the application of deep learning approaches, particularly Convolutional Neural Networks (CNNs) and Fully Convolutional Neural Networks (FCNNs), which produce pixel-wise classifications in order to create semantically segmented maps. These methods have proven effective in identifying geomorphological features such as bedrock outcrops, pockmarks, submarine dune and ridges, offering high accuracy and repeatability (Arosio et al., 2023; Garone et al., 2023). Additionally, 3D CNNs have been applied to automated denoising of MBES data, enhancing the efficiency of bathymetric data workflow (e.g., Stephens et al., 2020).

Nonetheless, a universally accepted and standardized methodology for geomorphological classification of the seafloor is still lacking. Indeed, existing approaches remain highly case-specific, depending on the study area, data quality, and research objective. Moreover, relatively limited attention has been devoted to the morphological characterization of Coralligenous bioconstructions, despite their ecological relevance. Indeed, only a few studies have attempt to map these complex biogenic structures in detail. Bracchi et al. (2017) proposed a categorization of coralligenous morphotypes on sub-horizontal substrate based on integrated acoustic data and ground-truthing, defining new morphological classes such as tabular banks, hybrid banks and discrete reliefs across the Apulian shelf. Subsequently, Marchese et al. (2020) proposed a protocol that combines acoustic datasets and geomorphometric analysis, performed using ArcGIS™, in order to define the 2D and 3D complexity of coralligenous build-ups and to quantify how much carbonate is deposited. More recently, Varzi et al. (2022) produced a morpho-bathymetric map for the continental shelf offshore Marzamemi (Sicily, Italy) that contained quantitative description for the distribution and extent of coralligenous reefs.

The mapping protocol approach proposed in this work, based on the workflow shown in Figure 2 3, represents the first attempt to define the benthic habitat in the Isola Capo Rizzuto Marine Protected Area and to quantify the extent and morphometric characteristics of coralligenous bioconstructions present therein using exclusively open-source software during post-processing phases.

## 5.1 Detected habitats-Spatial distribution of benthic habitats and seafloor morphology

The comparison between the bathymetric and backscatter data with the indices derived in QGIS and the model validation through ROV video transects allowed to identify several habitats: *Posidonia oceanica* meadows, mosaic of coralligenous and *Posidonia*, Coralligenous sensu stricto, and fine to medium sediment.

The *Posidonia* habitat, testified by its typical BS signal (intermittent speckled fabric of moderate backscatter), was recognised down to 25 m water depth. *Posidonia oceanica* habitat dominate in shallow areas, down to about 15 m depth, developing primarily on rocky substrate. The seafloor is characterized by the presence of sub-spherical rocky blocks (Fig. 6), which possibly result from gravitational processes affecting the 4<sup>th</sup> order terrace emerging landwards, and pockets of fine to medium sediments.



414 From 15 m to 25 m, *Posidonia* BS signal gradually attenuates and Coralligenous bioconstructions start to be discernible.  
 415 This transitional belt, that occupies about 0.37 km<sup>2</sup>, was classified as mosaic of Coralligenous and *Posidonia*. The visual  
 416 analysis of the ROV video transects, used as ground truth, suggests that in this zone bioconstructions, which  
 417 predominantly belong to the banks morphotype develop on a hard substrate that marks a widespread break in slope all  
 418 throughout the study area. This break marks the end of the transition zone, characterized by the simultaneous presence of  
 419 Coralligenous and *Posidonia*.  
 420 By comparing the morphological characteristics of the seabed with the alignment of the emerged marine terraces, the  
 421 presence of an additional submerged terraced surface becomes evident. It could represent a submerged portion of the 5<sup>th</sup>  
 422 order terrace, currently exposed only in the Le Castella area. The submersion of this portion of the terrace in the study  
 423 area would be justified by the presence of a tectonic feature with extensional kinematics, located approximately along the  
 424 coastline, which, in this area, shows a distinctly straight alignment with a N-S orientation. Further studies, focusing on  
 425 the geological characterization of the substrate on which coralligenous banks developed and the correlation of these  
 426 lithotypes with those outcropping on land, could confirm this hypothesis.  
 427 Deeper than 25 m, upon close MBES data and ROV inspection, *Posidonia* disappears and the predominant benthic habitat  
 428 is represented by Coralligenous sensu stricto. Bioconstructions, often associated with fine to medium sediment and maerl,  
 429 predominantly belong to the morphotype of discrete reliefs. Bioconstructions tend to align sub-parallel to the shoreline.  
 430 This distribution is associated with the presence of relatively pronounced seafloor structures, as revealed by ROV video  
 431 transects. This observation might suggest: i) a significant control of hydrodynamic conditions on the formation,  
 432 development and distribution of coralligenous build-ups, or ii) an overprint of the bioconstructions on a seafloor already  
 433 sculpted by the evolution of the bottom during glacial/interglacial cycles. However, further investigation is needed,  
 434 including bottom current monitoring using appropriate instruments (e.g., current meter), in order to better define these  
 435 bedforms.  
 436 The benthic habitat distribution identified in the study area exhibits a clear spatial zonation, which appear to be influenced  
 437 by both substrate characteristics and geomorphological features. In the shallowest sector (above -15m depth), *Posidonia*  
 438 *oceanica* represent the prevalent benthic habitat. In the intermediate depth range (down to approximately -25m depth), a  
 439 mosaic of *Posidonia* and coralligenous bioconstructions develops, indicating a transitional zone where environmental  
 440 conditions allow the coexistence of seagrass and algal reefs.  
 441 Comparison between the morphological characteristics of the seabed with the alignment and elevation of the emerged  
 442 marine terraces highlights the presence of a flat, laterally continuous submerged surface, as typically observed in relict  
 443 marine terraces (e.g., Savini et al., 2021; Lebrec et al., 2022). This sub-horizontal platform is bounded seaward by a break  
 444 in slope, located at approximately -15 m depth, interpreted as the outer margin of the terrace. Based on these evidences,  
 445 the submerged surface can be correlated with the 5<sup>th</sup> order terrace exposed near Le Castella, characterized by a gently  
 446 seaward-inclined surface and a morphological step interpreted as paleocliff (Bracchi et al., 2016). The different orientation  
 447 of the submerged scarp in the study area (NE-SW), compared to the emerged paleocliff associated with Le Castella marine  
 448 terrace (NW-SE to E-W), may be reasonably attributed to local coastal curvature and/or tectonic influences. The  
 449 submersion of this portion of the 5<sup>th</sup> order terrace in the study area would be justified by the possible presence of a tectonic  
 450 feature with extensional kinematics located approximately along the coastline, which shows a distinctly straight alignment  
 451 with a N-S orientation. However, further investigations are needed to confirm this hypothesis.  
 452 The inner portion of the submerged surface is characterized by the presence of sub-spherical blocks, often colonized by  
 453 *Posidonia oceanica*, which possibly result from gravitational processes affecting the adjacent 4<sup>th</sup> order marine terrace  
 454 located upslope. This interpretation is supported by their rounded morphology, typically associated with detachment and

downslope transport, and by the presence of scarps in the emerged portion of the study area, which could indicate past gravitational instability.

The outer portion and the edge of the submerged platform (down to approximately -25m) hosts several coralligenous build-ups, predominantly belonging to banks morphotype. Similar spatial arrangements have been observed in submerged terraces of southeastern Sicily (Varzi et al., 2022) and on wave-cut ravinement surfaces associated with fossil marine terraces, such as the mid-Pleistocene Cutro terrace (Nalin et al., 2006) and the emerged 5<sup>th</sup> order terrace of Le Castella (Bracchi et al., 2016).

In the deeper sector of the study area (below -25m depth), *Posidonia* is no longer present and the benthic assemblages are composed by Coralligenous *sensu stricto* associated with fine to medium sediments and maerl. These bioconstructions mainly belong to discrete reliefs morphotype and tend to follow a sub-parallel orientation relative to the shoreline, a distribution pattern that appears associated with relatively pronounced seafloor structures (as revealed by ROV-video transects). This spatial configuration suggests that environmental or geomorphological factors may influence the development and positioning of build-ups. Particularly, two hypotheses are proposed to explain this pattern: i) the influence of bottom currents and internal waves, which may promote the alignment of coralligenous bioconstructions, as observed in mesophotic carbonate systems of the Maltese shelf by Bialik et al. (2024); ii) an overprint of the build-ups onto inherited seabed morphologies, shaped by sea-level fluctuation and regional uplift during the Quaternary glacial/interglacial cycles, as documented on submerged terraces offshore Marzamemi (SE Sicily) by Varzi et al. (2022). However, further investigations, including in situ hydrodynamic and sediment transport measurements, are necessary to validate these hypotheses.

## 5.2 TPI-based feature extraction

Coralligenous build-ups were treated as distinct features in both two- and three-dimensional spaces, with the aim of using a geomorphometric parameters for their extraction from the seafloor. Variability of coralligenous morphotypes (Bracchi et al., 2017) poses several challenges to their automated extraction from DTM. Since build-ups raise from the surrounding seafloor, their detection could be performed by slope analysis. However, while slope proves effective for accurately segmenting isolated small-scale features (Savini et al., 2014; Bargain et al., 2017), it struggles to incorporate the inner areas of banks into the segmentation process. The high 3D complexity in these areas makes it challenging to create a continuous polygon. On the other hand, geomorphometric parameters like the rugosity index (i.e., TRI; Riley et al., 1999) are more successful in defining the overall distribution of bank morphotypes, but they fail to provide an accurate estimation of the size of discrete reliefs. Therefore, as noted by Marchese et al. (2020), TPI offers a good compromise for detecting coralligenous morphotypes. Indeed, it assesses the relative topographic position of a central point by calculating the difference between its elevation and the average elevation within a predefined neighbourhood. In this work, the input parameters for the calculation of the TPI have been refined in order to minimize the artifacts during the extraction process. Specifically, the choice of a threshold value of 0.2 (lower than 0.3 used by Marchese et al., 2020), combined with higher values of Power and Bandwidth compared to the default ones, has allowed for a 15% reduction in the artifact percentage compared to Marchese et al. (2020). These adjustments have therefore significantly reduced the manual review time, improving the automatization of the extraction process.

The threshold value adopted for the TPI analysis was defined through a trial-and-error procedure, as described in the methodological section. In particular, threshold values lower than 0.2 increased the morphological adherence of the extracted features to seabed forms, but at cost of a higher number of false positives (especially in areas covered by

495 *Posidonia oceanica*, where slight topographic variations were incorrectly interpreted as relevant morphotypes).  
496 Conversely, threshold values higher than 0.2 reduced the occurrence of artifacts but led to the omission of low-relief  
497 structures, thus compromising the completeness of mapping. In this work, a threshold value of 0.2 proved to be an  
498 effective compromise, ensuring a satisfactory balance between the accuracy of morphotype extraction and the  
499 minimization of false positive. This configuration allowed for the preservation of relevant coralligenous bioconstructions,  
500 including low-relief build-ups, while significantly limiting the occurrence of artifacts.  
501 The proposed approach, although developed only for a specific coastal area, can be transferred to other regions, provided  
502 that adequate calibration is performed. The effectiveness of TPI-based extraction depends on several factors, and no  
503 universally applicable threshold value exists, as it must be adapted to the resolution and quality of bathymetric data, as  
504 well as to the site-specific geomorphological and geobiological variability. To date, no standardized procedure is available  
505 for determining the optimal threshold; however, its selection can be refined through iterative testing supported by ground-  
506 thrut validation. Once the appropriate input parameter for TPI calculation (e.g., Power, Bandwidth, minimum and  
507 maximum radius) ad a suitable threshold value are identified, the method allows for the extraction of morphologically  
508 distinct features, provided these are sufficiently expressed relative to the surrounding seafloor.

509

### 510 5.3. Morphological development of coralligenous build-ups

511 ~~Computation of maximum diameter, surface and volume for each build-up were performed using vector field operation~~  
512 ~~in QGIS. Quantitative morphometric data extracted from the proposed benthic habitat model were plotted in the~~  
513 ~~scatterplots of Figure 8.~~ The quantitative morphometric data (i.e., surface, thickness, volume, maximum diameter and  
514 shape indices), extracted from the benthic habitat mapping model proposed in this work, were plotted in the scatterplots  
515 of Figure 8, providing new insights into spatial distribution, morphotype variability and growth pattern of the  
516 coralligenous build-ups across the study area.

517 Most polygons, representing aggregates of different coralligenous build-ups, are characterized by areas smaller than 200  
518 m<sup>2</sup> and less than 1 m thick (Fig. 8A). However, discrete reliefs and banks display some differences in their distribution:  
519 discrete reliefs tend to cluster in the lower part of the graph (smaller areas and lower thickness), whereas banks with  
520 similar thickness generally exhibit larger areas on average.

521 The volume of the build-ups is strongly dependent on thickness, suggesting that vertical growth plays a key role in the  
522 formation of these structures (Fig. 8B). However, discrete reliefs show a more irregular distribution, with a greater  
523 dispersion of data ( $R^2 = 0.36$  0.35). This trend suggests that volume increase depends not only on thickness but also on a  
524 significant lateral growth component. Conversely, banks exhibit a more regular trend, with volume increasing  
525 proportionally with thickness. The strong correlation between thickness and volume ( $R^2 = 0.83$ ) aligns with a growth  
526 pattern that is almost exclusively vertical for this morphotype.

527 The relationships between area and shape indices (SI) of coralligenous build-ups (Fig. 8C), despite a moderate data  
528 dispersion, revealed a positive correlation ( $R^2 = 0.61$ ), suggesting that more irregularly shaped bioconstructions (typically  
529 associated with the morphotypes of banks) tend to cover larger areas. Moreover, banks also tend to have larger maximum  
530 diameter (Dmax), as suggested by an  $R^2$  value of 0.78 (Fig. 8D). However, the greater variability in area might reflect  
531 higher spatial complexity in the distribution of these structures.

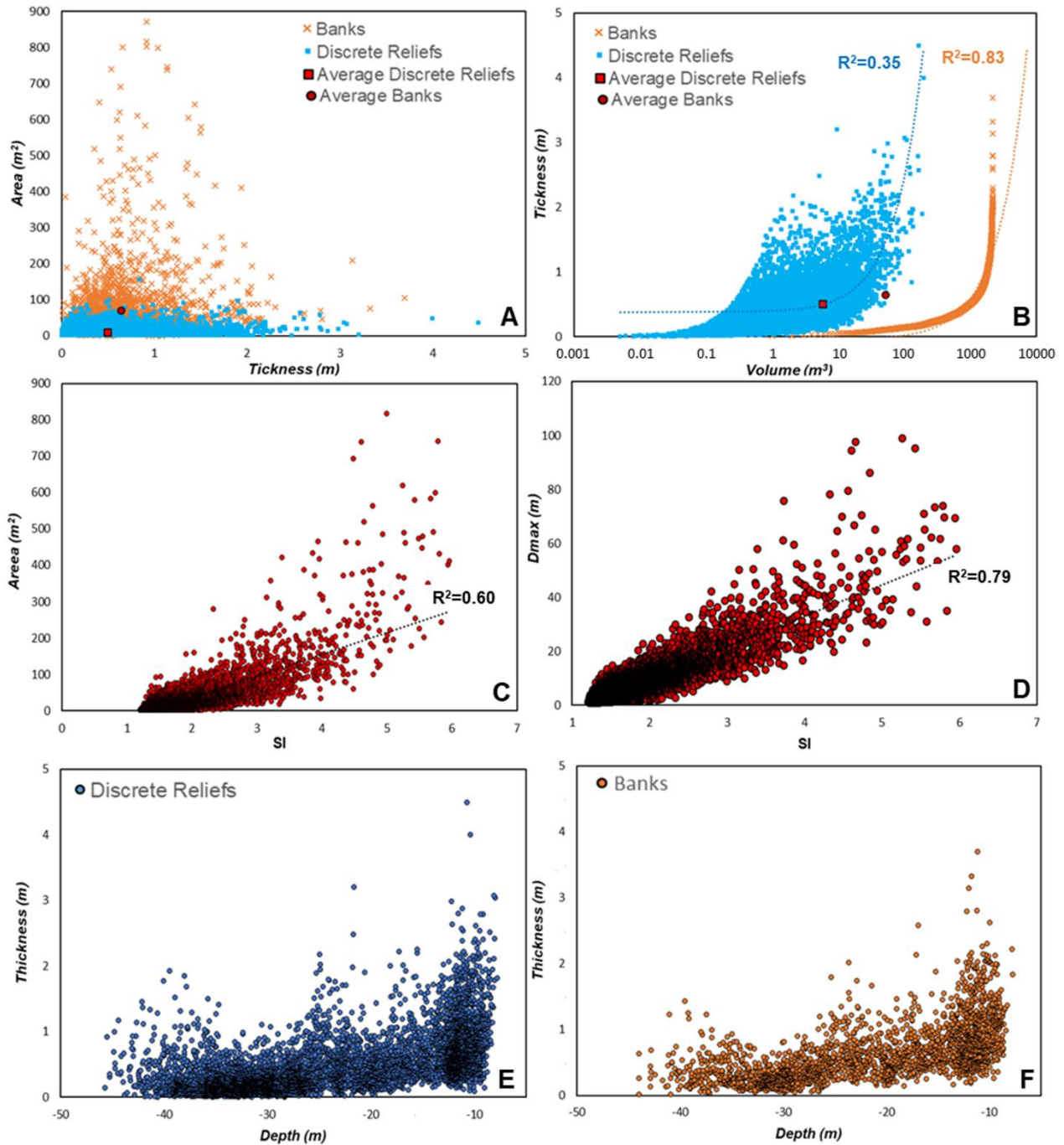
532 The relationship between depth and thickness of coralligenous bioconstructions, divided into banks (Fig. 8F) and discrete  
533 reliefs (Fig. 8E), reveals that both morphotypes exhibit average decreasing thickness with increasing depth. However,  
534 discrete reliefs show greater thickness variability, with higher dispersion of data at depths shallower than -25 m, whereas

535 for the banks, data distribution is more regular. The decrease in the thickness of bioconstructions with increasing depth  
536 could be attributed to various causes, including changes in hydrodynamic energy, the characteristics of the substrate on  
537 which the bioconstructions develop, or sedimentation conditions.

538 To date, no previous study has provided morphometric analysis of coralligenous build-ups based on quantitative extraction  
539 of 2D/3D parameters (e.g., area, thickness, volume, shape indices) from high-resolution MBES data. Therefore, a direct  
540 comparison of our results with other Mediterranean coralligenous fields is currently not possible. Nonetheless, several  
541 works have described the geomorphological variability of coralligenous morphotypes across the Mediterranean basin  
542 (e.g., Bracchi et al., 2015, 2017, 2022; Marchese et al., 2020). These studies recognize the coexistence of morphotypes  
543 such as banks and discrete reliefs, often occurring over short spatial scale and associated with different environmental  
544 conditions. The same spatial mixing of these morphotypes, which may be due to small-scale variations in substrate type,  
545 hydrodynamic regime, or inherited seabed features, which locally favour distinct growth mode despite spatial proximity  
546 (Bracchi et al., 2017; Marchese et al., 2020; Varzi et al., 2022), was also observed in our study area.

547





**Figure 8:** Scatterplot representing relationships between: area and thickness (A); thickness and volume (B); area and shape index (C); maximum diameter and shape index (D); thickness and depth for banks (E) and discrete relief (F). These quantitative geometric data were extracted by the benthic habitat mapping model proposed in this work. SI: shape index; Dmax: maximum diameter.

## CONCLUSIONS

A new mapping protocol approach starting from high-resolution acoustic data acquired through MBES surveys performed offshore Capo Bianco (Isola Capo Rizzuto Marine Protected Area) was developed and presented here. The method protocol represents a step forward, as it builds on an integrated two foundational approaches in coralligenous habitat studies: the morphotyping of Coralligenous based on the shape index, and their spatial and volumetric quantification. The innovation of this work lies in the synthesis of these methodologies, which were applied and refined in a new study area. Moreover, the approach protocol, which integrates bathymetric and backscatter data with geomorphological and

geomorphometric indices, was performed using open-source software, providing a detailed workflow that can be freely reproduced and adopted by organizations involved in research, monitoring and conservation of marine habitats. The resulting model proved capable not only in identifying and differentiating the benthic habitats but also in providing new quantitative information regarding the spatial distribution and 2D/3D geometric characteristics of the extracted coralligenous build-ups. This innovative aspect, compared to the traditional mapping protocol, is crucial for the quantification of the structural complexity of these bioconstructions. Moreover, this approach enables monitoring of variations not only in terms of the habitat's areal extent, but also in terms of vertical development of Coralligenous relative to the substrate from which build-ups form. Indeed, the quantitative geomorphometric data obtained from the mapping model of Capo Bianco seafloor were analyzed, revealing significant insights into the covered surface, volume and thickness of build-ups, as well as the relationships among these parameters. In particular, the results highlighted that the discrete reliefs morphotype exhibit a much more pronounced lateral growth component compared to the banks. If confirmed through an accurate geobiological characterization, these finding could provide important new insights about the tempo and mode of the inception and development of these hard-biogenic substrates, crucial for the conservation of Mediterranean biodiversity.

#### **Author contributions**

Conceptualization: G.M., A.G.; Methodology: G.M, A.G., G.I., F.M.; Formal analysis and investigation: G.M., M.C., G.I.; U.S.; F.M.; Writing – original draft preparation: G.M., M.C., G.V., F.P., A.L., E.C., R.S.; Writing – review and editing: R.D., C.A., F.B., V.A.B., D.B., A.R., A.G.; Funding acquisition: A.G., F.B.; Resources: R.D., F.B., A.L., E.C., A.G.; Supervision: A.G.

#### **Competing interests**

The contact author has declared that none of the authors has any competing interests.

#### **Acknowledgments**

We would like to express our sincere gratitude to the Geobiology and Marine Laboratories of the DiBEST, University of Calabria, for their invaluable support and contribution to this work.

#### **Financial support**

This work was funded by the Next Generation EU – Tech4You – “Technologies for climate change adaptation and quality of life improvement – Tech4You”, Project “Development of tools and applications for integrated marine communities and substrates monitoring”, PP 2.3.1 – Action 1 “Development of hardware and software systems for three-dimensional detection, sampling and mapping of underwater environments”, CUP H23C22000370006. This work reflects only the authors' views and opinions, neither the Ministry for University and Research nor the European Commission can be considered responsible for them.

#### **Open Research**

The data sets needed to evaluate results and conclusion in this paper are available at [http://geocube.unical.it/gmaruca/Dataset\\_Benthic\\_Habitat\\_Mapping.zip](http://geocube.unical.it/gmaruca/Dataset_Benthic_Habitat_Mapping.zip) (Maruca et al., 2025). The raw data used in this study were acquired through MBES survey using a pole-mounted, Norbit WBMS Basic multibeam sonar system

integrated with GNSS/INS (Applanix OceanMaster). The processing of MBES bathymetric data was performed using QPS Qimera (<https://qps.nl/qimera/>). Backscatter data processing was performed using QPS Fledermaus (<https://qps.nl/fledermaus/>). Figures 1, 3, 4, 6, 7 were made with QGIS 3.34.9 “Prizren” software (<https://qgis.org/project/overview/>). Figures 8 were generated using Microsoft Excel (<https://www.microsoft.com/it-it/microsoft-365>). Data used to generate the figures are available upon request to the corresponding author.

## REFERENCES

- Abdullah, M. Z., Chuah, L.F., Zakariya, R., Syed, A., Rozaimi, C. H., Mahmud, S. M., Abdallah M. E., Bokhari, A., Muhammad, S. A. and Al-Shwaiman, H. A.: Evaluating climate change impacts on reef environments via multibeam echosounder and Acoustic Doppler Current profiler technology. *Environmental Research*, Volume 252, Part 3, 118858, <https://doi.org/10.1016/j.envres.2024.118858>, 2024.
- Arosio, R., Hobley, B., Wheeler, A. J., Sacchetti, F., Conti, L. A., Furey, T. and Lim, A.: Fully convolutional neural networks applied to large-scale marine morphology mapping. *Frontiers in Marine Science*, 10-1228967, <https://doi.org/10.3389/fmars.2023.1228867>, 2023.
- Ballesteros, E.: Mediterranean Coralligenous Assemblages: a synthesis of present knowledge. *Oceanography and Marine Biology*, Annual Review, 44, 123–195, 2006.
- Basso, D., Bracchi, V. A., Bazzicalupo, P., Martini, M., Maspero, F. and Bavestrello, G.: Living coralligenous as geo-historical structure built by coralline algae. *Frontiers in Earth Science*, 10, 961632, <https://doi.org/10.3389/feart.2022.961632>, 2022.
- Bazzicalupo, P., Cipriani, M., Guido, A., Bracchi, V. A., Rosso, A. and Basso, D.: Calcareous nannoplankton inside coralligenous build-ups: the case of Marzamemi (SE, Sicily). *Bollettino della Società Paleontologica Italiana*, 63 (1), 89–99, <https://dx.doi.org/10.4435/BSPI.2024.09>, 2024.
- Belluomini, G., Gliozzi, E., Ruggieri, G., Branca, M. and Delitala, L.: First dates on the terraces of the Cortone Peninsula (Calabria, southern Italy). *Italian Journal of Geosciences*, 107 (1), 249–254, 1988.
- Betzler, C., Brachert, T. C., Braga, J. C. and Martin, J. M.: Nearshore, temperate, carbonate depositional systems (lower Tortonian, Agua Amarga Basin, southern Spain): Implications for carbonate sequence stratigraphy. *Sedimentary Geology*, 113, 27–53, 1977.
- Bishop, M. P., James, L. A., Shroder, J. F. & Walsh, S. J.: Geospatial technologies and digital geomorphological mapping: Concepts, issues and research. *Geomorphology*, 137, 5–26, <http://dx.doi.org/10.1016/j.geomorph.2011.06.027>, 2012.
- Bonardi, G., Cavazza, W., Perrone, V. and Rossi, S.: Calabria–Peloritani terrane and northern Ionian Sea. In Vai, G. B. & Martini, I. P. (eds.), *Anatomy of an Orogen: The Apennines and Adjacent Mediterranean Basins*, Kluwer Academic Publishers (pp. 287–306), [http://dx.doi.org/10.1007/978-94-015-9829-3\\_17](http://dx.doi.org/10.1007/978-94-015-9829-3_17), 2001.

634 Bracchi, V. A., Basso, D., Marchese, F., Corselli, C. and Savini, A.: Coralligenous morphotypes on subhorizontal  
635 substrate: A new categorization. *Continental Shelf Research*, 144, 10–20. <http://dx.doi.org/10.1016/j.csr.2017.06.005>,  
636 2017.  
637

638 Bracchi, V. A., Bazzicalupo, P., Fallati, L., Varzi, A. G., Savini, A., Negri, M. P., Rosso, A., Sanfilippo, R., Guido, A.,  
639 Bertolino, M., Costa, G., De Ponti, E., Leonardi, R., Muzzupappa, M., and Basso, D.: The Main Builders of Mediterranean  
640 Coralligenous: 2D and 3D Quantitative Approaches for its Identification. *Frontiers in Earth Science*, 10, 910522  
641 <https://doi.org/10.3389/feart.2022.910522>, 2022.  
642

643 Bracchi, V. A., Nalin, R. and Basso D.: Morpho-structural heterogeneity of shallow–water coralligenous in a Pleistocene  
644 marine terrace (Le Castella, Italy). *Palaeogeography, Palaeoclimatology, Palaeoecology*, 454, 101–112,  
645 <http://dx.doi.org/10.1016/j.palaeo.2016.04.014>, 2016.  
646

647 Bracchi, V. A., Nalin, R. and Basso, D.: Paleoeology and dynamics of coralline–dominated facies during a Pleistocene  
648 transgressive–regressive cycle (Capo Colonna marine terrace, Southern Italy). *Palaeogeography, Palaeoclimatology,*  
649 *Palaeoecology*, 414, 296–309, <http://dx.doi.org/10.1016/j.palaeo.2014.09.016>, 2014.  
650

651 Bracchi, V. A., Savini, A., Marchese, F., Palamara, S., Basso, D. and Corselli C.: Coralligenous habitat in the  
652 Mediterranean Sea: a geomorphological description from remote data. *Italian Journal Geosciences*, 134 (1), 32–40,  
653 <https://doi.org/10.3301/IJG.2014.16>, 2015.  
654

655 Brown, C. J., Sameoto, J. A., & Smith, S. J.: Multiple methods, maps, and management applications: Purpose made  
656 seafloor maps in support of ocean management. *Journal of Sea Research*, 72, 1–13,  
657 <https://doi.org/10.1016/j.seares.2012.04.009>, 2012.  
658

659 Cavazza, W., Blenkinsop, J., De Celles, P. G., Patterson, R. T. and Reinhardt, E. G.: Stratigrafia e sedimentologia della  
660 sequenza sedimentaria oligocenica–quaternaria del bacino Calabro–Ionico. *Bollettino della Società Paleontologica*  
661 *Italiana*, 116, 51–77, 1997.  
662

663 Chiocci, F. L., Budillon, F., Ceramicola, S., Gamberi, F. and Orrù, P.: Atlante dei lineamenti di pericolosità geologica dei  
664 mari italiani. CNR edizioni, RM: Risultati del progetto MaGIC, 2021.  
665

666 Cipriani, M., Apollaro, C., Basso, D., Bazzicalupo, P., Bertolino, M., Bracchi, V. A., Bruno, F., Costa, G., Dominici, R.,  
667 Gallo, A., Muzzupappa, M., Rosso, A., Sanfilippo, S., Sciuto, F., Vespasiano, G. and Guido, A.: Origin and role of non–  
668 skeletal carbonate in coralligenous build–ups: new geobiological perspectives in biomineralization processes.  
669 *Biogeosciences*, 21, 49–72, <https://doi.org/10.5194/bg-21-49-2024>, 2024.  
670

671 Cipriani, M., Basso, D., Bazzicalupo, P., Bertolino, M., Bracchi, V. A., Bruno, F., Costa, G., Dominici, R., Gallo, A.,  
672 Muzzupappa, M., Rosso, A., Perri, F., Sanfilippo, R., Sciuto, F. and Guido, A.: The role of non–skeletal carbonate  
673 component in Mediterranean Coralligenous: new insight from the CRESCIBLUREEF project. *Rendiconti Online Società*  
674 *Geologica Italiana*, 59, 75–79. <https://doi.org/10.3301/ROL.2023.12>, 2023.



675 Conrad, O., Bechtel, B., Bock, M., Dietrich, H., Fischer, E., Gerlitz, L., Wehberg, J., Wichmann, V. and Bohner, J.:  
676 System for Automated Geoscientific Analyses (SAGA). Geoscientific model development, 8.  
677 <https://doi.org/10.5194/gmd-8-1991-2015>, 2015.

678

679 Cosentino, D., Gliozzi, E. and Salvini, F.: Brittle deformations in the Upper Pleistocene deposits of the Crotona Peninsula,  
680 Calabria, southern Italy. Tectonophysics, 163, 205–217, 1989.

681

682 Cutter, G. R., Rzhano, Y. and Mayer, L. A.: Automated segmentation of seafloor bathymetry from multibeam  
683 echosounder data using local fourier histogram texture features. Journal of Experimental Marine Biology and Ecology,  
684 285, 355–370. [http://dx.doi.org/10.1016/S0022-0981\(02\)00537-3](http://dx.doi.org/10.1016/S0022-0981(02)00537-3), 2003.

685

686 De Falco, G., Conforti, A., Brambilla, W., Budillon, F., Ceccherelli, G. and De Luca, M.: Coralligenous banks along the  
687 western and northern continental shelf of Sardinia Island (Mediterranean Sea). Journal of Maps, 18(2), 200–209.  
688 <https://doi.org/10.1080/17445647.2021.2020179>, 2022.

689

690 De Falco, G., Tonielli, R., Di Martino, G., Innangi, S., Simeone, S. and Parnum, I. M.: Relationships between multibeam  
691 backscatter, sediment grain size and Posidonia oceanica seagrass distribution. Continental Shelf Research, 30(18), 1941–  
692 1950. <https://doi.org/10.1016/j.csr.2010.09.006>, 2010.

693

694 Deias, C., Guido, A., Sanfilippo, R., Apollaro, C., Dominici, R., Cipriani, M., Barca, D., and Vespasiano, G.: Elemental  
695 Fractionation in Sabellariidae (Polychaeta) Biocement and Comparison with Seawater Pattern: A New Environmental  
696 Proxy in a High-Biodiversity Ecosystem? Water, 15, 1549, <https://doi.org/10.3390/w15081549>, 2023.

697

698 Di Geronimo, I., Di Geronimo, R., Improta, S., Rosso, A. and Sanfilippo, R.: Preliminary observation on a columnar  
699 coralline build-up from off SE Sicily. Biologia Marina Mediterranea, 8(1), 229–237, 2001.

700

701 Donato, G., Sanfilippo, R., Basso, D., Bazzicalupo, P., Bertolino, M., Bracchi, V. A., Cipriani, M., D’Alpa, F., Guido,  
702 A., Negri, M. P., Sciuto, F., Serio, D. and Rosso, A.: Biodiversity associated with a coralligenous build-up off Sicily  
703 (Ionian Sea). Regional Studies in Marine Science, 80, 103868, <https://doi.org/10.1016/j.rsma.2024.103868>, 2024.

704

705 Faccenna, C., Becker, T. W., Lucente, F. P., Jolivet, L. and Rossetti, F.: History of subduction and back-arc extension in  
706 the Central Mediterranean. Geophysical Journal International, 145 (3), 809–820. <http://dx.doi.org/10.1046/j.0956-540x.2001.01435>, 2001.

707

708

709 Faccenna, C., Molin, P., Orecchio, B., Olivetti, V., Bellier, O., Funiciello, F., Minelli, L., Piromallo, C. and Billi, A.:  
710 Topography of the Calabria subduction zone (Southern Italy): clues for the origin of Mt. Etna. Tectonics, 30, TC1003.  
711 <http://dx.doi.org/10.1029/2010TC002694>. 2011.

712

713 Fakiris, E. and Papatheodorou, G.: Quantification of regions of interest in swath sonar backscatter images using grey-  
714 level and shape geometry descriptors: The TargAn software. Marine Geophysical Research, 33, 169–183,  
715 <http://dx.doi.org/10.1007/s11001-012-9153-5>, 2012.

716 Foglini, F., Grande, V., Marchese, F., Bracchi, V. A., Prampolini, M., Angeletti, L., Castellan, G., Chimienti, G., Hansen,  
717 I. M., Gudmundsen, M., Meroni, A. N., Mercorella, A., Vertino, A., Badalamenti, F., Corselli, C., Erdal, I., Martorelli,  
718 E., Savini, A. and Taviani, M.: Application of Hyperspectral Imaging to Underwater Habitat Mapping, Southern Adriatic  
719 Sea. *Sensors*, 19, 2261, <https://doi.org/10.3390/s19102261>, 2019.

720

721 **Fonseca, L., and Mayer, L.: Remote estimation of surficial seafloor properties through the application of angular range**  
722 **analysis to multibeam sonar data. *Marine Geophysical Research*, 28, 119–126, [https://doi.org/10.1007/s11001-007-9019-](https://doi.org/10.1007/s11001-007-9019-4)**  
723 **4, 2007.**

724

725 **Garone, R.V., Lønmo, T., I., B., Schimel, A. C. G., Diesing, M., Thorsnes, T. and Løvstakken, L.: Seabed classification**  
726 **of multibeam echosounder data into bedrock/non-bedrock using deep learning. *Frontiers in Earth Science*, 11:1285368,**  
727 **<https://doi.org/10.3389/feart.2023.1285368>, 2023.**

728

729 Gerovasileiou V. and Bianchi, C. N.: Mediterranean marine caves: a synthesis of current knowledge. In S. J. Hawkins,  
730 A. J. Lemasson, A. L. Allcock, A. E. Bates, M. Byrne, A. J. Evans, L. B. Firth, E. M. Marzinelli, B. D. Russell, I. P.  
731 Smith, S. E. Swearer, P. A. (Eds.), *Oceanography and Marine Biology: An Annual Review*, (Vol. 59, pp. 1–88). Todd,  
732 Editors Taylor & Francis, <https://doi.org/10.1201/9781003138846-1>, 2021.

733

734 Gliozzi, E.: I terrazzi marini del Pleistocene superiore della penisola di Crotone (Calabria). *Geologica Romana*, 26, 17–  
735 79, 1987.

736

737 Guido, A., Gerovasileiou, V., Russo, F., Rosso, A., Sanfilippo, R., Voultsiadou, E. and Mastandrea, A.: Composition and  
738 biostratigraphy of sponge-rich biogenic crusts in submarine caves (Aegean Sea, Eastern Mediterranean). *Palaeogeography,*  
739 *Palaeoclimatology, Palaeoecology*, 534, 109338, <https://doi.org/10.1016/j.palaeo.2019.109338>, 2019a.

740

741 Guido, A., Gerovasileiou, V., Russo, F., Rosso, A., Sanfilippo, R., Voultsiadou, E. and Mastandrea, A.: Dataset of  
742 biogenic crusts from submarine caves of the Aegean Sea: An example of sponges vs microbialites competitions in cryptic  
743 environments.” *Data in brief*, 27, 104745, <https://doi.org/10.1016/j.dib.2019.104745>, 2019b.

744

745 Guido, A., Heindel, K., Birgel, D., Rosso, A., Mastandrea, A., Sanfilippo, R., Russo, F. and Peckmann, J.: Pendant  
746 bioconstructions cemented by microbial carbonate in submerged marine cave (Holocene, SE Sicily). *Palaeogeography,*  
747 *Palaeoclimatology, Palaeoecology*, 388, 166–180. <http://dx.doi.org/10.1016/j.palaeo.2013.08.007>, 2013.

748

749 Guido, A., Jimenez, C., Achilleos, K., Rosso, A., Sanfilippo, R., Hadjioannou, L., Petrou, A., Russo, F. and Mastandrea,  
750 A.: Cryptic serpulid-microbialite bioconstructions in the Kakoskali submarine cave (Cyprus, Eastern Mediterranean).  
751 *Facies*, 63(21), <http://dx.doi.org/10.1007/s10347-017-0502-3>, 2017b.

752

753 Guido, A., Rosso, A., Sanfilippo, R., Miriello, D. and Belmonte, G.: Skeletal vs microbialite geobiological role in  
754 bioconstructions of confined marine environments. *Palaeogeography, Palaeoclimatology, Palaeoecology*, 593, 110920,  
755 <https://doi.org/10.1016/j.palaeo.2022.110920>, 2022.

756 Guido, A., Rosso, A., Sanfilippo, R., Russo, F. and Mastandrea, A.: Frutexites from microbial/metazoan bioconstructions  
757 of recent and Pleistocene marine caves (Sicily, Italy). *Palaeogeography, Palaeoclimatology, Palaeoecology*, 453, 127–  
758 138. <http://dx.doi.org/10.1016/j.palaeo.2016.04.025>, 2016.

759

760 Guido, A., Rosso, A., Sanfilippo, R., Russo, F. and Mastandrea, A.: Microbial Biomineralization in Biotic Crusts from a  
761 Pleistocene Marine Cave (NW Sicily, Italy).” *Geomicrobiology Journal*, 34 (10), 864–872,  
762 <https://doi.org/10.1080/01490451.2017.1284283>, 2017a.

763

764 Innangi, S., Barra, M., Di Martino, G., Parnum, I. M., Tonielli, R. and Mazzola, S.: Reson SeaBat 8125 backscatter data  
765 as a tool for seabed characterization (Central Mediterranean, Southern Italy): Results from different processing  
766 approaches. *Applied Acoustics*, 87, 109–122, <https://doi.org/10.1016/j.apacoust.2014.06.014>, 2015.

767

768 Innangi, S., Ferraro, L., Innangi, M., Di Martino, G., Giordano, L., Bracchi, V.A. and Tonielli, R.: Linosa island: a unique  
769 heritage of Mediterranean biodiversity. *Journal of Maps*, 20(1), 2297989,  
770 <https://doi.org/10.1080/17445647.2023.2297989>, 2024.

771

772 Ismail, K., Huvenne, V. A. I. and Masson, D. G.: Objective automated classification technique for marine landscape  
773 mapping in submarine canyons. *Marine Geology*, 362, 17–32, <https://doi.org/10.1016/j.margeo.2015.01.006>, 2015.

774

775 Janowski, L., Trzcinska, K., Tegowski, J., Kruss, A., Rucinska-Zjadacz, M. and Pocwiardowski P.: Nearshore Benthic  
776 Habitat Mapping Based on Multi-Frequency, Multibeam Echosounder Data Using a Combined Object-Based Approach:  
777 A Case Study from the Rowy Site in the Southern Baltic Sea. *Remote Sensing*, 10, 1983,  
778 <https://doi.org/10.3390/rs10121983>, 2018.

779

780 Laborel, J.: Marine biogenic constructions in the Mediterranean. A review. *Scientific Reports of Port-Cros National Park*  
781 13, 97–126, 1987.

782

783 Lamarche G. and Lurton X.: Recommendations for improved and coherent acquisition and processing of backscatter data  
784 from seafloor-mapping sonars. *Marine Geophysical Research*, 39:5-22, <https://doi.org/10.1007/s11001-017-9315-6>,  
785 2018.

786

787 Lebrech, U., Riera, R., Paumard, V., Leary, M. J. O. and Lang, S. C.: Morphology and distribution of Submerged  
788 palaeoshorelines: Insights from the North West Shelf of Australia. *Earth-Science Reviews*, 224, 103864,  
789 <https://doi.org/10.1016/j.earscirev.2021.103864>, 2022.

790

791 Lecours, V., Devillers, R., Schneider, D. C., Lucieer, V. L., Brown, C. J., and Edinger, E. N.: Spatial scale and geographic  
792 context in benthic habitat mapping: Review and future directions. *Marine Ecology Progress Series*, 535, 259–284,  
793 <https://doi.org/10.3354/meps11378>, 2015.

794

795 Lecours, V., Dolan, M. F. J., Micallef, A. and Lucieer, V. L.: A review of marine geomorphometry, the quantitative study  
796 of the seafloor. *Hydrology and Earth System Sciences*, 20, 3207–3244, <https://doi.org/10.5194/hess-20-3207-2016>, 2016.

797 Lo Iacono, C., Savini, A. and Basso, D.: Cold-Water carbonate bioconstructions. In Micallef A., Krastel S. & Savini A.  
798 (Eds.) Submarine geomorphology, (pp. 425–455). Springer, ISBN: 425-3-319-57851-4, [https://doi.org/10.1007/978-3-](https://doi.org/10.1007/978-3-319-57852-1_22)  
799 [319-57852-1\\_22](https://doi.org/10.1007/978-3-319-57852-1_22), 2018.

800

801 Lucieer, V. and Lamarche, G.: Unsupervised fuzzy classification and object-based image analysis of multibeam data to  
802 map deep water substrates, Cook Strait, New Zealand. *Continental Shelf Research*, 31, 1236–1247.  
803 <https://doi.org/10.1016/j.csr.2011.04.016>, 2011.

804

805 Malinverno, A. and Ryan, W. B. F.: Extension in the Tyrrhenian Sea and shortening in the Apennines as result of arc  
806 migration driven by sinking of the lithosphere. *Tectonics*, 5 (2), 227–245. <http://dx.doi.org/10.1029/TC005i002p00227>,  
807 1986.

808

809 Marchese, F., Bracchi, V. A., Lisi, G., Basso, D., Corselli, C. and Savini, S.: Assessing Fine-Scale Distribution and  
810 Volume of Mediterranean Algal Reefs through Terrain Analysis of Multibeam Bathymetric Data. A Case Study in the  
811 Southern Adriatic Continental Shelf, *Water*, 12, 157. [10.3390/w12010157](https://doi.org/10.3390/w12010157), 2020.

812

813 Maruca, G., Cipriani, M., Dominici, R., Imbrogno, G., Vespasiano, G., Apollaro, C., Perri, F., Bruno, F., Lagudi, A.,  
814 Severino, U., Bracchi, V. A., Basso, D., Cellini, E., Mauri, F., Rosso, A., Sanfilippo, R. and Guido, A.: Dataset Benthic  
815 Habitat Mapping [data set], [http://geocube.unical.it/gmaruca/Dataset\\_Benthic\\_Habitat\\_Mapping.zip](http://geocube.unical.it/gmaruca/Dataset_Benthic_Habitat_Mapping.zip), 2025.

816

817 Massari, F. and Prosser, G.: Late Cenozoic tectono-stratigraphic sequences of the Croton Basin: insights on the  
818 geodynamic history of the Calabrian arc and Tyrrhenian Sea. *Basin Research*, 25, 26–51,  
819 <http://dx.doi.org/10.1111/j.1365-2117.2012.00549>, 2013.

820

821 Mauz, B. and Hassler, U.: Luminescence chronology of late Pleistocene raised beaches on Southern Italy: new data on  
822 relative sea-level changes. *Marine Geology*, 170, 187–203, [http://dx.doi.org/10.1016/S0025-3227\(00\)00074-8](http://dx.doi.org/10.1016/S0025-3227(00)00074-8), 2000.

823 McGarigal, K. and Marks, B. J. F.: Spatial Pattern Analysis Program for Quantifying Landscape Structure (General  
824 Technical Report) Washington, DC, USA, 1995.

825

826 Micallef, A., Le Bas, T.P., Huvenne, V. A. I., Blondel, P., Hühnerbach, V. and Deidun, A.: A multi-method approach  
827 for benthic habitat mapping of shallow coastal areas with high-resolution multibeam data. *Continental Shelf Research*,  
828 39, 14–26, <https://doi.org/10.1016/j.csr.2012.03.008>, 2012.

829

830 Milia, A. and Torrente, M. M.: Early-stage rifting of the southern Tyrrhenian region: the Calabria–Sardinia breakup.  
831 *Journal of Geodynamics*, 81, 17–29, <http://dx.doi.org/10.1016/j.jog.2014.06.001>, 2014.

832

833 Minelli, L. and Faccenna, C.: Evolution of the Calabrian accretionary wedge (Central Mediterranean). *Tectonics*, 29,  
834 TC4004, <http://dx.doi.org/10.1029/2009TC002562>, 2010.

835

836 Nalin, R. and Massari, F.: Facies and stratigraphic anatomy of a temperate carbonate sequence (Capo Colonna Terrace,  
837 late Pleistocene, Southern Italy). *Journal of sedimentary research*, 79 (4), 210–225.  
838 <http://dx.doi.org/10.2110/jsr.2009.027>, 2009.

839

840 Nalin, R., Basso, D. and Massari, F.: Pleistocene coralline algal build-ups (coralligène de plateau) and associated  
841 bioclastic deposits in the sedimentary cover of Cutro marine terrace (Calabria, Southern Italy). In Pedley, H.M.,  
842 Carannante, G. (Eds.), *Cool–Water Carbonates: Depositional Systems and Palaeoenvironmental Controls*. The Geological  
843 Society of London (pp.11–22), <http://dx.doi.org/10.1144/GSL.SP.2006.255.01.02>, 2006.

844

845 Nalin, R., Bracchi, V. A., Basso D. and Massari, F.: *Persististrombus latus* (Gmelin) in the upper Pleistocene deposits of  
846 the marine terraces of the Crotona peninsula (Southern Italy). *Italian Journal of Geosciences*, 131 (1), 95–101.  
847 <http://dx.doi.org/10.3301/IJG.2011.25>, 2012.

848

849 Nalin, R., Massari, F. and Zecchin, M.: Superimposed cycles of composite marine terraces: the example of Cutro Terrace  
850 (Calabria, Southern Italy). *Journal of sedimentary research*, 77, 340–354. <http://dx.doi.org/10.2110/jsr.2007.030>, 2007.

851

852 Palmentola, G., Carobene, L., Mastronuzzi, G. and Sansò, P.: I terrazzi marini pleistocenici della Penisola di Crotona  
853 (Italia). *Geografia Fisica e Dinamica Quaternaria*, 13, 75–80, 1990.

854

855 Pepe, F., Sulli, A., Bertotti, G., and Cella F.: Architecture and Neogene to Recent evolution of the western Calabrian  
856 continental margin: An upper plate perspective to the Ionian subduction system, central Mediterranean. *Tectonics*, 29,  
857 TC3007, <https://doi.org/10.1029/2009TC002599>, 2010.

858

859 Pérès, J. M. and Picard, J. : *Nouveau manuel de bionomie benthique de la Mer Méditerranée*. *Recent Travaux de la Station*  
860 *Marine d'Endoume*, 31 (47),137, 1964.

861

862 Pérès, J. M.: Structure and dynamics of assemblages in the benthic. *Marine Ecology*, 5 (1),119–185, 1982.

863

864 Picone, F. and Chemello, R.: Seascape characterization of a Mediterranean vermetid reef: a structural complexity  
865 assessment. *Frontiers in Marine Science*, 10, 1134385, doi:10.3389/fmars.2023.1134385, 2023.

866

867 Reitz, M. A. and Seeber, L.: Arc-parallel strain in a short rollback-subduction system: the structural evolution of the  
868 Crotona basin (Northeastern Calabria, Southern Italy). *Tectonics*, 31, TC4017, <http://dx.doi.org/10.1029/2011TC003031>,  
869 2012.

870

871 Riley, S. J., De Gloria, S. D. and Elliot, R.: A Terrain Ruggedness Index that Quantifies Topographic Heterogeneity.  
872 *International Journal of Scientific Research*, 5, 23–27, 1999.

873

874 Rosso, A., Donato, G., Sanfilippo, R., Serio, D., Sciuto, F., D'Alpa, F., Bracchi, V.A., Negri, M.P. and Basso D.: The  
875 bryozoan *Margaretta cereoides* as a habitat-former in the Coralligenous of Marzamemi (SE Sicily, Mediterranean Sea).



876 In Koulouri P., Gerovasileiou V. & Dailianis T. (Eds), Marine Benthic Biodiversity of Eastern Mediterranean Ecosystems,  
877 Journal of Marine Science and Engineering, (Vol. 11, 590), <https://doi.org/10.3390/jmse11030590>, 2023.

878

879 Rueda, J.L., Urra, J., Aguilar, R., Angeletti, L., Bo, M., García-Ruiz, C. Gonzalez-Duarte, M. M., Lopez, E., Madurell,  
880 T., Maldonado, M., Mateo-Ramirez, A., Megina, C., Moreira, J., Moya, F., Ramalho, L. V., Rosso, A., Sitjà, C. and  
881 Taviani, M.: Cold–Water Coral Associated Fauna in the Mediterranean Sea and Adjacent Areas. In Orejas C., Jiménez  
882 C. (Eds.), Mediterranean Cold–Water Corals: Past, Present and Future, Coral Reefs of the World (Vol. 9 (29), pp. 295–  
883 333) Springer International Publishing AG, part of Springer Nature, <https://doi.org/10.1007/978-3-319-91608-829>, 2019.

884

885 Sanfilippo, R., Rosso, A., Mastandrea, A., Viola, A., Deias, C. and Guido, A.: Sabellaria alveolata sandcastle worm from  
886 the Mediterranean Sea: New insights on tube architecture and biocement. Journal of Morphology, 280, 1839–1849,  
887 <https://doi.org/10.1002/jmor.21069>, 2019.

888

889 Sanfilippo, R., Rosso, A., Viola, A., Guido, A. and Deias, C.: Architecture and tube structure of Sabellaria spinulosa  
890 (Leuckart, 1849): comparison with the Mediterranean S. alveolata congener. Journal of Morphology, 283, 1350–1358,  
891 <https://doi.org/10.1002/jmor.21507>, 2022.

892

893 Santagati, P., Guerrieri, S., Borrelli, M. and Perri, E.: Calcareous bioconstructions formation during the last interglacial  
894 (MIS 5) in the central Mediterranean: A consortium of algal, metazoan, and microbial framebuilders (Capo Colonna–  
895 Crotone Basin South Italy). Marine and Petroleum Geology, 167, 106950,  
896 <https://doi.org/10.1016/j.marpetgeo.2024.106950>, 2024.

897

898 Santoro, E., Mazzella, M. E., Rerranti, L., Randisi, A., Napolitano, E., Rittner, S. and Radtke, U.: Raised coastal terraces  
899 along the Ionian Sea coast of Northern Calabria, Italy, suggest space and time variability of tectonic uplift rates.”  
900 Quaternary International, 206, 78–101, <http://dx.doi.org/10.1016/j.quaint.2008.10.003>, 2009.

901

902 Savini, A., Borrelli, M., Vertino, A., Mazzella, F., and Corselli, C.: Terraced Landforms Onshore and Offshore the Cilento  
903 Promontory (Southern Tyrrhenian Margin): New Insights into the Geomorphological Evolution, Water, 13 (4), 566,  
904 <https://doi.org/10.3390/w13040566>, 2021.

905

906 Savini, A., Vertino, A., Marchese, F., Beuck, L. and Freiwald, A.: Mapping cold–water coral habitats at different scales  
907 within the Northern Ionian Sea (central Mediterranean): An assessment of coral coverage and associated vulnerability.  
908 PLoS ONE, 9, e87108. <https://doi.org/10.1371/journal.pone.0087108>, 2014.

909

910 Schlager, W.: Accommodation and supply–A dual control on stratigraphic sequences. Sedimentary Geology, 86, 111–  
911 136, 1993.

912

913 Schlager, W.: Depositional bias and environmental change–important factors in sequence stratigraphy. Sedimentary  
914 Geology, 70, 109–130, 1991.

915

916 Sciuto, F., Altieri, C., Basso, D., D'Alpa, F., Donato, G., Bracchi, V. A., Cipriani, M., Guido, A., Rosso, A., Sanfilippo,  
 917 R., Serio, D. and Viola, A.: Preliminary data on ostracods and foraminifers living on coralligenous bioconstructions  
 918 Offshore Marzamemi (Ionian Sea, Sicily). *Revue de Micropaléontologie*, 18, 100711,  
 919 <https://doi.org/10.1016/j.revmic.2023.100711>, 2023.  
 920  
 921 Severino, U., Lagudi, A., Barbieri, L., Scarfone, L., and Bruno, F.: A SLAM-Based Solution to Support ROV Pilots in  
 922 Underwater Photogrammetric Survey. In *International Conference of the Italian Association of Design Methods and Tools*  
 923 for Industrial Engineering (pp. 443–450). Cham: Springer Nature Switzerland,  
 924 [https://link.springer.com/chapter/10.1007/978-3-031-58094-9\\_49](https://link.springer.com/chapter/10.1007/978-3-031-58094-9_49), 2023.  
 925  
 926 SNPA, Methodological Sheets used in the monitoring program of the second cycle of the Marine Strategy Directive  
 927 (Ministerial Decree 2 February 2021) SNPA technical publications, [https://www.snpambiente.it/snpa/schede-](https://www.snpambiente.it/snpa/schede-metodologiche-utilizzate-nei-programmi-di-monitoraggio-del-secondo-ciclo-della-direttiva-strategia-marina-d-m-2-febbraio-2021/)  
 928 [metodologiche-utilizzate-nei-programmi-di-monitoraggio-del-secondo-ciclo-della-direttiva-strategia-marina-d-m-2-](https://www.snpambiente.it/snpa/schede-metodologiche-utilizzate-nei-programmi-di-monitoraggio-del-secondo-ciclo-della-direttiva-strategia-marina-d-m-2-febbraio-2021/)  
 929 [febbraio-2021/](https://www.snpambiente.it/snpa/schede-metodologiche-utilizzate-nei-programmi-di-monitoraggio-del-secondo-ciclo-della-direttiva-strategia-marina-d-m-2-febbraio-2021/), 2024.  
 930  
 931 Stephens, D., Smith, A., Redfern, T., Talbot, A., Lessnoff, A. and Dempsey, K.: Using three dimensional convolutional  
 932 neural networks for denoising echosounder point cloud data. *Applied Computing and Geosciences*, 5-100016,  
 933 <https://doi.org/10.1016/j.acags.2019.100016>, 2020.  
 934  
 935 Varzi, G. A., Fallati, L., Savini, A., Bracchi, V. A., Bazzicalupo, P., Rosso, A., Sanfilippo, R., Bertolino, M., Muzzupappa,  
 936 M., and Basso, D.: Geomorphology of coralligenous reefs offshore southeastern Sicily (Ionian Sea).” *Journal of Maps*,  
 937 19 (1), <https://doi=10.1080/17445647.2022.2161963>, 2023.  
 938  
 939 Vosselman, G.: Slope based filtering of laser altimetry data. *IAPRS*, Vol. XXXIII, Amsterdam, 2020.  
 940  
 941 Westaway, R. and Bridgland, D: Late Cenozoic uplift of Southern Italy deduced from fluvial and marine sediments:  
 942 coupling between surface processes and lower-crustal flow. *Quaternary International*, 175, 86–124,  
 943 <http://dx.doi.org/10.1016/j.quaint.2006.11.015>, 2007.  
 944  
 945 Westaway, R.: Quaternary uplift of Southern Italy. *Journal of Geophysical Research*, 98 (B12), 21741–21772,  
 946 <http://dx.doi.org/10.1029/93JB01566>, 1993.  
 947  
 948 Zecchin, M. and Caffau, M.: Key features of mixed carbonate–siliciclastic shallow–marine systems: the case of Capo  
 949 Colonna terrace (southern Italy). *Italian Journal of Geosciences*, 130 (3), 370 – 379.  
 950 <http://dx.doi.org/10.3301/IJG.2011.12>, 2011.  
 951  
 952 Zecchin, M., Caffau, M., Civile, D. and Roda, C.: Facies and cycle architecture of a Pleistocene marine terrace (Crotone,  
 953 southern Italy): a sedimentary response to late Quaternary, high–frequency glacio–eustatic changes. *Sedimentary*  
 954 *Geology*, 216, 138–157, <http://dx.doi.org/10.1016/j.sedgeo.2009.03.004>, 2009.  
 955

956 Zecchin, M., Caffau, M., Civile, D., Critelli, S., Di Stefano, A., Maniscalco, R., Muto, F., Sturiale, G., and Roda, C.: The  
 957 Plio–Pleistocene evolution of the Croton Basin (Southern Italy): interplay between sedimentation, tectonics and eustasy  
 958 in the frame of Calabrian arc migration.” *Earth Science Reviews*, 115, 273–303.  
 959 <http://dx.doi.org/10.1016/j.earscirev.2012.10.005>, 2012.  
 960  
 961 Zecchin, M., Nalin, R. and Roda, C.: Raised Pleistocene marine terraces of the Croton peninsula (Calabria, southern  
 962 Italy): facies analysis and organization of their deposits. *Sedimentary Geology*, 172, 165–185. doi:  
 963 10.1016/j.sedgeo.2004.08.003, 2004.  
 964  
 965 Zevenbergen, L.W. and Thorne C. R.: Quantitative analysis of land surface topography. *Earth Surface Processes and*  
 966 *Landforms*, 12 (1), 47–56. <https://doi.org/10.1002/esp.3290120107>, 1987.

# Mapping benthic marine habitats featuring coralligenous bioconstructions: a new approach to support geobiological research

Giuseppe Maruca<sup>1\*</sup>, Mara Cipriani<sup>1\*</sup>, Rocco Dominici<sup>1</sup>, Gianpietro Imbrogno<sup>1</sup>, Giovanni Vespasiano<sup>1</sup>, Carmine Apollaro<sup>1</sup>, Francesco Perri<sup>1</sup>, Fabio Bruno<sup>2</sup>, Antonio Lagudi<sup>2</sup>, Umberto Severino<sup>2</sup>, Valentina A. Bracchi<sup>3</sup>, Daniela Basso<sup>3</sup>, Emilio Cellini<sup>4</sup>, Fabrizio Mauri<sup>4</sup>, Antonietta Rosso<sup>5</sup>, Rossana Sanfilippo<sup>5</sup>, Adriano Guido<sup>1</sup>.

<sup>1</sup>Department of Biology, Ecology and Earth Sciences, University of Calabria, 87036, Rende, Italy;

<sup>2</sup>Department of Mechanical, Energy and Management Engineering, University of Calabria, 87036, Rende, Italy;

<sup>3</sup>Department of Earth and Environmental Sciences, University of Milano–Bicocca, 20126, Milan, Italy;

<sup>4</sup>Regional Agency for the Environment (ARPACAL), Regional Marine Strategy Centre (CRSM), 8890, Crotone Italy.

<sup>5</sup>Department of Biological, Geological and Environmental Sciences, University of Catania, 95129, Catania, Italy;

*Correspondence to:* Giuseppe Maruca ([giuseppe.maruca@unical.it](mailto:giuseppe.maruca@unical.it)); Mara Cipriani ([mara.cipriani@unical.it](mailto:mara.cipriani@unical.it))

**Abstract.** Seabed mapping represents a very useful tool for seascape characterization and benthic habitat study, and requires advanced technologies for acquiring, processing and interpreting remote data. Particularly, acoustic instruments, such as high-resolution swath bathymetry sounder (*i.e.*, Multibeam Echosounder: MBES), allows to recognize, identify and map the extension of benthic habitats without applying invasive mechanical procedures. Bathymetry and backscatter (BS) data are crucial to perform modern habitat mapping. Although the acquisition and processing of bathymetric data follows standardized procedure (*e.g.*, Hydrographic Organization guidelines), and recent studies proposed recommendation for backscatter acquisition and processing, a broadly validated methodological approach, integrating geomorphometric analysis for benthic habitat mapping, is still lacking. In this work, a new approach for benthic habitat mapping, with focus on coralligenous bioconstructions, was developed using the open-source software QGIS. This methodology, tested within the Isola Capo Rizzuto Marine Protected Area (Calabria, Italy), is designed to be freely reproducible by researchers working in the field of marine ecosystem monitoring and conservation. Through the proposed mapping procedure, it is possible to: i) identify benthic habitats on selected study areas by combining bathymetry and BS data with geomorphological indices performed in QGIS; ii) quantitatively define the 2D and 3D distribution of coralligenous bioconstructions in terms of surface covered, thickness and volume. Moreover, the statistical analysis of quantitative morphometric data allowed for comparison of geometric characteristics of different coralligenous morphotypes. The obtained results, combined with improvement of minimally invasive sampling and geobiological–geochemical characterization, can contribute to the development of protocols aimed at monitoring marine bioconstructed ecosystems, many of which protected by national and international regulations due to their importance for Mediterranean biodiversity preservation, and plan actions for their protection and persistence.

## 1 Introduction

Bioconstructions are geobiological bodies formed in situ by growth of skeletonised organisms and represent habitats that host a great variety of benthic species. They experience a wide array of dynamic phenomena, resulting from the balance between the action of habitat builders, dwelling organisms and bioeroders over decadal to millennial timescale. Along



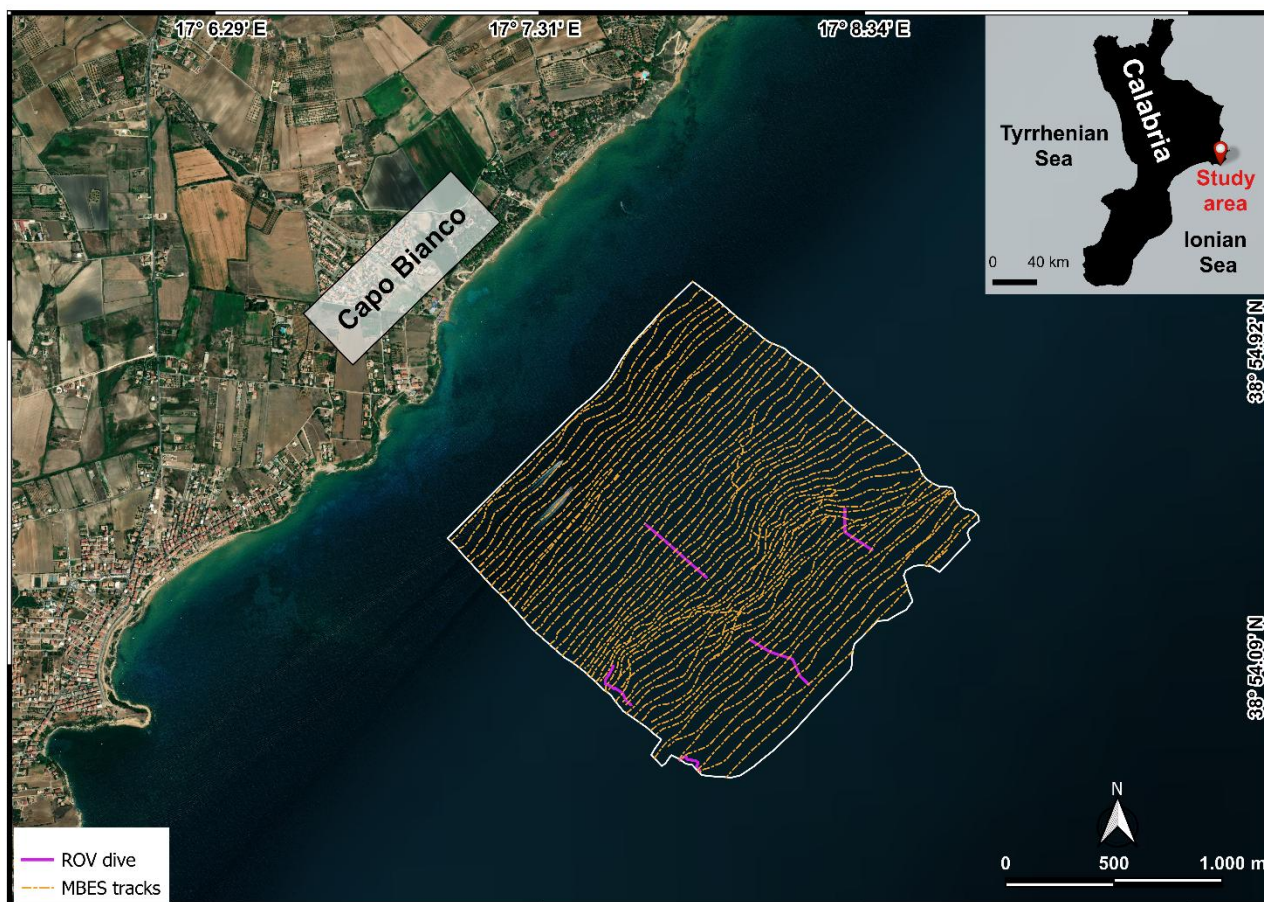
the Mediterranean continental shelf, the most conspicuous bioconstructed habitats are represented by coralligenous build-ups (Bracchi et al., 2015, 2017, 2022; Basso et al., 2022; Cipriani et al., 2023, 2024), vermetid reefs (Picone and Chemello, 2023), sabellariid build-ups (Sanfilippo et al., 2019, 2022; Deias et al., 2023) and polychaetes–bryozoan bioconstructions (Guido et al., 2013, 2016, 2017a, b, 2019a, b, 2022), whereas cold–water corals occur in deeper settings (Rueda et al. 2019, Foglini et al., 2019). Coralligenous is known as a biocenosis complex consisting of a hard biogenic substrate primarily generated by the superimposition of calcareous red algae able to form 3D structures, supporting a high biodiversity (*e.g.*, Ballesteros, 2006; Bracchi et al., 2022; Rosso et al., 2023; Sciuto et al., 2023; Donato et al., 2024). Pérès and Picard (1964) and Pérès (1982) identified Coralligenous as the ecological climax stage for the Mediterranean circalittoral zone, with some bioconstructions also occurring in dim–light very shallow settings (Ballesteros, 2006; Bracchi et al., 2016; Basso et al., 2022). Coralligenous produces various morphotypes on the seafloor and plays a key role in the formation and transformation of seascape over geological time (Bracchi et al., 2017; Marchese et al., 2020). Architecture and morphology are mainly influenced by biological carbonate production, that responds to different factors, like physiography, oceanography, terrigenous supply and climate (Schlager, 1991, 1993; Betzler et al., 1997; Bracchi et al., 2017). Based upon the nature of the substrates, coralligenous morphotypes have been categorized in two main groups: i) banks, flat frameworks mainly built on horizontal substrata and, and ii) rims, structures on submarine vertical cliffs or close to the entrance of submarine caves (Pérès & Picard, 1964; Laborel, 1987; Ballesteros, 2006; Bracchi et al., 2017; Marchese et al., 2020; Gerovasileiou & Bianchi, 2021). Moreover, Bracchi et al. (2017) introduced a new classification for coralligenous morphotypes on sub–horizontal substrate using a shape geometry descriptor, in order to obtain a more objective description of these morphologies, classified in: i) tabular banks, *i.e.*, large tabular structures with a significant lateral continuity that completely cover the seafloor, forming an extensive habitat; ii) discrete reliefs, *i.e.*, smaller, distinct structures often arranged in clusters that do not fully cover the seafloor, leaving patches of sediment between them; and iii) hybrid banks, a category grouping morphologies intermediate between tabular banks and discrete reliefs. These structures can coalesce into a larger formation, resembling tabular banks, while still maintain individual characteristics. Hybrid banks often occur alongside other habitats, and their distribution is influenced by local sediment and hydrodynamic conditions (Bracchi et al., 2017).

Although coralligenous bioconstructions occur along almost the entire Mediterranean continental shelf, they have been mapped only in few areas and their distribution is still underestimated (De Falco et al 2010, 2022; Innangi et al 2024). In addition, as known hot spot of biodiversity, along with its low accretion rate of 0.06–0.27 mm/yr and its sensitivity to natural and anthropogenic impacts (Di Geronimo et al., 2001; Bertolino et al., 2014; Basso et al., 2022; Cipriani et al., 2023, 2024), Coralligenous is acknowledged as a priority habitat for protection under the EU Habitats Directive, is part of the Natura 2000 network (92/43/CE), and is subject to specific conservation plans within the framework of the Barcelona Convention (UNEP–MAP–RAC/SPA, 2008; UNEP–MAP–RAC/SPA, 2017). Moreover, together with other vulnerable settings (*e.g.*, Cold–Water Corals), Coralligenous is monitored under the Marine Strategy Framework Directive (MSFD, EC, 2008; SNPA, 2024). As a result, non–destructive methods have been developed to assess the health status and ecological quality of this habitat (Bracchi et al., 2022). For all these reasons, seabed mapping can provide a very useful tool for seascape characterization and mapping of Coralligenous and other vulnerable habitats (Chiocci et al., 2021). In particular, acoustic instruments, such as high–resolution swath bathymetry sounder, side scan sonar and acoustic profiling, enable the quick detection and identification of benthic habitats and thus mapping their extension without any direct contact that might represent a threat for these vulnerable ecosystems (Bracchi et al., 2017; Chiocci et al., 2021). Several studies have demonstrated that such technologies, especially when combined with backscatter (BS) data and geometric descriptors, significantly enhance the study of seafloor properties and the discrimination of benthic habitats,

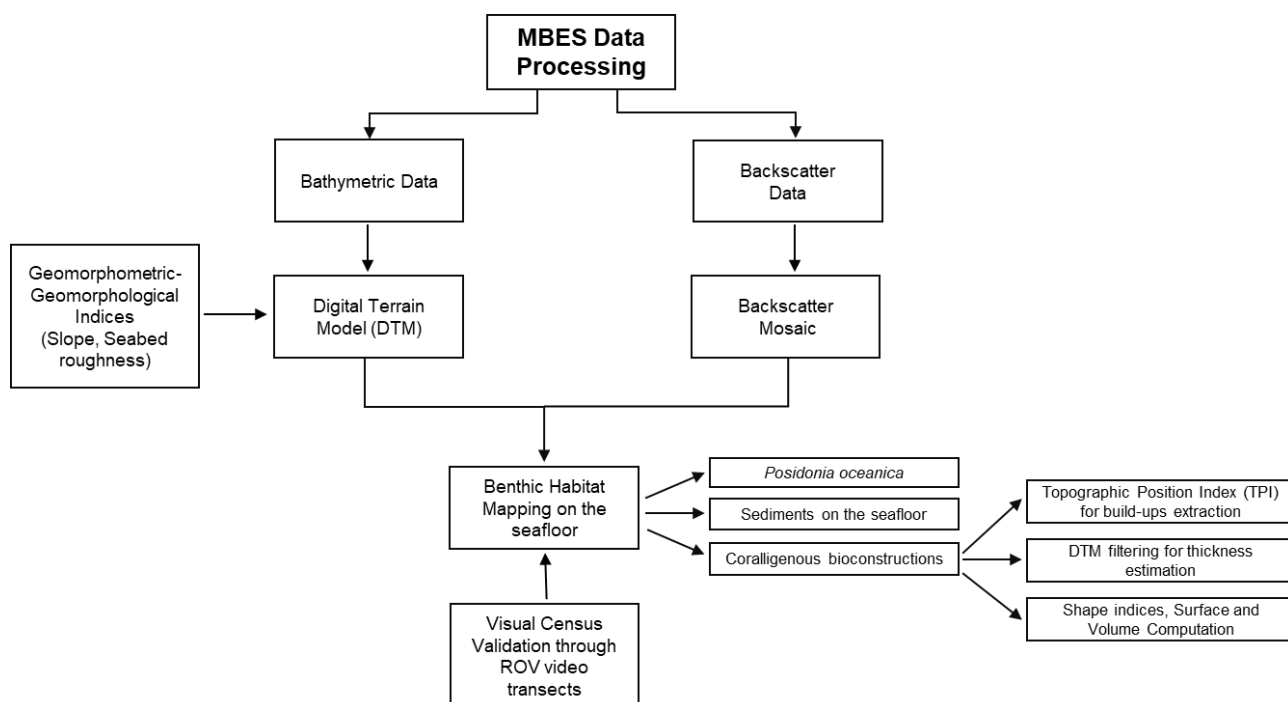
such as coral reefs, improving the understanding of their spatial distribution and ecological significance (Fonseca and Mayer, 2007, Lecours et al., 2015; Brown et al., 2012; Lamarche and Lurton, 2018; Abdullah et al., 2024). In this work, a semi-automated GIS-based approach for benthic habitat mapping was proposed and tested in shallow coastal waters, off Capo Bianco, within the Isola Capo Rizzuto Marine Protected Area (Crotone, Southern Italy). The method combines high-resolution bathymetric and BS data obtained through MBES surveys and geomorphological and geomorphometric indices in order to develop innovative approaches for eco-geomorphological and geobiological characterisation of the seafloor. The benthic habitat mapping here proposed has proven capable not only of identifying marine bioconstructions, but also of quantitatively defining their spatial and three-dimensional distribution in terms of area, volume and height relative to the substrate from which they arise. For these reasons, the procedure represents a powerful tool for accurately delineate the extension of the bioconstructions and evaluate their evolution over time in response to natural and/or anthropogenic changes. Furthermore, the combination of this mapping approach with minimally invasive sampling systems and geobiological-geochemical characterization of marine bioconstructions, may represent a potent tool for monitoring these delicate habitats.

## 2 Methodological approach

High-resolution acoustic data of the study area offshore Capo Bianco were collected during several MBES surveys (Fig. 1) performed between February and July 2024 as part of the project “Tech4You PP2.3.1: Development of tools and applications for integrated marine communities and substrates monitoring; Action 1: Development of hardware and software systems for three-dimensional detection, sampling and mapping of underwater environments”, in implementation to the previous bathymetric and backscatter data acquisition and elaboration of CRSM-ARPACAL. The approach proposed for benthic habitat mapping and defining of spatial and three-dimensional distribution of coralligenous bioconstruction is shown in Figure 2. In particular, mapping operations were conducted using QGIS 3.34.9 “Prizren”. The most representative morphological indices, represented by slope and seafloor roughness, were extracted from the Digital Terrain Model (DTM). Due to the large amount of data resulting from the need to obtain a high-resolution mapping of benthic habitats, backscatter and bathymetry values, together with geomorphological-geomorphometric indices, were imported and queried into PostgreSQL, an open-source and free relational database management system (RDBMS) capable of executing queries in SQL language.



**Figure 1:** Study area off Capo Bianco (Calabria, Italy) and location of the MBES tracks and ROV–video transect (basemap from Esri World Imagery).



**Figure 2:** Conceptual model of the workflow for the development of the proposed benthic habitat mapping approach.

114 Once the spatial extension and distribution of the benthic habitat have been defined by combination of bathymetric,  
115 backscatter, slope and seafloor roughness data, the extraction of coralligenous build-ups was performed using the  
116 Topographic Position Index (TPI), according to Marchese et al. (2020). Moreover, area, Shape Index (SI), maximum  
117 diameter (Dmax) thickness and volume were calculated for each extracted polygon. Finally, the benthic habitat mapping  
118 model was ground-truthed by visual analysis of ROV-video transect performed along specific paths within the study  
119 area. The underwater video surveys were obtained using a VideoRay Defender equipped with a functional prototype of  
120 the optical module dedicated to mapping, comprising a stereo-camera, a high-resolution camera and a lightning system  
121 (Severino et al., 2023). Both cameras have been meticulously calibrated to correct for optical distortions, ensuring  
122 accurate and reliable data acquisition. The selected cameras were the GoPro Hero 9 Black, serving as the high-resolution  
123 camera, and the Stereolabs ZED2i, serving as the stereo camera. The GoPro Hero 9 Black is a small-sized action camera  
124 with a 26.3 MP CMOS sensor capable of acquiring videos at a resolution of 5120×2880 at 30 fps, digital stabilization,  
125 and a horizontal field of view up to 128°. The ZED2i is a stereo camera with dual 4 MP sensors of 2 mm pixel size, a  
126 depth range between 0.3 m to 20 m, capable of acquiring video with a resolution of 2208×1242 at 15 fps, and a horizontal  
127 field of view of 110°. The stereo-camera communicates with the surface control unit by means of a single-board  
128 microcomputer, a NVIDIA Jetson Nano, which supports the CUDA architecture for parallel elaboration. The GoPro Hero  
129 9 Black features Bluetooth Low Energy (BLE) and Wi-Fi communication capabilities. The acquisition parameters for  
130 both cameras can be configured via the enclosure using a custom user interface accessible on the surface computer.

## 131 **2.1 Bathymetric and backscatter data**

132 MBES surveys have been carried out using a pole-mounted, Norbit iWBMS Long Range Turnkey Multibeam Sonar  
133 System integrated with GNSS/INS (Applanix OceanMaster), operating with Real Time Kinematic (RTK) corrections,  
134 ensuring high positioning accuracy during the surveys. Data were collected in 59 tracks with a swath overlap of 20–40 %  
135 performed at an average speed of 4.5 knots. A total of three sound velocity profiles per day were collected before starting  
136 the acquisition using a Sound Velocity Profiler–Valeport miniSVP. Considering the absence of freshwater inputs and the  
137 relative stability of the water column across the depth range, this was deemed sufficient to ensure reliable sound speed  
138 correction.

139 The MBES survey provided both bathymetry and BS data. The processing of MBES bathymetric data was performed  
140 using QPS Qimera and included corrections for tide, heading, heave, pitch and roll. The correction of sound velocity was  
141 carried out using profiles obtained with the Valeport miniSVP. Subsequently, the soundings underwent manual cleaning  
142 to remove spikes. The bathymetric dataset was exported as a 32-bit raster file with a cell size of 0.05 m. BS data were  
143 processed using QPS Fledermaus, and the final output was exported as an 8-bit raster file with 0.05 m cell size.

## 144 **2.2 Geomorphological–geomorphometric indices**

145 Geomorphologic and geomorphometric indices were obtained using SAGA (System for Automated Geoscientific  
146 Analysis; Conrad et al., 2015) Next Gen Provider and GDAL plugins. In particular, the slope, expressed in degrees, was  
147 calculated using the dedicated function implemented in the GDAL plugin using a ratio of vertical units to horizontal of  
148 1.0 and applying the Zevenbergen–Thorne formula instead of the Horn’s one. Indeed, the Zevenbergen–Thorne method  
149 (1987), that considers a second-order finite difference, is more dedicated to geomorphological applications as it uses a  
150 particular weighting scheme that emphasizes changes in curvature and terrain shape. Seabed roughness was assessed  
151 using the Terrain Roughness Index (TRI), which provides a quantitative measure of terrain heterogeneity (Riley et al.,  
152 1999). In particular, TRI values close to 0 indicate fairly regular and uniform surfaces, moderate TRI values correspond



153 to more pronounced irregularities, while high TRI values identify rugged morphologies and/or complex structures on the  
154 seafloor. TRI was calculated using SAGA module “Terrain Roughness Index” with the following settings: circle as search  
155 mode; a search radius of 0.5 map units (m.u.); gaussian weighting function: a value of 3.00 for the power; a bandwidth  
156 of 75.00. The values of these parameters were selected through a trial-and-error method in order to best highlight the  
157 heterogeneity of the seabed.

## 158 2.3 Topographic Position Index

159 The Topographic Position Index (TPI) was calculated at the finest possible scale (min radius: 1.00 m.u.; max radius: 5.00  
160 m.u.) according to the DTM resolution and using a Power of 3.00 and a Bandwidth of 150.00. TPI is a morphometric  
161 parameter based on neighbouring areas useful in DTM analysis (Wilson and Gallant, 2000). Specifically, positive TPI  
162 values indicate areas that are higher than the average of their surroundings, TPI values near zero correspond to flat areas  
163 or region with a constant slope, while negative TPI values represent areas lower than their surroundings. In order to  
164 facilitate the extraction of coralligenous build-ups from surrounding seafloor and reduce the occurrence of artifact, a TPI  
165 threshold of 0.2 was used and all the grid cells below this value were not considered as coralligenous bioconstructions.  
166 TPI scale (1.00–5.00 m.u.) and value (0.2) were chosen through a trial-and-error approach in order to preserve the high  
167 resolution of the extraction which is crucial for accurate volume computation.

## 168 2.4 DTM filtering

169 TPI parameters extracted the distribution of the coralligenous build-ups with high-resolution in terms of perimeter  
170 boundary. The thickness calculation for each coralligenous build-up was developed by the creation of a “reference  
171 surface” (without build-ups) using the SAGA “DTM Filter (Slope-Based)” tool implemented in QGIS 3.34.9. This tool  
172 uses concept as described by Vosselman (2000) and can be used to filter a DTM, categorizing its cell into ground and  
173 non-ground (object) cell. A cell is considered ground if there is no other cell within the kernel radius where the height  
174 difference exceeds the allowed maximum terrain slope at the distance between the two cells. The thickness estimation of  
175 each coralligenous build-up was obtained by subtracting the average depth of each polygon extracted using TPI from the  
176 average depth value of the reference surface at that specific zone.

177 After estimating the height of each build-up relative to the seabed on which it developed, the Shape Index (SI–McGarigal  
178 et al., 1995) was calculated using the module “Polygon Shape Indices” of SAGA in order to describe a seafloor landscape  
179 characterized by distinct Coralligenous morphotypes. Finally, covered surface and volume of each polygon were  
180 calculated using vector field operation implemented into QGIS.

## 181 3 Geological setting

182 The study area, located offshore Capo Bianco (Isola Capo Rizzuto, Calabria, Italy), belongs to the Crotona Basin (CB)  
183 (Fig. 3). The CB is the widest Neogene basin of the Calabria region, partly exposed along the Ionian coast and in part  
184 documented offshore. It represents a segment of the Ionian fore arc basin on the inner portion of the Calabrian accretionary  
185 wedge (Cavazza et al., 1997; Bonardi et al., 2001; Minelli and Faccenna, 2010). The basin infill is structured into several  
186 distinct tectono-stratigraphic sequences, which reflect an extensional to transtensional tectonic regime, occasionally  
187 interrupted by transpressional to compressional events (Malinverno and Ryan, 1986; Faccenna et al., 2001; Reitz and  
188 Seeber, 2012; Zecchin et al., 2012; Massari and Prosser, 2013; Milia and Torrente, 2014).

189 Since the mid–Pleistocene a significant uplift (0.70–1.25 m/ky; Zecchin et al., 2004), combined with glacio–eustatic sea  
190 level fluctuations, led to the formation in the Crotona Peninsula of five orders of marine terraces (Palmentola et al., 1990;  
191 Westaway, 1993; Westaway and Bridgland, 2007; Santoro et al., 2009; Faccenna et al., 2011; Bracchi et al., 2014;  
192 Santagati et al., 2024 which unconformably overlie the Piacenzian–Calabrian marly clays of the Cutro Formation (Zecchin  
193 et al., 2004).

194 The Cutro Terrace (1<sup>st</sup> order terrace), ascribed to MIS 7 by Zecchin et al. (2011), is a mixed marine to continental terrace,  
195 consisting of the products of carbonate (algal build-ups and biocalcarene passing into shoreface and foreshore deposits)  
196 to siliciclastic (shoreface, fluvial channel fill, lagoon-estuarine and lacustrine deposits) sequences (Zecchin et al., 2011).  
197 The 2<sup>nd</sup> order (MIS 5e), represented by the Campolongo-La Mazzotta terrace, is characterized by bioclastic and  
198 siliciclastic sandstones, with local bioclastic deposits and algal patch reefs (Maunz and Hassler, 2000, Zecchin et al.,  
199 2011).

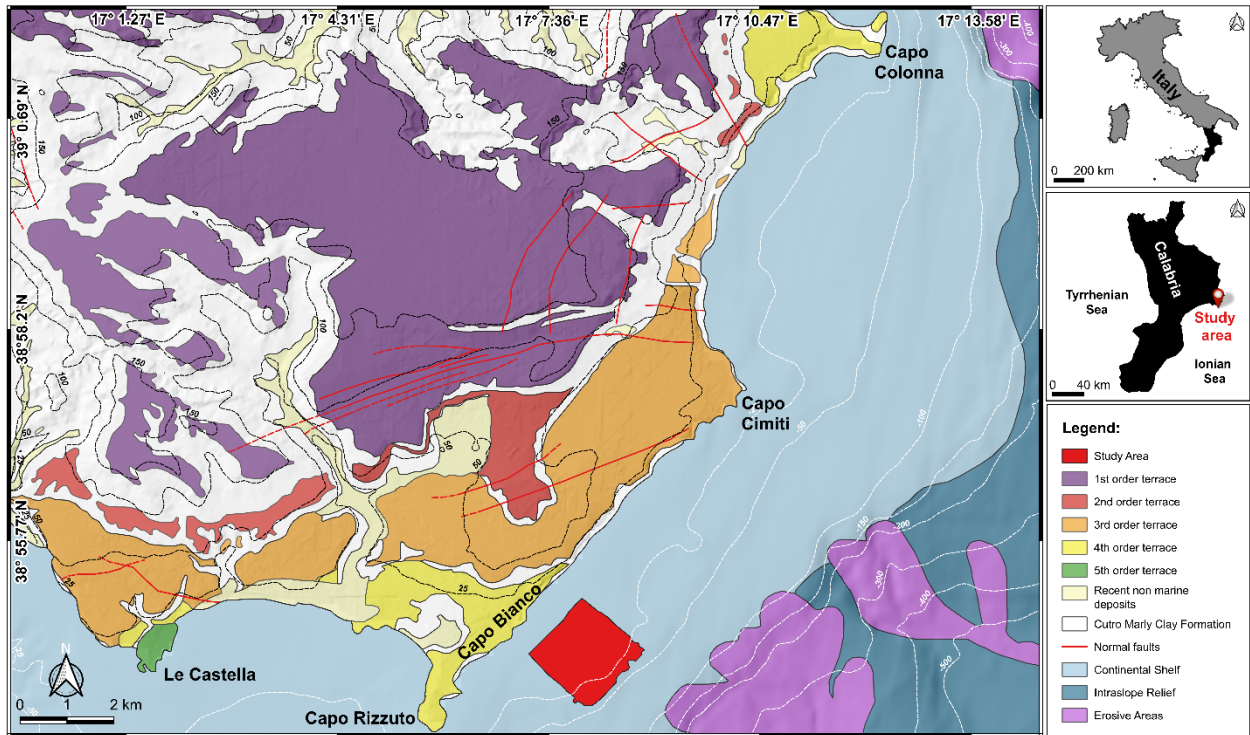
200 The Le Castella–Capo Cimiti terrace (3<sup>rd</sup> order terrace), probably associated to the MIS 5c (Maunz and Hassler, 2000),  
201 shows extensive algal reefs and shoreface deposits, with elevations variation due to normal fault displacement (Zecchin  
202 et al., 2004; Nalin et al., 2012).

203 The Capo Colonna marine terrace (4<sup>th</sup> order terrace), correlated to MIS 5.3 (Palmentola et al., 1990; Zecchin et al., 2004,  
204 2009), or MIS 5.1 (ca 80 ka; Gliozzi 1987; Belluomini et al., 1988; Nalin et al., 2006; Nalin & Massari, 2009), consists  
205 of a planar surface with a sedimentary cover overlaid by a wedge of colluvium tapering (Bracchi et al., 2014).

206 The Le Castella marine terrace (5<sup>th</sup> order terrace) records an unconformity-bounded transgressive-regressive cycle (Nalin  
207 et al., 2007; Nalin & Massari, 2009; Zecchin et al., 2010; Bracchi et al., 2014; Bracchi et al., 2016), with two different  
208 facies for coralline algal build-ups and associated bioclastic deposits in the lower portion (Zecchin et al., 2004, 2011).  
209 The age of these deposits remains debated, as they have been correlated with MIS 5.3 (Gliozzi, 1987), MIS 5.1  
210 (Palmentola et al., 1990) and MIS 3 (Zecchin et al., 2004; Maunz & Hassler, 2000; Santagati et al., 2024).

211 The marine terraces exposed in emerged portion near the study area demonstrated extensive carbonate production due to  
212 the development of algal bioconstruction throughout the Late Pleistocene. This production also appears to currently affect  
213 the seafloor. However, although the onshore portion of the CB has been well studied, its offshore extension is still less  
214 known (Pepe et al., 2010). Nevertheless, data from the MaGIC Project related to Sheet 39 “Crotona” covered a vast area  
215 extending from the Neto Submarine Canyon to the Capo Rizzuto Swell. In this section, the continental shelf reaches up  
216 to 7 km wide, with the shelf break located at depths of 80–120 m. The slope encompasses the southern portion of the Neto  
217 Canyon headwall and the Esaro Canyon along with its tributaries. The average continental slope gradient is less than 5°  
218 and is characterised by an undulating morphology including the Luna and the Capo Rizzuto Swell. The southern section  
219 of the sheet covers the offshore extension of the Crotona forearc basin (Chiocci et al., 2021). This work aims to enhance  
220 the understanding of the Crotona Basin offshore features, with focus on underwater bioconstructed habitats.

221

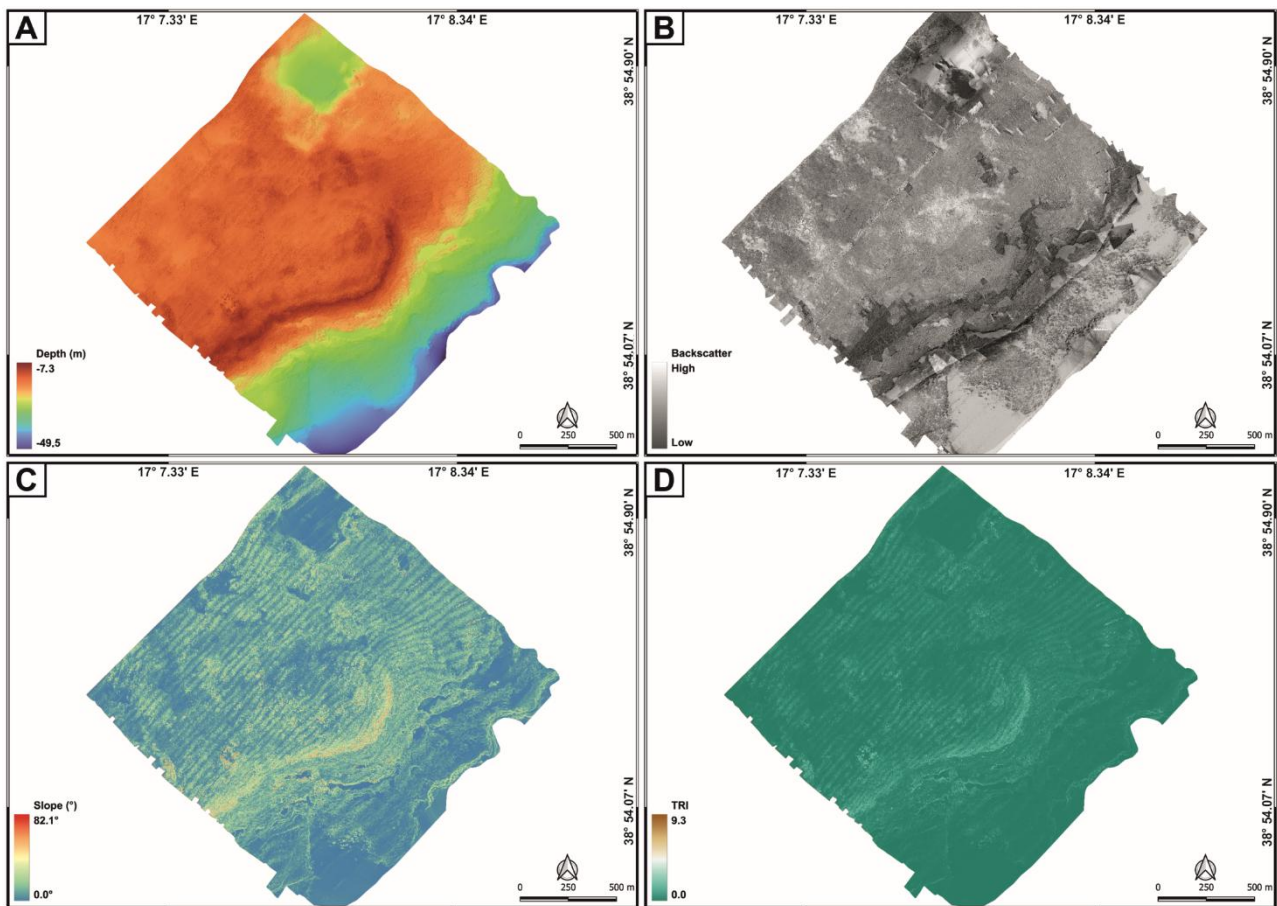


**Figure 3:** Conflated geological map of the Crotone peninsula, with the indication of the five order terraces (modified from Bracchi et al., 2014), and physiographic domains identified offshore the area in the frame of the MaGIC Project (modified from Chiocci et al., 2021).

## 4 Results

### 4.1 Morpho-acoustic characteristics of the seafloor

The comparison between bathymetric (Fig. 4A) and backscatter (Fig. 4B) data with those related to slope (Fig. 4C) and seafloor roughness (Fig. 4D) allowed for the definition of the morphological and morpho-acoustic characteristics of the study area off Capo Bianco (Calabria, Italy) and the identification of the benthic habitats. In particular, bathymetric data revealed a seafloor with depths ranging from -7.3 m to -49.5 m (Fig. 4A). The transition towards the deeper areas is not gradual but shows an evident break in slope (starting from about -15m depth), especially in the central zone of the study area. The shallower portion is characterized by widespread irregularities, while the deeper areas appear generally more regular, with less pronounced variations. Slope analysis (Fig. 4C) reveals maximum values (up to about 80°) along the break in slope, highlighting a steep and well-defined margin. The surrounding areas show lower slopes, with scattered peaks associated with seafloor irregularities. The Terrain Ruggedness Index showed: i) a higher roughness along the break in slope (where the highest TRI values were recorded) and in its immediate vicinity; ii) the presence of scattered roughness associated with irregularities on the seafloor (Fig. 4D).




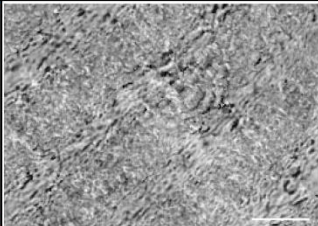

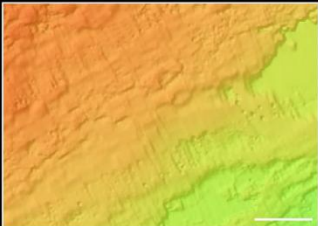
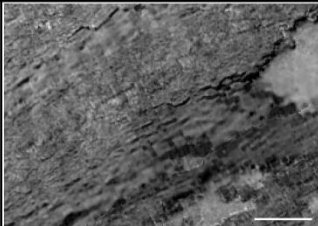

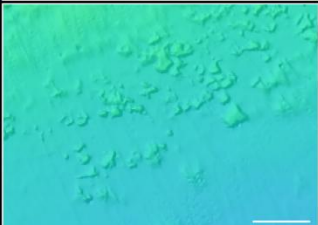
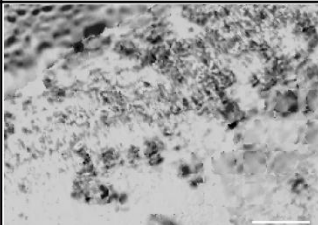
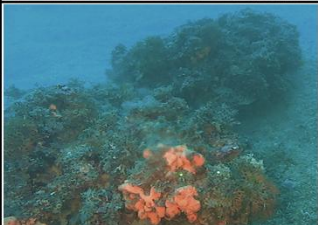
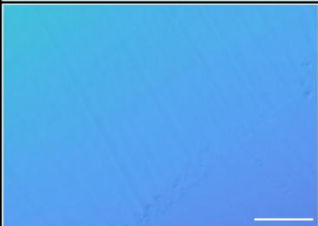
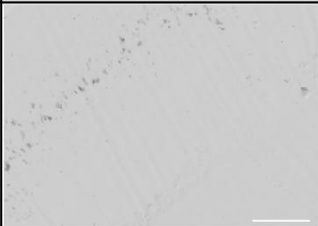



**Figure 4:** Geomorphological characters of the study area expressed through processed bathymetric (A), backscatter (B) data and geomorphometric indices, like slope (C) and Terrain Roughness Index (D).

Combining bathymetric and backscatter (Fig. 4B) data with slope and seafloor roughness values, different morpho-acoustic features were identified (Fig. 5):

- *Posidonia oceanica* meadows, characterized by an intermittent speckled fabric of moderate backscatter. *Posidonia* covers seabed areas characterized by low slopes and slight roughness, spanning a depth range from about -6 m to -25 m. In the depth range from -15 m to -25 m, analysis of ROV-video transects showed that *Posidonia* meadow forms a mosaic with the coralligenous habitat;
- banks of Coralligenous, characterized by a complex fabric of moderate to low backscatter. They covered areas characterized by moderate to high slopes and medium to high roughness, spanning a depth range from about -15 m to -25 m;
- discrete coralligenous build-ups surrounded by medium to coarse sediment and maerl are characterized by a dotted pattern of moderate backscatter. They covered areas characterized by low slopes and medium roughness and occupy the area between the end of the banks and the final depth of the MBES survey, at approximately -40 m depth;
- fine to medium sediment, characterized by homogeneous pattern of medium to high backscatter. It covers scattered portions throughout the study area at various depths and is characterized by very low TRI values.



Bathymetry -7.33  -49.51 m. (b.s.l.)	Backscatter High  Low	Seabed image (ROV–video transects)	Seabed Description
			<i>Posidonia oceanica</i> developing on sub-spherical rocky blocks
			Banks of Coralligenous partly covered with <i>Posidonia Oceanica</i>
			Discrete coralligenous build-ups surrounded by medium to coarse sediment and maerl
			Fine to medium sediment

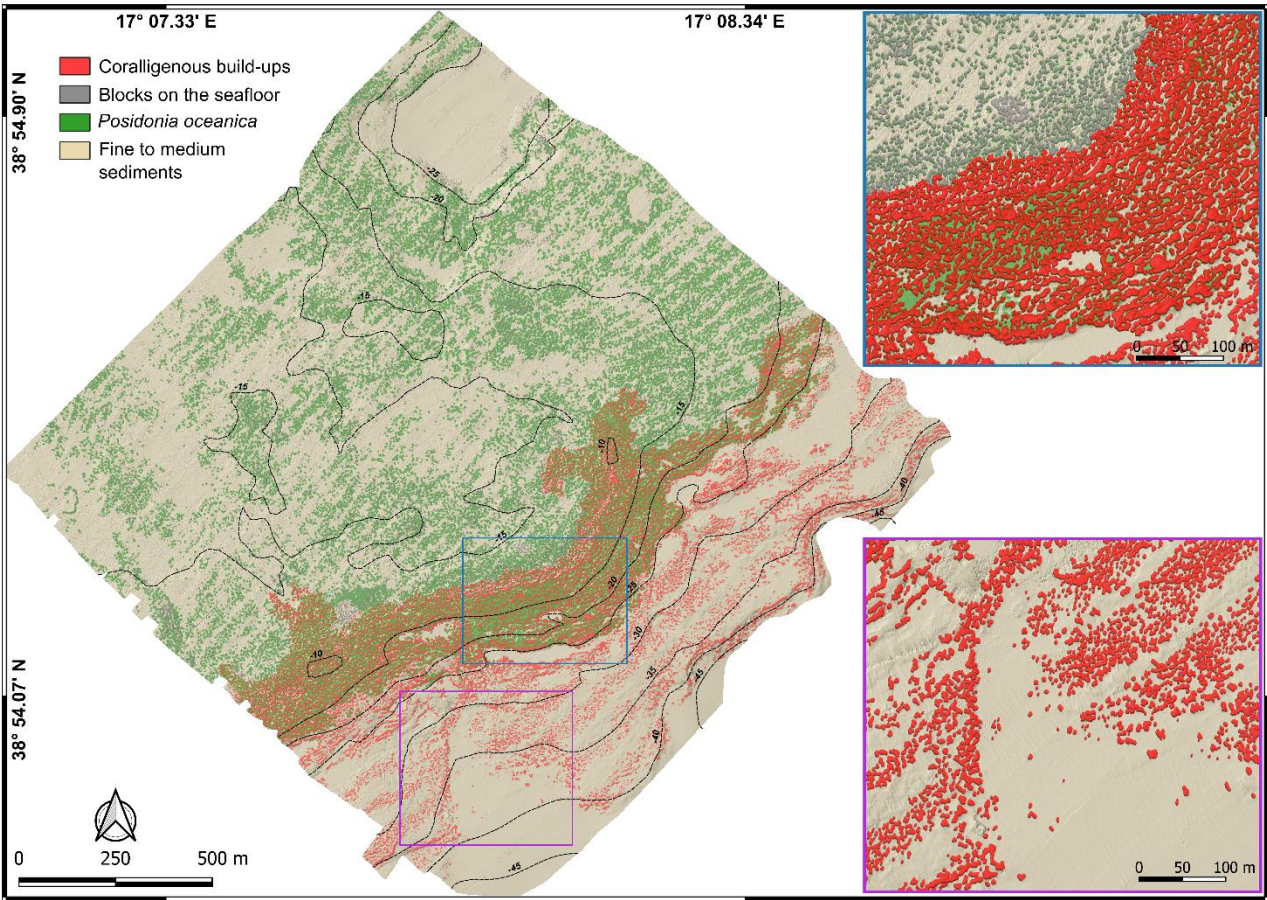
**Figure 5:** Morpho–acoustic features identified by bathymetric and BS data, together with ROV videos interpretation. White scale bar is 20 m.

The combination of the various morpho–acoustic features enabled the identification of four main benthic habitats (Fig. 6): i) *Posidonia oceanica* meadows; ii) mosaic of coralligenous and *Posidonia*; iii) Coralligenous *sensu stricto* (i.e., bioconstructions that are not spatially intermixed with *Posidonia oceanica*); iv) fine to medium sediment.

The *Posidonia* habitat, testified by its typical BS signal (intermittent speckled fabric of moderate backscatter), dominate in shallow areas (down to about -15 m depth), where it primarily colonizes rocky substrate. In this area, ROV imagery and bathymetric data also highlight the occurrence of sub-spherical rocky blocks on the seabed, often surrounded by *Posidonia oceanica* (Fig. 5).

Between -15 m and -25 m, the *Posidonia* backscatter signal gradually attenuates and coralligenous bioconstructions start to be discernible. This transitional belt, that occupies about 0.37 km<sup>2</sup>, was classified as a mosaic of Coralligenous and *Posidonia oceanica*. Visual analysis of ROV-video transects, used as ground-truth, indicates that in this zone bioconstructions, mainly belonging to the banks morphotype, develop on a hard substrate that marks the widespread break in slope throughout the study area.

Below -25 m, *Posidonia* is no longer detected and the predominant benthic habitat is represented by Coralligenous *sensu stricto*. These bioconstructions, often associated with fine to medium sediment and maerl, predominantly belong to the discrete reliefs morphotype and tend to align sub-parallel to the shoreline.



**Figure 6:** Mapping model of the underwater benthic habitats in the study area off Capo Bianco (Calabria, Italy). Note, in the blue and purple boxes, two magnifications of representative areas of the model where coralligenous bioconstructions and rocky blocks on the seabed are depicted in 2.5D.

#### 4.2 Extraction of coralligenous build-ups

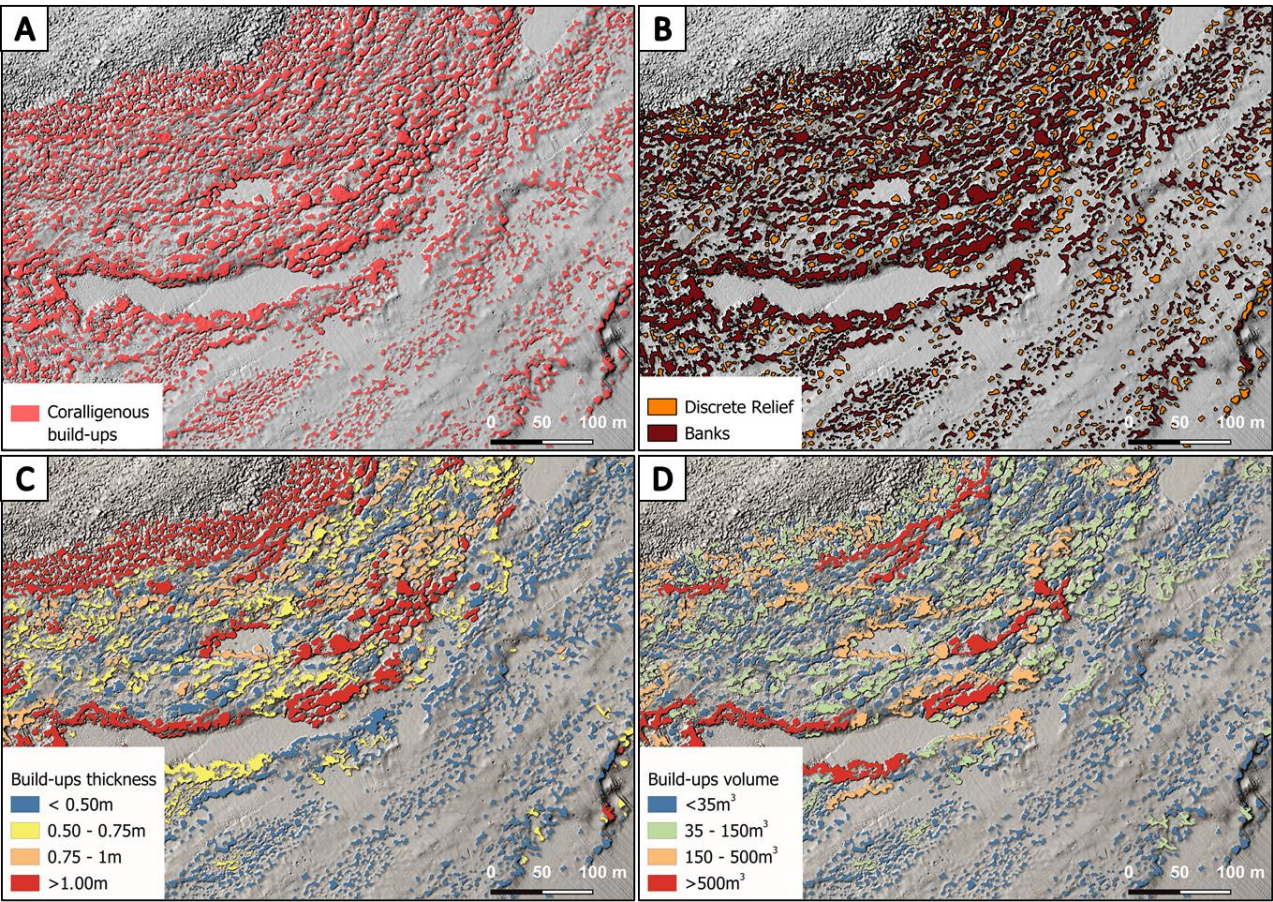
The model extracted 12384 polygons, but only 9211 positive morphologies were finally related to coralligenous build-ups considering the hillshade values and validation from ROV-video transects collected within the study area (Fig. 7A). This means that about 25 % of the polygons extracted using the TPI were found to be artifacts after the re-classification and the polygonization of resulting raster. According to Marchese et al. (2020), the artifacts may be due to: i) occurrence of *Posidonia oceanica* (Innangi et al., 2015) (Fig. 8A); ii) bad roll correction (Fig. 8C); iii) artifacts concentration on DTM boundaries (Fig.8E). While artifacts of types ii) and iii) can be reduced by performing more accurate MBES surveys (*i.e.*, larger coverage, greater overlapping, and narrower swath width), those related to *Posidonia oceanica* represent real morphological features that cannot be removed by improving survey quality. The identification of artifacts was based on specific pattern inconsistent with expected Coralligenous morphologies, and their removal was carried out manually as part of the data cleaning process (Fig. 8B, D, F). The time required for the cleaning phase strongly depends on the quality of the survey execution, the geomorphological and ecological complexity of the study area and the experience of the operator performing the cleaning. These factors can significantly influence the extent and efficiency of manual artifact removal.



Regarding the distinction between coralligenous bioconstructions and *Posidonia oceanica* in the mosaic area, the separation was primarily based on the characteristics of the backscatter signal. Specifically, as discussed previously, *Posidonia* is associated with a moderate, speckled acoustic texture, while coralligenous bioconstructions exhibit a more complex and spatially structured acoustic signature. These interpretations were supported by ROV video transects, which help to validate the differentiation.

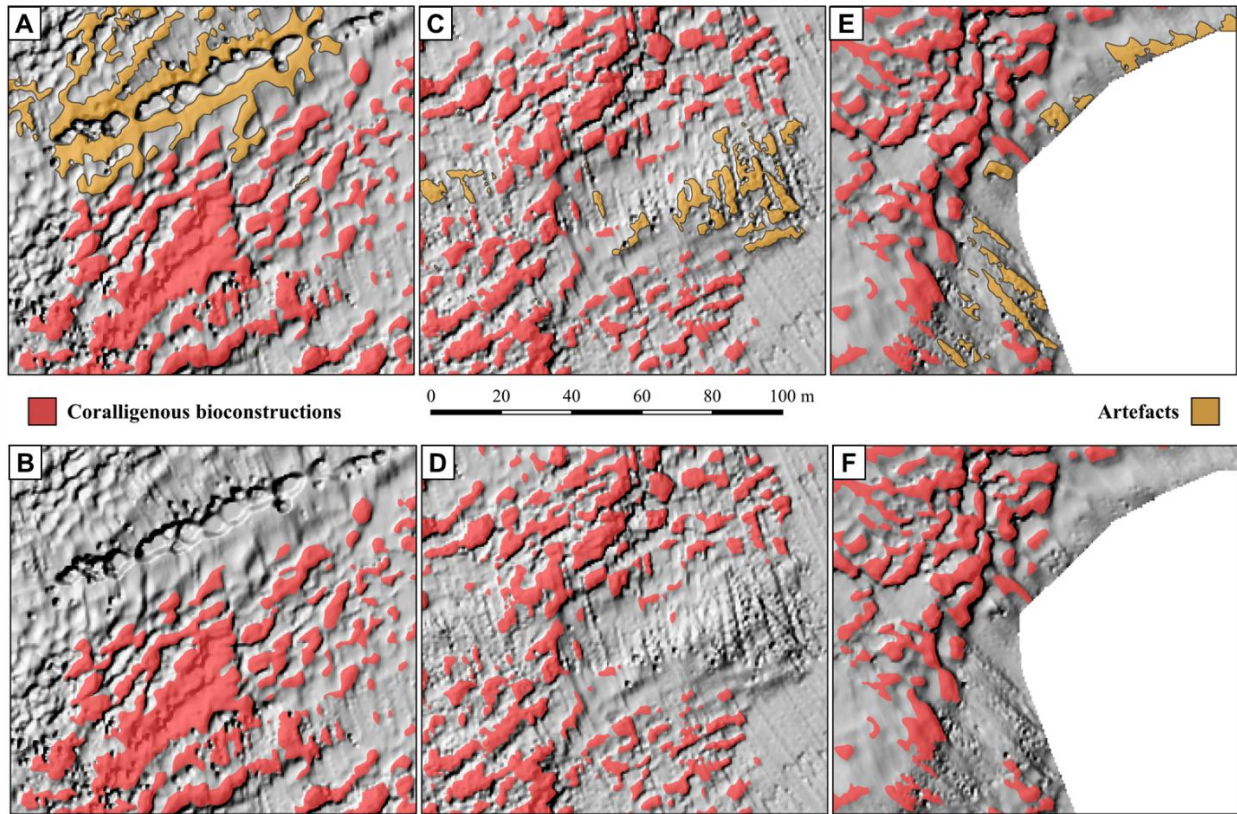
### 4.3 Shape index, thickness, surface and volume of coralligenous build-ups

Shape Index (SI) values allowed to distinguish between banks (tabular bank *sensu* Bracchi et al., 2016;  $SI \leq 2$ ) and discrete reliefs (discrete reliefs and hybrid banks *sensu* Bracchi et al., 2016;  $SI > 2$ ) (Fig. 7B). Following this approach, it was possible to identify 7001 polygons belonging to the morphotype of the banks and 2210 classified as discrete reliefs. As shown in Table 1, banks have a greater average thickness (Fig. 7C) compared to discrete reliefs (0.65 m vs 0.49 m, respectively) and cover an area of 155677 m<sup>2</sup>, which represents about 5.2 % of the seabed in the study area. In contrast, discrete reliefs cover only 2.6 % of the seafloor, with a surface area of 69830 m<sup>2</sup>. The volume (Fig. 7D) occupied by discrete reliefs (40806 m<sup>3</sup>) is also significantly lower than that of the banks (116094 m<sup>3</sup>). This data is consistent with the fact that discrete reliefs are characterized by smaller extent and thickness compared to the banks.



**Figure 7:** (A) Result of build-ups extraction using TPI. (B) Differentiation of coralligenous build-ups into discrete relief and banks based on the SI value. (C) Estimation of build-ups thickness. (D) Calculation of the volume for each coralligenous polygon.





**Figure 8:** Examples of artifacts identified during polygon extraction and their manual removal. (A) False positive caused by the presence of *Posidonia oceanica* and (B) the same area after removal; (C) artifact due to bad roll correction and (D) corrected version; (E) artifacts at the boundary of the DTM and (F) cleaned result.

**Table 1:** Classification of coralligenous polygons, based on SI values, and results in terms of area and volume.

Morphotype	Shape Index Values	Average Thickness (m)	Area (m <sup>2</sup> )	Volume (m <sup>3</sup> )
Banks	$\leq 2$	0.65	155677	116094
Discrete Reliefs	$> 2$	0.49	69830	40806

## 5 DISCUSSION

Acoustic techniques, such as high-resolution swath bathymetry sounder (including backscatter), side scan sonar and acoustic profiling are optimal tools for quickly recognize and identify the extension of benthic habitats on the seabed and map their distribution without mechanical collection of samples, which would damage this delicate ecosystem (Bracchi et al., 2017).

Traditionally, the segmentation of MBES data sets have been performed manually, despite the process might be inaccurate and subjective (Cutter et al., 2003; Bishop et al., 2012). Initial attempts at automation employed object-oriented methods using object-based image analysis (OBIA) or considered a comprehensive set of remote data to accurately characterize seabed landforms for documenting the extension of benthic habitat (e.g., Lucieer and Lamarche, 2011; Ismail et al., 2015; Janowski et al., 2018; Fakiris et al., 2019). More recently, the growing availability of high-resolution MBES data has encouraged the application of deep learning approaches, particularly Convolutional Neural Networks (CNNs) and Fully Convolutional Neural Networks (FCNNs), which produce pixel-wise classifications in order to create semantically segmented maps. These methods have proven effective in identifying geomorphological features such as bedrock outcrops, pockmarks, submarine dune and ridges, offering high accuracy and repeatability (Arosio et al., 2023; Garone et



al., 2023). Additionally, 3D CNNs have been applied to automated denoising of MBES data, enhancing the efficiency of bathymetric data workflow (e.g., Stephens et al., 2020).

Nonetheless, a universally accepted and standardized methodology for geomorphological classification of the seafloor is still lacking. Indeed, existing approaches remain highly case-specific, depending on the study area, data quality, and research objective. Moreover, relatively limited attention has been devoted to the morphological characterization of Coralligenous bioconstructions, despite their ecological relevance. Indeed, only a few studies have attempt to map these complex biogenic structures in detail. Bracchi et al. (2017) proposed a categorization of coralligenous morphotypes on sub-horizontal substrate based on integrated acoustic data and ground-truthing, defining new morphological classes such as tabular banks, hybrid banks and discrete reliefs across the Apulian shelf. Subsequently, Marchese et al. (2020) proposed a protocol that combines acoustic datasets and geomorphometric analysis, performed using ArcGIS™, in order to define the 2D and 3D complexity of coralligenous build-ups and to quantify how much carbonate is deposited. More recently, Varzi et al. (2022) produced a morpho-bathymetric map for the continental shelf offshore Marzamemi (Sicily, Italy) that contained quantitative description for the distribution and extent of coralligenous reefs.

The approach proposed in this work, based on the workflow shown in Figure 2, represents the first attempt to define the benthic habitat in the Isola Capo Rizzuto Marine Protected Area and to quantify the extent and morphometric characteristics of coralligenous bioconstructions present therein using exclusively open-source software during post-processing phases.

## 5.1 Spatial distribution of benthic habitats and seafloor morphology

The benthic habitat distribution identified in the study area exhibits a clear spatial zonation, which appear to be influenced by both substrate characteristics and geomorphological features. In the shallowest sector (above -15m depth), *Posidonia oceanica* represent the prevalent benthic habitat. In the intermediate depth range (down to approximately -25m depth), a mosaic of *Posidonia* and coralligenous bioconstructions develops, indicating a transitional zone where environmental conditions allow the coexistence of seagrass and algal reefs.

Comparison between the morphological characteristics of the seabed with the alignment and elevation of the emerged marine terraces highlights the presence of a flat, laterally continuous submerged surface, as typically observed in relict marine terraces (e.g., Savini et al., 2021; Lebrec et al., 2022). This sub-horizontal platform is bounded seaward by a break in slope, located at approximately -15 m depth, interpreted as the outer margin of the terrace. Based on these evidences, the submerged surface can be correlated with the 5<sup>th</sup> order terrace exposed near Le Castella, characterized by a gently seaward-inclined surface and a morphological step interpreted as paleoclipf (Bracchi et al., 2016). The different orientation of the submerged scarp in the study area (NE-SW), compared to the emerged paleoclipf associated with Le Castella marine terrace (NW-SE to E-W), may be reasonably attributed to local coastal curvature and/or tectonic influences. The submersion of this portion of the 5<sup>th</sup> order terrace in the study area would be justified by the possible presence of a tectonic feature with extensional kinematics located approximately along the coastline, which shows a distinctly straight alignment with a N-S orientation. However, further investigations are needed to confirm this hypothesis.

The inner portion of the submerged surface is characterized by the presence of sub-spherical blocks, often colonized by *Posidonia oceanica*, which possibly result from gravitational processes affecting the adjacent 4<sup>th</sup> order marine terrace located upslope. This interpretation is supported by their rounded morphology, typically associated with detachment and downslope transport, and by the presence of scarps in the emerged portion of the study area, which could indicate past gravitational instability.

377 The outer portion and the edge of the submerged platform (down to approximately -25m) hosts several coralligenous  
378 build-ups, predominantly belonging to banks morphotype. Similar spatial arrangements have been observed in submerged  
379 terraces of southeastern Sicily (Varzi et al., 2022) and on wave-cut ravinement surfaces associated with fossil marine  
380 terraces, such as the mid-Pleistocene Cutro terrace (Nalin et al., 2006) and the emerged 5<sup>th</sup> order terrace of Le Castella  
381 (Bracchi et al., 2016).

382 In the deeper sector of the study area (below -25m depth), *Posidonia* is no longer present and the benthic assemblages are  
383 composed by Coralligenous *sensu stricto* associated with fine to medium sediments and maerl. These bioconstructions  
384 mainly belong to discrete reliefs morphotype and tend to follow a sub-parallel orientation relative to the shoreline, a  
385 distribution pattern that appears associated with relatively pronounced seafloor structures (as revealed by ROV-video  
386 transects). This spatial configuration suggests that environmental or geomorphological factors may influence the  
387 development and positioning of build-ups. Particularly, two hypotheses are proposed to explain this pattern: i) the  
388 influence of bottom currents and internal waves, which may promote the alignment of coralligenous bioconstructions, as  
389 observed in mesophotic carbonate systems of the Maltese shelf by Bialik et al. (2024); ii) an overprint of the build-ups  
390 onto inherited seabed morphologies, shaped by sea-level fluctuation and regional uplift during the Quaternary  
391 glacial/interglacial cycles, as documented on submerged terraces offshore Marzamemi (SE Sicily) by Varzi et al. (2022).  
392 However, further investigations, including in situ hydrodynamic and sediment transport measurements, are necessary to  
393 validate these hypotheses.

394

## 395 5.2 TPI-based feature extraction

396 Coralligenous build-ups were treated as distinct features in both two- and three-dimensional spaces, with the aim of  
397 using a geomorphometric parameters for their extraction from the seafloor. Variability of coralligenous morphotypes  
398 (Bracchi et al., 2017) poses several challenges to their automated extraction from DTM. Since build-ups raise from the  
399 surrounding seafloor, their detection could be performed by slope analysis. However, while slope proves effective for  
400 accurately segmenting isolated small-scale features (Savini et al., 2014; Bargain et al., 2017), it struggles to incorporate  
401 the inner areas of banks into the segmentation process. The high 3D complexity in these areas makes it challenging to  
402 create a continuous polygon. On the other hand, geomorphometric parameters like the rugosity index (i.e., TRI; Riley et  
403 al., 1999) are more successful in defining the overall distribution of bank morphotypes, but they fail to provide an accurate  
404 estimation of the size of discrete reliefs. Therefore, as noted by Marchese et al. (2020), TPI offers a good compromise for  
405 detecting coralligenous morphotypes. Indeed, it assesses the relative topographic position of a central point by calculating  
406 the difference between its elevation and the average elevation within a predefined neighbourhood. In this work, the input  
407 parameters for the calculation of the TPI have been refined in order to minimize the artifacts during the extraction process.  
408 Specifically, the choice of a threshold value of 0.2 (lower than 0.3 used by Marchese et al., 2020), combined with higher  
409 values of Power and Bandwidth compared to the default ones, has allowed for a 15% reduction in the artifact percentage  
410 compared to Marchese et al. (2020). These adjustments have therefore significantly reduced the manual review time,  
411 improving the automatization of the extraction process.

412 The threshold value adopted for the TPI analysis was defined through a trial-and-error procedure, as described in the  
413 methodological section. In particular, threshold values lower than 0.2 increased the morphological adherence of the  
414 extracted features to seabed forms, but at cost of a higher number of false positives (especially in areas covered by  
415 *Posidonia oceanica*, where slight topographic variations were incorrectly interpreted as relevant morphotypes).  
416 Conversely, threshold values higher than 0.2 reduced the occurrence of artifacts but led to the omission of low-relief

417 structures, thus compromising the completeness of mapping. In this work, a threshold value of 0.2 proved to be an  
418 effective compromise, ensuring a satisfactory balance between the accuracy of morphotype extraction and the  
419 minimization of false positive. This configuration allowed for the preservation of relevant coralligenous bioconstructions,  
420 including low-relief build-ups, while significantly limiting the occurrence of artifacts.

421 The proposed approach, although developed only for a specific coastal area, can be transferred to other regions, provided  
422 that adequate calibration is performed. The effectiveness of TPI-based extraction depends on several factors, and no  
423 universally applicable threshold value exists, as it must be adapted to the resolution and quality of bathymetric data, as  
424 well as to the site-specific geomorphological and geobiological variability. To date, no standardized procedure is available  
425 for determining the optimal threshold; however, its selection can be refined through iterative testing supported by ground-  
426 thrut validation. Once the appropriate input parameter for TPI calculation (e.g., Power, Bandwidth, minimum and  
427 maximum radius) ad a suitable threshold value are identified, the method allows for the extraction of morphologically  
428 distinct features, provided these are sufficiently expressed relative to the surrounding seafloor.

429

### 430 **5.3. Morphological development of coralligenous build-ups**

431 The quantitative morphometric data (*i.e.*, surface, thickness, volume, maximum diameter and shape indices), extracted  
432 from the benthic habitat mapping model proposed in this work, were plotted in the scatterplots of Figure 8, providing new  
433 insights into spatial distribution, morphotype variability and growth pattern of the coralligenous build-ups across the study  
434 area.

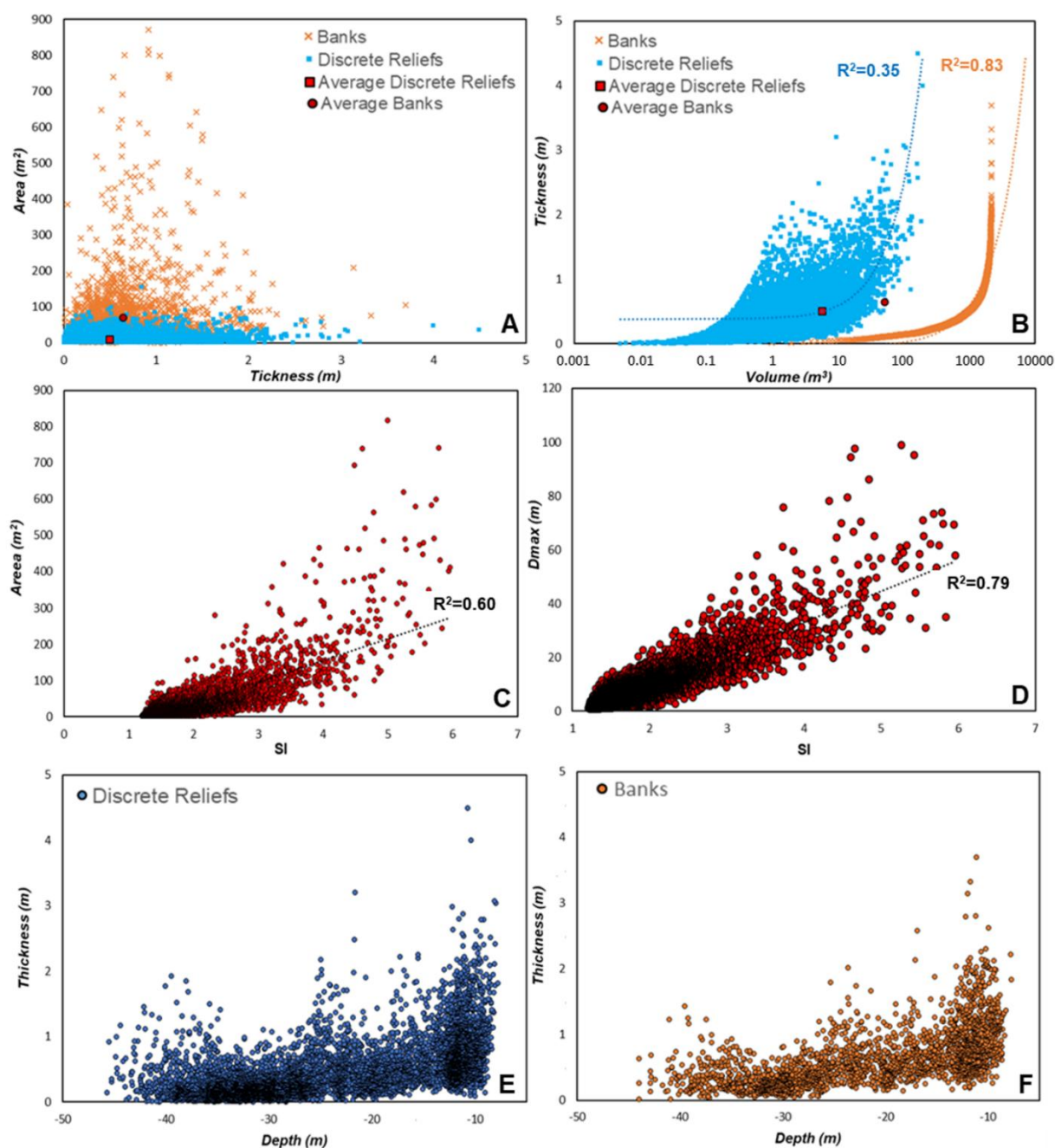
435 Most polygons, representing aggregates of different coralligenous build-ups, are characterized by areas smaller than 200  
436 m<sup>2</sup> and less than 1 m thick (Fig. 8A). However, discrete reliefs and banks display some differences in their distribution:  
437 discrete reliefs tend to cluster in the lower part of the graph (smaller areas and lower thickness), whereas banks with  
438 similar thickness generally exhibit larger areas on average.

439 The volume of the build-ups is strongly dependent on thickness, suggesting that vertical growth plays a key role in the  
440 formation of these structures (Fig. 8B). However, discrete reliefs show a more irregular distribution, with a greater  
441 dispersion of data ( $R^2 = 0.35$ ). This trend suggests that volume increase depends not only on thickness but also on a  
442 significant lateral growth component. Conversely, banks exhibit a more regular trend, with volume increasing  
443 proportionally with thickness. The strong correlation between thickness and volume ( $R^2 = 0.83$ ) aligns with a growth  
444 pattern that is almost exclusively vertical for this morphotype.

445 The relationships between area and shape indices (SI) of coralligenous build-ups (Fig. 8C), despite a moderate data  
446 dispersion, revealed a positive correlation ( $R^2 = 0.61$ ), suggesting that more irregularly shaped bioconstructions (typically  
447 associated with the morphotypes of banks) tend to cover larger areas. Moreover, banks also tend to have larger maximum  
448 diameter (Dmax), as suggested by an  $R^2$  value of 0.78 (Fig. 8D). However, the greater variability in area might reflect  
449 higher spatial complexity in the distribution of these structures.

450 The relationship between depth and thickness of coralligenous bioconstructions, divided into banks (Fig. 8F) and discrete  
451 reliefs (Fig. 8E), reveals that both morphotypes exhibit average decreasing thickness with increasing depth. However,  
452 discrete reliefs show greater thickness variability, with higher dispersion of data at depths shallower than -25 m, whereas  
453 for the banks, data distribution is more regular. The decrease in the thickness of bioconstructions with increasing depth  
454 could be attributed to various causes, including changes in hydrodynamic energy, the characteristics of the substrate on  
455 which the bioconstructions develop, or sedimentation conditions.

456 To date, no previous study has provided morphometric analysis of coralligenous build-ups based on quantitative extraction  
 457 of 2D/3D parameters (e.g., area, thickness, volume, shape indices) from high-resolution MBES data. Therefore, a direct  
 458 comparison of our results with other Mediterranean coralligenous fields is currently not possible. Nonetheless, several  
 459 works have described the geomorphological variability of coralligenous morphotypes across the Mediterranean basin  
 460 (e.g., Bracchi et al., 2015, 2017, 2022; Marchese et al., 2020). These studies recognize the coexistence of morphotypes  
 461 such as banks and discrete reliefs, often occurring over short spatial scale and associated with different environmental  
 462 conditions. The same spatial mixing of these morphotypes, which may be due to small-scale variations in substrate type,  
 463 hydrodynamic regime, or inherited seabed features, which locally favour distinct growth mode despite spatial proximity  
 464 (Bracchi et al., 2017; Marchese et al., 2020; Varzi et al., 2022), was also observed in our study area.



466  
 467 **Figure 8:** Scatterplot representing relationships between: area and thickness (A); thickness and volume (B); area and shape index (C);  
 468 maximum diameter and shape index (D); thickness and depth for banks (E) and discrete relief (F). These quantitative geometric data  
 469 were extracted by the benthic habitat mapping model proposed in this work. SI: shape index; Dmax: maximum diameter.



## 470 CONCLUSIONS

471 A new mapping approach starting from high-resolution acoustic data acquired through MBES surveys performed offshore  
 472 Capo Bianco (Isola Capo Rizzuto Marine Protected Area) was developed and presented here. The method represents a  
 473 step forward, as it builds on an integrated two foundational approaches in coralligenous habitat studies: the morphotyping  
 474 of Coralligenous based on the shape index, and their spatial and volumetric quantification.

475 The innovation of this work lies in the synthesis of these methodologies, which were applied and refined in a new study  
 476 area. Moreover, the approach, which integrates bathymetric and backscatter data with geomorphological and  
 477 geomorphometric indices, was performed using open-source software, providing a detailed workflow that can be freely  
 478 reproduced and adopted by organizations involved in research, monitoring and conservation of marine habitats.

479 The resulting model proved capable not only in identifying and differentiating the benthic habitats but also in providing  
 480 new quantitative information regarding the spatial distribution and 2D/3D geometric characteristics of the extracted  
 481 coralligenous build-ups. This innovative aspect, compared to the traditional mapping protocol, is crucial for the  
 482 quantification of the structural complexity of these bioconstructions. Moreover, this approach enables monitoring of  
 483 variations not only in terms of the habitat's areal extent, but also in terms of vertical development of Coralligenous relative  
 484 to the substrate from which build-ups form. Indeed, the quantitative geomorphometric data obtained from the mapping  
 485 model of Capo Bianco seafloor were analyzed, revealing significant insights into the covered surface, volume and  
 486 thickness of build-ups, as well as the relationships among these parameters. In particular, the results highlighted that the  
 487 discrete reliefs morphotype exhibit a much more pronounced lateral growth component compared to the banks. If  
 488 confirmed through an accurate geobiological characterization, these finding could provide important new insights about  
 489 the tempo and mode of the inception and development of these hard-biogenic substrates, crucial for the conservation of  
 490 Mediterranean biodiversity.

## 491 Author contributions

492 Conceptualization: G.M., A.G.; Methodology: G.M, A.G., G.I., F.M.; Formal analysis and investigation: G.M., M.C.,  
 493 G.I.; U.S.; F.M.; Writing – original draft preparation: G.M., M.C., G.V., F.P., A.L., E.C., R.S.; Writing – review and  
 494 editing: R.D., C.A., F.B., V.A.B., D.B., A.R., A.G.; Funding acquisition: A.G., F.B.; Resources: R.D., F.B., A.L., E.C.,  
 495 A.G.; Supervision: A.G.

## 496 Competing interests

497 The contact author has declared that none of the authors has any competing interests.

## 498 Acknowledgments

499 We would like to express our sincere gratitude to the Geobiology and Marine Laboratories of the DiBEST, University  
 500 of Calabria, for their invaluable support and contribution to this work.

## 501 Financial support

502 This work was funded by the Next Generation EU – Tech4You – “Technologies for climate change adaptation and quality  
 503 of life improvement – Tech4You”, Project “Development of tools and applications for integrated marine communities and  
 504 substrates monitoring”, PP 2.3.1 – Action 1 “Development of hardware and software systems for three-dimensional  
 505 detection, sampling and mapping of underwater environments”, CUP H23C22000370006. This work reflects only the

506 authors' views and opinions, neither the Ministry for University and Research nor the European Commission can be  
507 considered responsible for them.

508

## 509 **Open Research**

510 The data sets needed to evaluate results and conclusion in this paper are available at  
511 [http://geocube.unical.it/gmaruca/Dataset\\_Benthic\\_Habitat\\_Mapping.zip](http://geocube.unical.it/gmaruca/Dataset_Benthic_Habitat_Mapping.zip) (Maruca et al., 2025). The raw data used in this  
512 study were acquired through MBES survey using a pole-mounted, Norbit WBMS Basic multibeam sonar system  
513 integrated with GNSS/INS (Applanix OceanMaster). The processing of MBES bathymetric data was performed using  
514 QPS Qimera (<https://qps.nl/qimera/>). Backscatter data processing was performed using QPS Fledermaus  
515 (<https://qps.nl/fledermaus/>). Figures 1, 3, 4, 6, 7 were made with QGIS 3.34.9 “Prizren” software  
516 (<https://qgis.org/project/overview/>). Figures 8 were generated using Microsoft Excel ([https://www.microsoft.com/it-](https://www.microsoft.com/it-it/microsoft-365)  
517 [it/microsoft-365](https://www.microsoft.com/it-it/microsoft-365)). Data used to generate the figures are available upon request to the corresponding author.

## 518 **REFERENCES**

519 Abdullah, M. Z., Chuah, L.F., Zakariya, R., Syed, A., Rozaimi, C. H., Mahmud, S. M., Abdallah M. E., Bokhari, A.,  
520 Muhammad, S. A. and Al-Shwaiman, H. A.: Evaluating climate change impacts on reef environments via multibeam  
521 echosounder and Acoustic Doppler Current profiler technology. *Environmental Research*, Volume 252, Part 3, 118858,  
522 <https://doi.org/10.1016/j.envres.2024.118858>, 2024.

523

524 Arosio, R., Hobley, B., Wheeler, A. J., Sacchetti, F., Conti, L. A., Furey, T. and Lim, A.: Fully convolutional neural  
525 networks applied to large-scale marine morphology mapping. *Frontiers in Marine Science*, 10-1228967,  
526 <https://doi.org/10.3389/fmars.2023.1228867>, 2023.

527

528 Ballesteros, E.: Mediterranean Coralligenous Assemblages: a synthesis of present knowledge. *Oceanography and Marine*  
529 *Biology, Annual Review*, 44, 123–195, 2006.

530

531 Basso, D., Bracchi, V. A., Bazzicalupo, P., Martini, M., Maspero, F. and Bavestrello, G.: Living coralligenous as geo-  
532 historical structure built by coralline algae. *Frontiers in Earth Science*, 10, 961632,  
533 <https://doi.org/10.3389/feart.2022.961632>, 2022.

534

535 Bazzicalupo, P., Cipriani, M., Guido, A., Bracchi, V. A., Rosso, A. and Basso, D.: Calcareous nannoplankton inside  
536 coralligenous build-ups: the case of Marzamemi (SE, Sicily). *Bollettino della Società Paleontologica Italiana*, 63 (1), 89–  
537 99, <https://dx.doi.org/10.4435/BSPI.2024.09>, 2024.

538

539 Belluomini, G., Gliozzi, E., Ruggieri, G., Branca, M. and Delitala, L.: First dates on the terraces of the Cortone Peninsula  
540 (Calabria, southern Italy). *Italian Journal of Geosciences*, 107 (1), 249–254, 1988.

541

542 Betzler, C., Brachert, T. C., Braga, J. C. and Martin, J. M.: Nearshore, temperate, carbonate depositional systems (lower  
543 Tortonian, Agua Amarga Basin, southern Spain): Implications for carbonate sequence stratigraphy. *Sedimentary Geology*,  
544 113, 27–53, 1977.

545

546 Bishop, M. P., James, L. A., Shroder, J. F. & Walsh, S. J.: Geospatial technologies and digital geomorphological mapping:  
547 Concepts, issues and research. *Geomorphology*, 137, 5–26, <http://dx.doi.org/10.1016/j.geomorph.2011.06.027>, 2012.

548

549 Bonardi, G., Cavazza, W., Perrone, V. and Rossi, S.: Calabria–Peloritani terrane and northern Ionian Sea. In Vai, G. B.  
550 & Martini, I. P. (eds.), *Anatomy of an Orogen: The Apennines and Adjacent Mediterranean Basins*, Kluwer Academic  
551 Publishers (pp. 287–306), [http://dx.doi.org/10.1007/978-94-015-9829-3\\_17](http://dx.doi.org/10.1007/978-94-015-9829-3_17), 2001.

552 Bracchi, V. A., Basso, D., Marchese, F., Corselli, C. and Savini, A.: Coralligenous morphotypes on subhorizontal  
553 substrate: A new categorization. *Continental Shelf Research*, 144, 10–20. <http://dx.doi.org/10.1016/j.csr.2017.06.005>,  
554 2017.

555

556 Bracchi, V. A., Bazzicalupo, P., Fallati, L., Varzi, A. G., Savini, A., Negri, M. P., Rosso, A., Sanfilippo, R., Guido, A.,  
557 Bertolino, M., Costa, G., De Ponti, E., Leonardi, R., Muzzupappa, M., and Basso, D.: The Main Builders of Mediterranean  
558 Coralligenous: 2D and 3D Quantitative Approaches for its Identification. *Frontiers in Earth Science*, 10, 910522  
559 <https://doi.org/10.3389/feart.2022.910522>, 2022.

560

561 Bracchi, V. A., Nalin, R. and Basso D.: Morpho-structural heterogeneity of shallow–water coralligenous in a Pleistocene  
562 marine terrace (Le Castella, Italy). *Palaeogeography, Palaeoclimatology, Palaeoecology*, 454, 101–112,  
563 <http://dx.doi.org/10.1016/j.palaeo.2016.04.014>, 2016.

564

565 Bracchi, V. A., Nalin, R. and Basso, D.: Paleoeecology and dynamics of coralline–dominated facies during a Pleistocene  
566 transgressive–regressive cycle (Capo Colonna marine terrace, Southern Italy). *Palaeogeography, Palaeoclimatology,*  
567 *Palaeoecology*, 414, 296–309, <http://dx.doi.org/10.1016/j.palaeo.2014.09.016>, 2014.

568

569 Bracchi, V. A., Savini, A., Marchese, F., Palamara, S., Basso, D. and Corselli C.: Coralligenous habitat in the  
570 Mediterranean Sea: a geomorphological description from remote data. *Italian Journal Geosciences*, 134 (1), 32–40,  
571 <https://doi.org/10.3301/IJG.2014.16>, 2015.

572

573 Brown, C. J., Sameoto, J. A., & Smith, S. J.: Multiple methods, maps, and management applications: Purpose made  
574 seafloor maps in support of ocean management. *Journal of Sea Research*, 72, 1–13,  
575 <https://doi.org/10.1016/j.seares.2012.04.009>, 2012.

576

577 Cavazza, W., Blenkinsop, J., De Celles, P. G., Patterson, R. T. and Reinhardt, E. G.: Stratigrafia e sedimentologia della  
578 sequenza sedimentaria oligocenica–quaternaria del bacino Calabro–Ionico. *Bollettino della Società Paleontologica*  
579 *Italiana*, 116, 51–77, 1997.

580

581 Chiocci, F. L., Budillon, F., Ceramicola, S., Gamberi, F. and Orrù, P.: Atlante dei lineamenti di pericolosità geologica dei  
582 mari italiani. CNR edizioni, RM: Risultati del progetto MaGIC, 2021.

583  
584  
585  
586  
587  
588  
589  
590  
591  
592  
593  
594  
595  
596  
597  
598  
599  
600  
601  
602  
603  
604  
605  
606  
607  
608  
609  
610  
611  
612  
613  
614  
615  
616  
617  
618  
619  
620  
621  
622

Cipriani, M., Apollaro, C., Basso, D., Bazzicalupo, P., Bertolino, M., Bracchi, V. A., Bruno, F., Costa, G., Dominici, R., Gallo, A., Muzzupappa, M., Rosso, A., Sanfilippo, S., Sciuto, F., Vespasiano, G. and Guido, A.: Origin and role of non-skeletal carbonate in coralligenous build-ups: new geobiological perspectives in biomineralization processes. *Biogeosciences*, 21, 49–72, <https://doi.org/10.5194/bg-21-49-2024>, 2024.

Cipriani, M., Basso, D., Bazzicalupo, P., Bertolino, M., Bracchi, V. A., Bruno, F., Costa, G., Dominici, R., Gallo, A., Muzzupappa, M., Rosso, A., Perri, F., Sanfilippo, R., Sciuto, F. and Guido, A.: The role of non-skeletal carbonate component in Mediterranean Coralligenous: new insight from the CRESCIBLUREEF project. *Rendiconti Online Societa Geologica Italiana*, 59, 75–79. <https://doi.org/10.3301/ROL.2023.12>, 2023.

Conrad, O., Bechtel, B., Bock, M., Dietrich, H., Fischer, E., Gerlitz, L., Wehberg, J., Wichmann, V. and Böhner, J.: System for Automated Geoscientific Analyses (SAGA). *Geoscientific model development*, 8, <https://doi.org/10.5194/gmd-8-1991-2015>, 2015.

Cosentino, D., Gliozzi, E. and Salvini, F.: Brittle deformations in the Upper Pleistocene deposits of the Croton Peninsula, Calabria, southern Italy. *Tectonophysics*, 163, 205–217, 1989.

Cutter, G. R., Rzhannov, Y. and Mayer, L. A.: Automated segmentation of seafloor bathymetry from multibeam echosounder data using local fourier histogram texture features. *Journal of Experimental Marine Biology and Ecology*, 285, 355–370. [http://dx.doi.org/10.1016/S0022-0981\(02\)00537-3](http://dx.doi.org/10.1016/S0022-0981(02)00537-3), 2003.

De Falco, G., Conforti, A., Brambilla, W., Budillon, F., Ceccherelli, G. and De Luca, M.: Coralligenous banks along the western and northern continental shelf of Sardinia Island (Mediterranean Sea). *Journal of Maps*, 18(2), 200–209. <https://doi.org/10.1080/17445647.2021.2020179>, 2022.

De Falco, G., Tonielli, R., Di Martino, G., Innangi, S., Simeone, S. and Parnum, I. M.: Relationships between multibeam backscatter, sediment grain size and *Posidonia oceanica* seagrass distribution. *Continental Shelf Research*, 30(18), 1941–1950. <https://doi.org/10.1016/j.csr.2010.09.006>, 2010.

Deias, C., Guido, A., Sanfilippo, R., Apollaro, C., Dominici, R., Cipriani, M., Barca, D., and Vespasiano, G.: Elemental Fractionation in Sabellariidae (Polychaeta) Biocement and Comparison with Seawater Pattern: A New Environmental Proxy in a High-Biodiversity Ecosystem? *Water*, 15, 1549, <https://doi.org/10.3390/w15081549>, 2023.

Di Geronimo, I., Di Geronimo, R., Improta, S., Rosso, A. and Sanfilippo, R.: Preliminary observation on a columnar coralline build-up from off SE Sicily. *Biologia Marina Mediterranea*, 8(1), 229–237, 2001.

Donato, G., Sanfilippo, R., Basso, D., Bazzicalupo, P., Bertolino, M., Bracchi, V. A., Cipriani, M., D’Alpa, F., Guido, A., Negri, M. P., Sciuto, F., Serio, D. and Rosso, A.: Biodiversity associated with a coralligenous build-up off Sicily (Ionian Sea). *Regional Studies in Marine Science*, 80, 103868, <https://doi.org/10.1016/j.rsma.2024.103868>, 2024.



623 Faccenna, C., Becker, T. W., Lucente, F. P., Jolivet, L. and Rossetti, F.: History of subduction and back–arc extension in  
624 the Central Mediterranean. *Geophysical Journal International*, 145 (3), 809–820. [http://dx.doi.org/10.1046/j.0956-](http://dx.doi.org/10.1046/j.0956-540x.2001.01435.2001)  
625 540x.2001.01435, 2001.

626

627 Faccenna, C., Molin, P., Orecchio, B., Olivetti, V., Bellier, O., Funiciello, F., Minelli, L., Piromallo, C. and Billi, A.:  
628 Topography of the Calabria subduction zone (Southern Italy): clues for the origin of Mt. Etna. *Tectonics*, 30, TC1003.  
629 <http://dx.doi.org/10.1029/2010TC002694>. 2011.

630

631 Fakiris, E. and Papatheodorou, G.: Quantification of regions of interest in swath sonar backscatter images using grey–  
632 level and shape geometry descriptors: The TargAn software. *Marine Geophysical Research*, 33, 169–183,  
633 <http://dx.doi.org/10.1007/s11001-012-9153-5>, 2012.

634 Foglini, F., Grande, V., Marchese, F., Bracchi, V. A., Prampolini, M., Angeletti, L., Castellan, G., Chimienti, G., Hansen,  
635 I. M., Gudmundsen, M., Meroni, A. N., Mercorella, A., Vertino, A., Badalamenti, F., Corselli, C., Erdal, I., Martorelli,  
636 E., Savini, A. and Taviani, M.: Application of Hyperspectral Imaging to Underwater Habitat Mapping, Southern Adriatic  
637 Sea. *Sensors*, 19, 2261, <https://doi.org/10.3390/s19102261>, 2019.

638

639 Fonseca, L., and Mayer, L.: Remote estimation of surficial seafloor properties through the application of angular range  
640 analysis to multibeam sonar data. *Marine Geophysical Research*, 28, 119–126, [https://doi.org/10.1007/s11001-007-9019-](https://doi.org/10.1007/s11001-007-9019-4)  
641 4, 2007.

642

643 Garone, R.V., Lønmo, T., I., B., Schimel, A. C. G., Diesing, M., Thorsnes, T. and Løvstakken, L.: Seabed classification  
644 of multibeam echosounder data into bedrock/non-bedrock using deep learning. *Frontiers in Earth Science*, 11:1285368,  
645 <https://doi.org/10.3389/feart.2023.1285368>, 2023.

646

647 Gerovasileiou V. and Bianchi, C. N.: Mediterranean marine caves: a synthesis of current knowledge. In S. J. Hawkins,  
648 A. J. Lemasson, A. L. Allcock, A. E. Bates, M. Byrne, A. J. Evans, L. B. Firth, E. M. Marzinelli, B. D. Russell, I. P.  
649 Smith, S. E. Swearer, P. A. (Eds.), *Oceanography and Marine Biology: An Annual Review*, (Vol. 59, pp. 1–88). Todd,  
650 Editors Taylor & Francis, <https://doi.org/10.1201/9781003138846-1>, 2021.

651

652 Gliozzi, E.: I terrazzi marini del Pleistocene superiore della penisola di Crotone (Calabria). *Geologica Romana*, 26, 17–  
653 79, 1987.

654

655 Guido, A., Gerovasileiou, V., Russo, F., Rosso, A., Sanfilippo, R., Voultsiadou, E. and Mastandrea, A.: Composition and  
656 biostratinomy of sponge–rich biogenic crusts in submarine caves (Aegean Sea, Eastern Mediterranean). *Palaeogeography*,  
657 *Palaeoclimatology*, *Palaeoecology*, 534, 109338, <https://doi.org/10.1016/j.palaeo.2019.109338>, 2019a.

658

659 Guido, A., Gerovasileiou, V., Russo, F., Rosso, A., Sanfilippo, R., Voultsiadou, E. and Mastandrea, A.: Dataset of  
660 biogenic crusts from submarine caves of the Aegean Sea: An example of sponges vs microbialites competitions in cryptic  
661 environments.” *Data in brief*, 27, 104745, <https://doi.org/10.1016/j.dib.2019.104745>, 2019b.

662

663 Guido, A., Heindel, K., Birgel, D., Rosso, A., Mastandrea, A., Sanfilippo, R., Russo, F. and Peckmann, J.: Pendant  
664 bioconstructions cemented by microbial carbonate in submerged marine cave (Holocene, SE Sicily). *Palaeogeography,*  
665 *Palaeoclimatology, Palaeoecology*, 388, 166–180. <http://dx.doi.org/10.1016/j.palaeo.2013.08.007>, 2013.

666

667 Guido, A., Jimenez, C., Achilleos, K., Rosso, A., Sanfilippo, R., Hadjioannou, L., Petrou, A., Russo, F. and Mastandrea,  
668 A.: Cryptic serpulid-microbialite bioconstructions in the Kakoskali submarine cave (Cyprus, Eastern Mediterranean).  
669 *Facies*, 63(21), <http://dx.doi.org/10.1007/s10347-017-0502-3>, 2017b.

670

671 Guido, A., Rosso, A., Sanfilippo, R., Miriello, D. and Belmonte, G.: Skeletal vs microbialite geobiological role in  
672 bioconstructions of confined marine environments. *Palaeogeography, Palaeoclimatology, Palaeoecology*, 593, 110920,  
673 <https://doi.org/10.1016/j.palaeo.2022.110920>, 2022.

674 Guido, A., Rosso, A., Sanfilippo, R., Russo, F. and Mastandrea, A.: Frutexitites from microbial/metazoan bioconstructions  
675 of recent and Pleistocene marine caves (Sicily, Italy). *Palaeogeography, Palaeoclimatology, Palaeoecology*, 453, 127–  
676 138. <http://dx.doi.org/10.1016/j.palaeo.2016.04.025>, 2016.

677

678 Guido, A., Rosso, A., Sanfilippo, R., Russo, F. and Mastandrea, A.: Microbial Biomineralization in Biotic Crusts from a  
679 Pleistocene Marine Cave (NW Sicily, Italy).” *Geomicrobiology Journal*, 34 (10), 864–872,  
680 <https://doi.org/10.1080/01490451.2017.1284283>, 2017a.

681

682 Innangi, S., Barra, M., Di Martino, G., Parnum, I. M., Tonielli, R. and Mazzola, S.: Reson SeaBat 8125 backscatter data  
683 as a tool for seabed characterization (Central Mediterranean, Southern Italy): Results from different processing  
684 approaches. *Applied Acoustics*, 87, 109–122, <https://doi.org/10.1016/j.apacoust.2014.06.014>, 2015.

685

686 Innangi, S., Ferraro, L., Innangi, M., Di Martino, G., Giordano, L., Bracchi, V.A. and Tonielli, R.: Linosa island: a unique  
687 heritage of Mediterranean biodiversity. *Journal of Maps*, 20(1), 2297989,  
688 <https://doi.org/10.1080/17445647.2023.2297989>, 2024.

689

690 Ismail, K., Huvenne, V. A. I. and Masson, D. G.: Objective automated classification technique for marine landscape  
691 mapping in submarine canyons. *Marine Geology*, 362, 17–32, <https://doi.org/10.1016/j.margeo.2015.01.006>, 2015.

692

693 Janowski, L., Trzcinska, K., Tegowski, J., Kruss, A., Rucinska-Zjadacz, M. and Pocwiardowski P.: Nearshore Benthic  
694 Habitat Mapping Based on Multi-Frequency, Multibeam Echosounder Data Using a Combined Object-Based Approach:  
695 A Case Study from the Rowy Site in the Southern Baltic Sea. *Remote Sensing*, 10, 1983,  
696 <https://doi.org/10.3390/rs10121983>, 2018.

697

698 Laborel, J.: Marine biogenic constructions in the Mediterranean. A review. *Scientific Reports of Port-Cros National Park*  
699 13, 97–126, 1987.

700

701 Lamarche G. and Lurton X.: Recommendations for improved and coherent acquisition and processing of backscatter data  
702 from seafloor-mapping sonars. *Marine Geophysical Research*, 39:5-22, <https://doi.org/10.1007/s11001-017-9315-6>,  
703 2018.

704  
705  
706  
707  
708  
709  
710  
711  
712  
713  
714  
715  
716  
717  
718  
719  
720  
721  
722  
723  
724  
725  
726  
727  
728  
729  
730  
731  
732  
733  
734  
735  
736  
737  
738  
739  
740  
741  
742  
743

Lebrec, U., Riera, R., Paumard, V., Leary, M. J. O. and Lang, S. C.: Morphology and distribution of Submerged palaeoshorelines: Insights from the North West Shelf of Australia. *Earth-Science Reviews*, 224, 103864, <https://doi.org/10.1016/j.earscirev.2021.103864>, 2022.

Lecours, V., Devillers, R., Schneider, D. C., Lucieer, V. L., Brown, C. J., and Edinger, E. N.: Spatial scale and geographic context in benthic habitat mapping: Review and future directions. *Marine Ecology Progress Series*, 535, 259–284, <https://doi.org/10.3354/meps11378>, 2015.

Lecours, V., Dolan, M. F. J., Micallef, A. and Lucieer, V. L.: A review of marine geomorphometry, the quantitative study of the seafloor. *Hydrology and Earth System Sciences*, 20, 3207–3244, <https://doi.org/10.5194/hess-20-3207-2016>, 2016.

Lo Iacono, C., Savini, A. and Basso, D.: Cold-Water carbonate bioconstructions. In Micallef A., Krastel S. & Savini A. (Eds.) *Submarine geomorphology*, (pp. 425–455). Springer, ISBN: 425-3-319-57851-4, [https://doi.org/10.1007/978-3-319-57852-1\\_22](https://doi.org/10.1007/978-3-319-57852-1_22), 2018.

Lucieer, V. and Lamarche, G.: Unsupervised fuzzy classification and object-based image analysis of multibeam data to map deep water substrates, Cook Strait, New Zealand. *Continental Shelf Research*, 31, 1236–1247. <https://doi.org/10.1016/j.csr.2011.04.016>, 2011.

Malinverno, A. and Ryan, W. B. F.: Extension in the Tyrrhenian Sea and shortening in the Apennines as result of arc migration driven by sinking of the lithosphere. *Tectonics*, 5 (2), 227–245. <http://dx.doi.org/10.1029/TC005i002p00227>, 1986.

Marchese, F., Bracchi, V. A., Lisi, G., Basso, D., Corselli, C. and Savini, S.: Assessing Fine-Scale Distribution and Volume of Mediterranean Algal Reefs through Terrain Analysis of Multibeam Bathymetric Data. A Case Study in the Southern Adriatic Continental Shelf, *Water*, 12, 157. [10.3390/w12010157](https://doi.org/10.3390/w12010157), 2020.

Maruca, G., Cipriani, M., Dominici, R., Imbrogno, G., Vespasiano, G., Apollaro, C., Perri, F., Bruno, F., Lagudi, A., Severino, U., Bracchi, V. A., Basso, D., Cellini, E., Mauri, F., Rosso, A., Sanfilippo, R. and Guido, A.: Dataset Benthic Habitat Mapping [data set], [http://geocube.unical.it/gmaruca/Dataset\\_Benthic\\_Habitat\\_Mapping.zip](http://geocube.unical.it/gmaruca/Dataset_Benthic_Habitat_Mapping.zip), 2025.

Massari, F. and Prosser, G.: Late Cenozoic tectono-stratigraphic sequences of the Croton Basin: insights on the geodynamic history of the Calabrian arc and Tyrrhenian Sea. *Basin Research*, 25, 26–51, <http://dx.doi.org/10.1111/j.1365-2117.2012.00549>, 2013.

Mauz, B. and Hassler, U.: Luminescence chronology of late Pleistocene raised beaches on Southern Italy: new data on relative sea-level changes. *Marine Geology*, 170, 187–203, [http://dx.doi.org/10.1016/S0025-3227\(00\)00074-8](http://dx.doi.org/10.1016/S0025-3227(00)00074-8), 2000.

McGarigal, K. and Marks, B. J. F.: *Spatial Pattern Analysis Program for Quantifying Landscape Structure (General Technical Report)* Washington, DC, USA, 1995.

744 Micallef, A., Le Bas, T.P., Huvenne, V. A. I., Blondel, P., Hühnerbach, V. and Deidun, A.: A multi-method approach  
745 for benthic habitat mapping of shallow coastal areas with high-resolution multibeam data. *Continental Shelf Research*,  
746 39, 14–26, <https://doi.org/10.1016/j.csr.2012.03.008>, 2012.

747

748 Milia, A. and Torrente, M. M.: Early-stage rifting of the southern Tyrrhenian region: the Calabria–Sardinia breakup.  
749 *Journal of Geodynamics*, 81, 17–29, <http://dx.doi.org/10.1016/j.jog.2014.06.001>, 2014.

750

751 Minelli, L. and Faccenna, C.: Evolution of the Calabrian accretionary wedge (Central Mediterranean). *Tectonics*, 29,  
752 TC4004, <http://dx.doi.org/10.1029/2009TC002562>, 2010.

753

754 Nalin, R. and Massari, F.: Facies and stratigraphic anatomy of a temperate carbonate sequence (Capo Colonna Terrace,  
755 late Pleistocene, Southern Italy). *Journal of sedimentary research*, 79 (4), 210–225.  
756 <http://dx.doi.org/10.2110/jsr.2009.027>, 2009.

757

758 Nalin, R., Basso, D. and Massari, F.: Pleistocene coralline algal build-ups (coralligène de plateau) and associated  
759 bioclastic deposits in the sedimentary cover of Cutro marine terrace (Calabria, Southern Italy). In Pedley, H.M.,  
760 Carannante, G. (Eds.), *Cool–Water Carbonates: Depositional Systems and Palaeoenvironmental Controls*. The Geological  
761 Society of London (pp.11–22), <http://dx.doi.org/10.1144/GSL.SP.2006.255.01.02>, 2006.

762

763 Nalin, R., Bracchi, V. A., Basso D. and Massari, F.: Persististrombus latus (Gmelin) in the upper Pleistocene deposits of  
764 the marine terraces of the Crotona peninsula (Southern Italy). *Italian Journal of Geosciences*, 131 (1), 95–101.  
765 <http://dx.doi.org/10.3301/IJG.2011.25>, 2012.

766

767 Nalin, R., Massari, F. and Zecchin, M.: Superimposed cycles of composite marine terraces: the example of Cutro Terrace  
768 (Calabria, Southern Italy). *Journal of sedimentary research*, 77, 340–354. <http://dx.doi.org/10.2110/jsr.2007.030>, 2007.

769

770 Palmentola, G., Carobene, L., Mastronuzzi, G. and Sansò, P.: I terrazzi marini pleistocenici della Penisola di Crotona  
771 (Italia). *Geografia Fisica e Dinamica Quaternaria*, 13, 75–80, 1990.

772

773 Pepe, F., Sulli, A., Bertotti, G., and Cella F.: Architecture and Neogene to Recent evolution of the western Calabrian  
774 continental margin: An upper plate perspective to the Ionian subduction system, central Mediterranean. *Tectonics*, 29,  
775 TC3007, <https://doi.org/10.1029/2009TC002599>, 2010.

776

777 Pérès, J. M. and Picard, J. : Nouveau manuel de bionomie benthique de la Mer Méditerranée. *Recent Travaux de la Station*  
778 *Marine d'Endoume*, 31 (47), 137, 1964.

779

780 Pérès, J. M.: Structure and dynamics of assemblages in the benthic. *Marine Ecology*, 5 (1), 119–185, 1982.

781

782 Picone, F. and Chemello, R.: Seascape characterization of a Mediterranean vermetid reef: a structural complexity  
783 assessment. *Frontiers in Marine Science*, 10, 1134385, doi:10.3389/fmars.2023.1134385, 2023.

784



785 Reitz, M. A. and Seeber, L.: Arc-parallel strain in a short rollback-subduction system: the structural evolution of the  
786 Crotone basin (Northeastern Calabria, Southern Italy). *Tectonics*, 31, TC4017, <http://dx.doi.org/10.1029/2011TC003031>,  
787 2012.

788

789 Riley, S. J., De Gloria, S. D. and Elliot, R.: A Terrain Ruggedness Index that Quantifies Topographic Heterogeneity.  
790 *International Journal of Scientific Research*, 5, 23–27, 1999.

791

792 Rosso, A., Donato, G., Sanfilippo, R., Serio, D., Sciuto, F., D’Alpa, F., Bracchi, V.A., Negri, M.P. and Basso D.: The  
793 bryozoan *Margaretta cereoides* as a habitat-former in the Coralligenous of Marzamemi (SE Sicily, Mediterranean Sea).  
794 In Koulouri P., Gerovasileiou V. & Dailianis T. (Eds), *Marine Benthic Biodiversity of Eastern Mediterranean Ecosystems*,  
795 *Journal of Marine Science and Engineering*, (Vol. 11, 590), <https://doi.org/10.3390/jmse11030590>, 2023.

796

797 Rueda, J.L., Urra, J., Aguilar, R., Angeletti, L., Bo, M., García-Ruiz, C. Gonzalez-Duarte, M. M., Lopez, E., Madurell,  
798 T., Maldonado, M., Mateo-Ramirez, A., Megina, C., Moreira, J., Moya, F., Ramalho, L. V., Rosso, A., Sitjà, C. and  
799 Taviani, M.: Cold-Water Coral Associated Fauna in the Mediterranean Sea and Adjacent Areas. In Orejas C., Jiménez  
800 C. (Eds.), *Mediterranean Cold-Water Corals: Past, Present and Future, Coral Reefs of the World* (Vol. 9 (29), pp. 295–  
801 333) Springer International Publishing AG, part of Springer Nature, <https://doi.org/10.1007/978-3-319-91608-829>, 2019.

802

803 Sanfilippo, R., Rosso, A., Mastandrea, A., Viola, A., Deias, C. and Guido, A.: *Sabellaria alveolata* sandcastle worm from  
804 the Mediterranean Sea: New insights on tube architecture and biocement. *Journal of Morphology*, 280, 1839–1849,  
805 <https://doi.org/10.1002/jmor.21069>, 2019.

806

807 Sanfilippo, R., Rosso, A., Viola, A., Guido, A. and Deias, C.: Architecture and tube structure of *Sabellaria spinulosa*  
808 (Leuckart, 1849): comparison with the Mediterranean *S. alveolata* congener. *Journal of Morphology*, 283, 1350–1358,  
809 <https://doi.org/10.1002/jmor.21507>, 2022.

810

811 Santagati, P., Guerrieri, S., Borrelli, M. and Perri, E.: Calcareous bioconstructions formation during the last interglacial  
812 (MIS 5) in the central Mediterranean: A consortium of algal, metazoan, and microbial framebuilders (Capo Colonna–  
813 Crotone Basin South Italy). *Marine and Petroleum Geology*, 167, 106950,  
814 <https://doi.org/10.1016/j.marpetgeo.2024.106950>, 2024.

815

816 Santoro, E., Mazzella, M. E., Rerranti, L., Randisi, A., Napolitano, E., Rittner, S. and Radtke, U.: Raised coastal terraces  
817 along the Ionian Sea coast of Northern Calabria, Italy, suggest space and time variability of tectonic uplift rates.”  
818 *Quaternary International*, 206, 78–101, <http://dx.doi.org/10.1016/j.quaint.2008.10.003>, 2009.

819

820 Savini, A., Borrelli, M., Vertino, A., Mazzella, F., and Corselli, C.: Terraced Landforms Onshore and Offshore the Cilento  
821 Promontory (Southern Tyrrhenian Margin): New Insights into the Geomorphological Evolution, *Water*, 13 (4), 566,  
822 <https://doi.org/10.3390/w13040566>, 2021.

823

824 Savini, A., Vertino, A., Marchese, F., Beuck, L. and Freiwald, A.: Mapping cold–water coral habitats at different scales  
825 within the Northern Ionian Sea (central Mediterranean): An assessment of coral coverage and associated vulnerability.  
826 PLoS ONE, 9, e87108. <https://doi.org/10.1371/journal.pone.0087108>, 2014.

827

828 Schlager, W.: Accommodation and supply–A dual control on stratigraphic sequences. *Sedimentary Geology*, 86, 111–  
829 136, 1993.

830

831 Schlager, W.: Depositional bias and environmental change–important factors in sequence stratigraphy. *Sedimentary*  
832 *Geology*, 70, 109–130, 1991.

833

834 Sciuto, F., Altieri, C., Basso, D., D’Alpa, F., Donato, G., Bracchi, V. A., Cipriani, M., Guido, A., Rosso, A., Sanfilippo,  
835 R., Serio, D. and Viola, A.: Preliminary data on ostracods and foraminifers living on coralligenous bioconstructions  
836 Offshore Marzamemi (Ionian Sea, Se Sicily). *Revue de Micropaléontologie*, 18, 100711,  
837 <https://doi.org/10.1016/j.revmic.2023.100711>, 2023.

838

839 Severino, U., Lagudi, A., Barbieri, L., Scarfone, L., and Bruno, F.: A SLAM–Based Solution to Support ROV Pilots in  
840 Underwater Photogrammetric Survey. In *International Conference of the Italian Association of Design Methods and Tools*  
841 *for Industrial Engineering* (pp. 443–450). Cham: Springer Nature Switzerland,  
842 [https://link.springer.com/chapter/10.1007/978-3-031-58094-9\\_49](https://link.springer.com/chapter/10.1007/978-3-031-58094-9_49), 2023.

843

844 SNPA, Methodological Sheets used in the monitoring program of the second cycle of the Marine Strategy Directive  
845 (Ministerial Decree 2 February 2021) SNPA technical publications, [https://www.snambiente.it/snpa/schede-](https://www.snambiente.it/snpa/schede-metodologiche-utilizzate-nei-programmi-di-monitoraggio-del-secondo-ciclo-della-direttiva-strategia-marina-d-m-2-febbraio-2021/)  
846 [metodologiche-utilizzate-nei-programmi-di-monitoraggio-del-secondo-ciclo-della-direttiva-strategia-marina-d-m-2-](https://www.snambiente.it/snpa/schede-metodologiche-utilizzate-nei-programmi-di-monitoraggio-del-secondo-ciclo-della-direttiva-strategia-marina-d-m-2-febbraio-2021/)  
847 [febbraio-2021/](https://www.snambiente.it/snpa/schede-metodologiche-utilizzate-nei-programmi-di-monitoraggio-del-secondo-ciclo-della-direttiva-strategia-marina-d-m-2-febbraio-2021/), 2024.

848

849 Stephens, D., Smith, A., Redfern, T., Talbot, A., Lessnoff, A. and Dempsey, K.: Using three dimensional convolutional  
850 neural networks for denoising echosounder point cloud data. *Applied Computing and Geosciences*, 5-100016,  
851 <https://doi.org/10.1016/j.acags.2019.100016>, 2020.

852

853 Varzi, G. A., Fallati, L., Savini, A., Bracchi, V. A., Bazzicalupo, P., Rosso, A., Sanfilippo, R., Bertolino, M., Muzzupappa,  
854 M., and Basso, D.: Geomorphology of coralligenous reefs offshore southeastern Sicily (Ionian Sea).” *Journal of Maps*,  
855 19 (1), <https://doi.org/10.1080/17445647.2022.2161963>, 2023.

856

857 Vosselman, G.: Slope based filtering of laser altimetry data. *IAPRS*, Vol. XXXIII, Amsterdam, 2020.

858

859 Westaway, R. and Bridgland, D: Late Cenozoic uplift of Southern Italy deduced from fluvial and marine sediments:  
860 coupling between surface processes and lower–crustal flow. *Quaternary International*, 175, 86–124,  
861 <http://dx.doi.org/10.1016/j.quaint.2006.11.015>, 2007.

862

863 Westaway, R.: Quaternary uplift of Southern Italy. *Journal of Geophysical Research*, 98 (B12), 21741–21772,  
864 <http://dx.doi.org/10.1029/93JB01566>, 1993.

865

866 Zecchin, M. and Caffau, M.: Key features of mixed carbonate–siliciclastic shallow–marine systems: the case of Capo  
867 Colonna terrace (southern Italy). *Italian Journal of Geosciences*, 130 (3), 370 – 379.  
868 <http://dx.doi.org/10.3301/IJG.2011.12>, 2011.

869

870 Zecchin, M., Caffau, M., Civile, D. and Roda, C.: Facies and cycle architecture of a Pleistocene marine terrace (Crotone,  
871 southern Italy): a sedimentary response to late Quaternary, high–frequency glacio–eustatic changes. *Sedimentary*  
872 *Geology*, 216, 138–157, <http://dx.doi.org/10.1016/j.sedgeo.2009.03.004>, 2009.

873

874 Zecchin, M., Caffau, M., Civile, D., Critelli, S., Di Stefano, A., Maniscalco, R., Muto, F., Sturiale, G., and Roda, C.: The  
875 Plio–Pleistocene evolution of the Crotone Basin (Southern Italy): interplay between sedimentation, tectonics and eustasy  
876 in the frame of Calabrian arc migration.” *Earth Science Reviews*, 115, 273–303.  
877 <http://dx.doi.org/10.1016/j.earscirev.2012.10.005>, 2012.

878

879 Zecchin, M., Nalin, R. and Roda, C.: Raised Pleistocene marine terraces of the Crotone peninsula (Calabria, southern  
880 Italy): facies analysis and organization of their deposits. *Sedimentary Geology*, 172, 165–185. doi:  
881 10.1016/j.sedgeo.2004.08.003, 2004.

882

883 Zevenbergen, L.W. and Thorne C. R.: Quantitative analysis of land surface topography. *Earth Surface Processes and*  
884 *Landforms*, 12 (1), 47–56. <https://doi.org/10.1002/esp.3290120107>, 1987.